

Supplementary Information

Antiviral Cyclic Peptides Targeting the Main Protease of SARS-CoV-2

Jason Johansen-Leete ^{ab}, Sven Ullrich ^c, Sarah E. Fry ^{ab}, Rebecca Frkic ^{cd}, Max J. Bedding ^{ab}, Anupriya Aggarwal ^e, Anneliese S. Ashhurst ^{abf}, Kasuni B. Ekanayake ^{cd}, Mithun C. Mahawaththa ^{cd}, Vishnu M. Sasi ^{cd}, Stephanie Luedtke ^g, Daniel J. Ford ^{ab}, Anthony J. O'Donoghue ^g, Toby Passioura ^{abhi}, Mark Larence ^{ij}, Gottfried Otting ^{cd}, Stuart Turville ^e, Colin J. Jackson ^{cd}, Christoph Nitsche ^{*c}, Richard J. Payne ^{*ab}

^a School of Chemistry, The University of Sydney, Sydney, NSW 2006, Australia

^b Australian Research Council Centre of Excellence for Innovations in Peptide and Protein Science, The University of Sydney, Sydney, NSW 2006, Australia

^c Research School of Chemistry, Australian National University, Canberra, ACT 2601, Australia

^d Australian Research Council Centre of Excellence for Innovations in Peptide and Protein Science, Australian National University, Canberra, ACT 2601, Australia

^e Kirby Institute, Sydney, NSW 2052, Australia

^f School of Medical Sciences, Faculty of Medicine and Health, The University of Sydney, Sydney, NSW 2006, Australia.

^g Skaggs School of Pharmacy and Pharmaceutical Sciences, University of California, San Diego, 9500 Gilman Dr., La Jolla, CA 92093, USA

^h School of Life and Environmental Sciences, The University of Sydney, Sydney NSW 2006, Australia

ⁱ Sydney Analytical, The University of Sydney, Sydney NSW 2006, Australia

^j Charles Perkins Centre, The University of Sydney, Sydney, NSW 2006, Australia

*Correspondence and requests for materials should be addressed to Richard J. Payne or Christoph Nitsche.

Email: richard.payne@sydney.edu.au or christoph.nitsche@anu.edu.au

Supplementary Methods

General Materials and Methods

Peptide grade *N,N*-dimethylformamide (DMF) and dichloromethane (CH₂Cl₂) for peptide synthesis were purchased from RCI Labscan and Merck, respectively. Gradient grade acetonitrile (CH₃CN) for chromatography was purchased from Sigma Aldrich and ultrapure water (Type 1) was obtained from a Merck Millipore Direct-Q 5 water purification system. Standard Fmoc-protected amino acids (Fmoc-Xaa-OH), coupling reagents and resins were purchased from Mimotopes and Novabiochem. PEG building blocks were purchased from Broadpharm. Fmoc-SPPS was performed manually with these reagents and solvents in polypropylene Teflon-fritted syringes purchased from Torviq or through automated synthesis on a SYRO I peptide synthesizer (Biotage). All other reagents were purchased from AK Scientific or Merck and used as received.

Preparative Chromatography

Preparative and semi-preparative reversed-phase high-performance liquid chromatography (RP-HPLC) was carried-out using a Waters 600E multisolvent delivery system with a Rheodyne 7725i injection valve fitted with a 5 mL loading loop, a Waters 500 pump and a Waters Fraction Collector III with detection using a Waters 490E programmable wavelength detector operating at 214 nm and 280 nm. Preparative RP-HPLC was carried-out using a Waters XBridge® C18 OBDTM Prep Column (5 μm, 30 x 150 mm) at a flow rate of 35 mL min⁻¹ using a mobile phase of H₂O with 0.1vol.% TFA (solvent A) and CH₃CN with 0.1vol.% TFA (solvent B) on linear gradients, unless otherwise specified. Semi-preparative RP-HPLC was performed using a Waters XBridge® BEH C18 OBDTM Prep Column (300 Å, 5 μm, 10 x 250 mm) at a flow rate of 5 mL min⁻¹ using a mobile phase of H₂O with 0.1vol.% TFA (solvent A) and CH₃CN with 0.1vol.% TFA (solvent B) on linear gradients, unless otherwise specified.

Liquid Chromatography-Mass Spectrometry

Liquid Chromatography-Mass Spectrometry (LC-MS) was performed on a Shimadzu 2020 UPLC-MS instrument with a Nexera X2 LC-30AD pump, Nexera X2 SPD-M30A UV/Vis diode array detector and a Shimadzu 2020 (ESI) mass spectrometer operating in positive ion mode. Separations were performed on a Waters Acquity BEH300 1.7 μm, 2.1 × 50 mm (C18) column at a flow rate of 0.6 mL min⁻¹. All separations were performed using a mobile phase of 0.1 vol.% formic acid in water (solvent A) and 0.1 vol.% formic acid in CH₃CN (solvent B) using linear gradients over 5 min.

Analytical RP-HPLC

Analytical RP-HPLC was performed on a Waters Alliance e2695 HPLC system equipped with a 2998 PDA detector (λ = 210–400 nm). Separations were performed on a Waters XBridge® Peptide BEH300 5 μm, 4.6 × 250 mm (C18) column at 40 °C with a flow rate of 1.0 mL min⁻¹. All separations were performed using a mobile phase of 0.1% TFA in water (Solvent A) and 0.1% TFA in CH₃CN (Solvent B) using linear gradients, unless otherwise specified.

***In vitro* Protein Expression**

Selectively isotope-labelled samples of M^{Pro} R298A and site-directed mutants thereof were prepared by cell-free protein synthesis.^{1, 2} Selectively ¹⁵N-labelled samples were prepared with Ala, Cys, Gly, Ile, Leu, Lys, Met, Ser, Thr, Val and Arg. ¹⁵N-HSQC cross-peaks of selectively labelled samples were obtained by systematic site-directed mutagenesis, using cell-free protein synthesis from PCR-amplified DNA³ to obtain 85 individual mutant protein samples (Supplementary Table 1). In each of these samples, the mutated residue type was labelled with ¹⁵N. Each cell-free reaction was conducted as two reactions, each with 1 mL inner and 10 mL outer buffer. The mutant proteins were purified using a 1 mL His GraviTrap™ TALON column (GE Healthcare, USA). Following the purification, the buffer was exchanged to NMR buffer and 10 % D₂O added afterwards to provide a lock signal.

Plasma stability Assessment

Plasma stability of peptides **1** and **6** was determined using a slightly modified method previously described by Teufel *et al.*⁴ Positive control: Propantheline bromide. The peptides (5 mM stock in DMSO) were added to citrated human plasma (from healthy volunteers) to a concentration of 200 μM. The peptides were incubated at 37 °C for 0, 1, 3, 6 or 24 h before being quenched with three volumes of 1:1 v/v MeOH: MeCN. The samples were centrifuged at 13,500 rpm for 5 minutes before removing an aliquot of the supernatant (20 μL) that was diluted with water (20 μL) and analysed by reverse-phase UHPLC-MS. The area under the starting peptide peak (normalised to total area under the chromatogram) was used to quantify the amount of uncleaved peptide remaining.

NMR Experiments

All NMR spectra of M^{Pro} R298A were recorded at 25 °C, using 3 mm NMR tubes on 800 MHz or 600 MHz Bruker Avance NMR spectrometers. 0.1–0.5 mM protein samples were used. Spectra recorded included 2D [¹⁵N,¹H]-HSQC (typical parameters: $t_{1max} = 42$ ms, $t_{2max} = 100$ ms, total recording time 2.5 h) and [¹⁵N,¹H]-TROSY ($t_{1max} = 82$ ms, $t_{2max} = 142$ ms, total recording time 2.2 h) and TROSY versions of 3D HNCA, HNCOC, HNCACB and HNCOCA experiments. NOEs were recorded using a 3D NOESY-¹⁵N-HSQC experiment with a mixing time of 150 ms.

NMR Resonance Assignments of M^{Pro} R298A

Selectively ¹⁵N-labelled samples were prepared by cell-free protein synthesis, which uses amino acids only sparingly (at a final concentration of 1 mM). Eleven different amino acid types, one at a time, were targeted by using ¹⁵N-labelled amino acids. In addition, 85 samples were prepared with site-directed mutagenesis to remove single peaks from the [¹⁵N,¹H]-HSQC spectrum of the selectively labelled samples. The side chains of all targeted residues were solvent exposed according to the crystal structure 6LU7.⁵ 41 HSQC cross-peaks could be assigned in this way (Supplementary Tables 1 and 2). In the remaining cases, the assignment was compromised as the mutation perturbed the appearance of the [¹⁵N,¹H]-HSQC spectrum too much or the cross-peak of the mutated amino acid was too weak to be observed in the first place. The resonance assignments made by site-directed mutation presented useful starting points for additional assignments made by 3D NMR spectra of ¹⁵N/²H/¹³C-labelled protein.

Ultimately, we assigned 143 [$^{15}\text{N}, ^1\text{H}$]-HSQC cross-peaks (Fig. S6b), which corresponds to almost half of the non-proline backbone amides. The assignments agree with previously published assignments made for the M^{pro} dimer.⁶

NMR Resonance Assignments of wild-type M^{pro}

Resonance assignments of backbone amides of dimeric wild-type M^{pro} were based on a comparison of 3D HNCO spectra recorded of $^{15}\text{N}/^{13}\text{C}/^2\text{H}$ -labelled wild-type M^{pro} and the R298A mutant, assuming conservation of the ^1H , ^{15}N and ^{13}C chemical shifts of resolved cross-peaks between both proteins. Our limited assignments of the backbone amides of wild-type M^{pro} obtained in this way (Figure S6a) agree in general also with those by Cantrelle et al.⁷, which were obtained under different conditions (pH 6.8 and 305 K), but significant differences (> 0.8 ppm in the ^1H dimension and/or > 2.5 ppm in the ^{15}N dimension) were observed for residues Asp48, Arg105, Ser121 and Gly183. In principle, chemical shift changes may arise from conformational changes between the monomeric and dimeric forms of M^{pro}, although the crystal structures of the wild-type dimer (PDB code 6LU7; Jin et al., 2020)⁵ and the R298A mutant of the corresponding M^{pro} protein from SARS-1 (PDB code 2QCY; Cheng et al., 2010)⁸ suggest high structural conservation of the chemical environment of the backbone amides of these residues.

Molecular Dynamics Simulations

The crystal structure of the cyclic peptide **Se-1** complexed with the SARS-CoV-2 M^{pro} homodimer was used to model the full-length peptide. For chain A, the starting peptide conformation was manually built as accurately as possible using the available electron density, in the canonical orientation as seen in crystal structure. As a negative control, for chain B, the peptide was modelled in the opposite orientation, i.e. where the S2 subcavity was occupied by Tyr4 group (rather than Leu2).

The co-crystallized structure was processed using the protein preparation wizard in Maestro.⁹ The sequence of steps involved in the preparation were the assignment of bond orders, addition of missing hydrogens, creating disulfide bonds, converting selenomethionines to methionines, and generation of het states using Epik program at a pH of 7.4 ± 0.02 . The hydrogen bond networks were optimized using the default parameters and the PROPKA program was selected to assign the protonation states of the residues at a pH of 7.4. This was followed by restrained minimization, where the heavy atoms were converged to an RMSD of 0.30 Å, using the OPLS3e forcefield. Overlapping bonds were fixed using the 3-D builder tool in Maestro before an H-bond optimization step.

The structure generated after the restrained minimization step was selected for molecular dynamics (MD) studies using Desmond.¹⁰ The Desmond System builder module was used to build the system, which involved enclosing the protein-ligand complex in an orthorhombic box with a buffer distance of (25x25x25) Å using the Transferable Intermolecular Potential 3P (TIP3P) water model. Counterions were added to neutralize the net charge, followed by the addition of 0.15 M NaCl to the system. The OPLS3e forcefield was selected for the study. The minimization step was carried out using the default parameters with a total simulation time of 100 ps.

The molecular dynamics module of Desmond was utilized to perform simulations of 330 ns duration in three replicates (0.99 μ s in total) starting from different random seeds. The NPT ensemble was chosen with an initial temperature and pressure of 300 K and 1.01325 bar respectively. The time step was set to 2.0 fs, while the Nose-Hoover chain Langevin thermostat and the Martyna-Tobias-Klein barometer was selected to control the temperature and pressure, respectively, during the simulation. The Cutoff method was chosen to determine the short-range Coulombic interactions and the cut-off radius was set to 9 Å. The default NVT ensemble was used to run a short minimization to properly equilibrate the system. After completion, the trajectories for all the three simulations were analyzed using Simulation Event Analysis (SEA) module of Desmond to study the protein and ligand RMSD plots. The simulation interaction diagram (SID) program of Desmond was utilized to view the ligand-protein interactions occurring throughout the simulation run time.

The Trajectory Frame Clustering module of Desmond was used to generate representative structures from the combined trajectories. Clustering was performed based on the backbone of the complex, with the frequency set to 10 and the maximum number of the reported clusters set to 10. All the generated structures were analyzed and the representative model from each simulation was identified for detailed binding interaction analysis. The structural figures were produced from PyMOL.¹¹

Plasmid construction

The gene of the SARS-CoV-2 main protease (M^{pro})¹² was cloned in between the *Nde*I and *Xho*I sites of the T7 vector pET-47b (+). The construct contains the M^{pro} self-cleavage-site (SAVLQ↓SGFRK; arrow indicating the cleavage site) at the N-terminus. At the C-terminus, the construct contains a modified PreScission cleavage site (SGVTFQ↓GP) connected to a His₆-tag. All plasmid constructions and mutagenesis were conducted with cloning and QuikChange protocols using mutant T4 DNA polymerase.

Protein expression

Wild-type M^{pro} was expressed in BL21 DE3 cells transformed with the desired plasmid. Protein expression was conducted in a Labfors 5 bioreactor (INFORS HT, Switzerland). After induction, the culture was grown at 18 °C overnight for protein expression. Cells were harvested by centrifugation at 5,000 g for 15 minutes and lysed by passing twice through a Emulsiflex-C5 homogenizer (Avestin, Canada). The lysate was centrifuged at 13,000 g for 60 minutes and the filtered supernatant was loaded onto a 5 mL Ni-NTA column (GE Healthcare, USA) equilibrated with binding buffer (50 mM Tris-HCl pH 7.5, 300 mM NaCl, 5 % glycerol). The protein was eluted with elution buffer (binding buffer containing, in addition, 300 mM imidazole) and the fractions were analyzed by 12% SDS-PAGE. PreScission cleavage and TEV cleavage were conducted in binding buffer in the presence of 1 mM DTT with a protein-to-protease ratio of 100:1. Following cleavage of the His₆-tag, the buffer was exchanged to 20 mM HEPES-KOH pH 7.0, 150 mM NaCl, 1 mM DTT, 1 mM EDTA. All samples were analyzed by mass spectrometry using an Orbitrap Fusion Tribrid mass spectrometer (Thermo Scientific, USA) coupled

with an UltiMate S4 3000 UHPLC (Thermo Scientific, USA). For SDS-PAGE and MALDI-TOF characterization refer to Figures S18 and S19 in the ESI.

Protein cross-linking

C-terminally His-tagged SARS-CoV-2 M^{pro} (25 μ M) was incubated with disuccinimidyl glutarate (H6/D6, Creative Molecules Inc.) (250 μ M) in aqueous buffer (20 mM HEPES pH 7.6, 100 mM NaCl) at 37 °C for 1 h before the reaction was quenched by dilution of the protein to 10 μ M (monomer concentration) by addition of aqueous buffer containing 20 mM Tris-HCl pH 7.6, 100 mM NaCl. Cross-linking efficiency was analyzed by 12% SDS-PAGE and stained with SyproTM Ruby.

Proteomics to determine crosslink sites on SARS-CoV-2 M^{pro}

Crosslinked proteins were digested with trypsin and peptides desalted as described previously¹³. Peptide mixtures were analyzed by LC-MS/MS using data dependent acquisition with HCD fragmentation on a Thermo Orbitrap Eclipse mass spectrometer. Crosslinked peptides were identified with a 2% false-discovery rate using the Byonic search engine (Protein Metrics) and a custom database containing the M^{pro} protein sequence and common proteomics contaminants (e.g. trypsin, albumin, keratins, etc.). DSG crosslinks and hydrolysis products were allowed for the M^{pro} protein only. Carbamidomethylation was specified as a fixed modification on C, while oxidation of methionine, deamidation of N/Q and pyro-Glu for N-terminal Q/E were variable modifications. Plots of crosslinked residues were generated using UCSF Chimera 1.15rc with the M^{pro} dimer structure (PDB: 6Y2E).

RaPID mRNA display selection

Library preparation and display selection were performed as described previously with slight modifications¹⁴⁻¹⁷. Briefly, an mRNA library comprising an AUG start codon, 4–15 NNS (N = A, C, G or T; S = C or G) codons, a TGC cysteine codon and a 3' region encoding a linking sequence (Gly-Asn-Leu-Ile) with mRNA lengths pooled proportional to theoretical diversity was prepared as described previously. The mRNA library was then ligated to a puromycin-linked oligonucleotide using T4 ligase. The puromycin-linked mRNA was then translated using the PURExpress Δ RF kit (New England Biolabs) with the addition of release factors 2 and 3 per the manufacturer's instructions along with a "Solution A" containing 19 amino acids (-Met) (prepared as previously described) and either tRNA^{fMet}_{ini}-N-chloroacetyl-L-Tyr or tRNA^{fMet}_{ini}-N-chloroacetyl-D-Tyr (25 μ M) to initiate translation and facilitate peptide macrocyclization. Translation was performed at 100 μ L scale for the first round and 2.5 μ L scale for subsequent rounds. Following translation, ribosomal denaturation was performed by addition of EDTA before reverse transcription with RNase H- reverse transcriptase. After exchange into selection buffer (50 mM Tris-HCl pH 8.0, 150 mM NaCl, 0.1% Tween-20) through G-25 resin the peptide-mRNA:cDNA libraries were incubated with cross-linked linked SARS-CoV-2 M^{pro} (200 nM) immobilized on DynabeadsTM His-tag Isolation & Pulldown (Life Technologies) at 4 °C for 30 min after which the beads were washed with ice-cold selection buffer (3 x 100 μ L). The beads were then suspended in aqueous 0.1 vol.% TritonTM X-100 (100 μ L) and heated to 95 °C for 5 min to recover binding peptides. The recovered cDNA was amplified by PCR, purified by ethanol precipitation and transcribed with T7

RNA polymerase to yield an enriched mRNA library to enter the following round of selection. Subsequent rounds were performed in the same manner with the addition of six negative selection steps against beads alone to remove bead binding sequences. Sequencing of recovered cDNA from rounds seven through nine was conducted using an iSeq high-throughput sequencer (Illumina).

SARS-CoV-2 M^{pro} activity assay

The M^{pro} inhibition assay protocol was adapted and modified from ^{12, 18} and was carried out with a reaction volume of 100 μ L in 96-well-plates (black, polypropylene, U-bottom; Greiner Bio-One, Austria) using an aqueous buffer composed of 20 mM Tris-HCl pH 7.3, 100 mM NaCl, 1 mM EDTA, 1 mM DTT. All measurements were performed in triplicate. The compounds were incubated with recombinant SARS-CoV-2 M^{pro} for 10 min at 37 °C. The enzymatic reaction was initiated by addition of the FRET substrate (DABCYL)-KTSAVLQ↓SGFRKM-E(EDANS)-NH₂ (Mimotopes, Australia). The final concentrations for IC₅₀ determination amounted to 25 nM M^{pro} and 25 μ M substrate, with inhibitor concentrations ranging from nanomolar to micromolar. The final concentrations for K_i determination amounted to 12.5 nM enzyme and 10, 20, 35 and 50 μ M substrate, with a control and three inhibitor concentrations ranging from nanomolar to micromolar. The fluorescence signal was monitored by a fluorophotometer (Infinite 200 PRO M Plex; Tecan, Switzerland) for 5 min at 490 nm, using an excitation wavelength of 340 nm. Initial velocities were derived from the linear range of the enzymatic reaction. For IC₅₀ determination, 100% enzymatic activity was defined as the initial velocity of control triplicates containing no inhibitor and the percentage of inhibition was calculated in relation to 100% enzymatic activity. An EDANS standard curve generated as described by Ma *et al.*¹⁹ was used to convert fluorescence intensity to the amount of cleaved substrate (calibration curve). Data sets were analyzed with Prism 9.2 (Graph Pad Software, USA) to generate dose-response curves and calculate IC₅₀ values, as well as to generate Michaelis-Menten curves and calculate K_i values assuming the appropriate inhibition mode.

Protease inhibition studies

SARS-CoV-2 PL^{pro} was purchased from Acro Biosystems (PAE-C518) and human TMPRSS2 was purchased from Cusabio Technology (CSB-YP023924HU). Other recombinant proteases were purchased from R&D Systems which included SARS-CoV-1 3CL/M^{pro} (E-718), MERS-CoV 3CL/M^{pro} (E-719), human cathepsin L (952-CY), human cathepsin B (953-CY), human cathepsin E (1294-AS) and human Furin (1503-SE). Fluorogenic peptide substrates were purchased from a variety of vendors and used at the following concentration, 50 μ M z-Arg-Leu-Arg-Gly-Gly-AMC (Bachem I1690), 5 μ M z-Phe-Arg-AMC (R&D Systems, ES009), 85.5 μ M Boc-Gln-Ala-Arg-AMC (Vivitide, MQR-3135-v), 50 μ M pGlu-Arg-Thr-Lys-Arg-AMC (Vivitide, MPR-3159-v), Ac-Abu-Tle-Leu-Gln-AMC (Vivitide, SFP-3250-v) and 5 μ M Mca-Gly-Lys-Pro-Ile-Leu-Phe-Phe-Arg-Leu-Lys(DNP)-DArg-NH₂ (CPC Scientific, SUBS-017A). Assay buffers for protease assays were as follows, Assay Buffer 1 (SARS-CoV-1 and MERS-CoV): 50 mM HEPES pH7.5, 150 mM NaCl, 1 mM EDTA, 1 mM DTT, 0.01% Tween; Assay Buffer 2 (SARS-CoV-2 PL^{pro}): 50 mM HEPES pH 6.5, 150 mM NaCl, 0.01% Tween 20, 0.1 mM DTT; Assay

Buffer 3 (Cathepsin L & B): 50 mM Na-Acetate pH 5.5, 5 mM DTT, 1 mM EDTA, 0.01 % BSA, 100 mM NaCl; Assay Buffer 4 (TMPRSS2 and Furin): 25 mM Tris, HCl, pH 8.0, 150 mM NaCl, 5 mM CaCl₂, 0.01% Triton X-100 and Assay Buffer 5 (Cathepsin D & E): 100 mM Na-Citrate, pH 3.6. Peptide inhibitors we made up as 10 mM stocks in DMSO. Initial assays were performed with 10 μ M of peptide **1**, **6** and **Se-1**. Control inhibitors include 10 μ M E-64 (Sigma E3132), 10 μ M Pepstatin (Sigma P5318), 1 mM AEBSF (Sigma 101500), 10 μ M GC373 (gift from John C. Vederas, University of Alberta), 1 μ M Camostat (gift from James Janetka, Washington University) and 10 μ M PI-I (in house PL^{pro} inhibitor). For dose-response assays compounds were first diluted to 2.5 mM in DMSO and then serially diluted by 3-fold in DMSO to 0.174 nM. Each diluent was subsequently diluted into the appropriate assay buffer and pre-incubated with protease for 15 minutes at 25 °C. The reaction was initiated by addition of substrate in assay buffer. All assays were performed at 25°C in triplicate wells and DMSO used as a vehicle control. The final volume of each reaction was 30 μ L in a 384-well plate, and fluorescence was measured at 360/460 nm (ex/em) for peptide-AMC substrates or 320/400 nm (ex/em) for internally quenched MCA-peptide-DNP substrates in a Biotek Synergy HTX fluorescence plate reader. The reaction velocity was calculated as relative fluorescent units per second over 20 mins, with readings taken in 2 min intervals. Activity was normalized to wells lacking inhibitor but containing 1% DMSO in assay buffer. IC₅₀ values were calculated using GraphPad Prism 9.

Crystallography

To obtain a crystallographic complex of SARS-CoV-2 M^{pro} and **1**, the peptide was dissolved in DMSO to a stock concentration of 50 mM. Protein, prepared as described above, was diluted to 4 mg/mL in TBS (50 mM Tris-HCl pH 7.5, 300 mM NaCl) and incubated with 2.5-fold molar excess (~300 μ M) **1** for 2 hours on ice to saturate the binding sites of the protease. The complex was briefly buffer exchanged to remove unbound peptide using an Amicon Ultra 0.5 mL centrifugal filter with a 10 kDa MWCO to a final protein concentration of 4 mg/mL. This complex was used for high-throughput crystallography trials at 18 °C using drop sizes of 0.5 μ L protein and 0.5 μ L reservoir, which yielded a hit in the Index sparse matrix screen (Hampton Research). This hit was optimized but did not yield crystals of suitable diffraction quality; however, the crystals were able to be crushed and used to seed crystals with better morphology. Serial seeding was performed using a protein concentration of 1 mg/mL for several rounds until crystals of suitable diffracting quality were obtained, which were formed at 18 °C in a drop size of 1 μ L reservoir, 1.5 μ L protein, and 0.5 μ L seed stock against a reservoir solution of 25% PEG 3350, 0.1 M Bis-Tris pH 6.5, 0.3 M NaCl. Crystals were flash frozen without cryoprotecting and diffraction data were collected at 100 K using the MX2 beamline at the Australian Synchrotron. As the diffraction was not adequate to unambiguously model the inhibitor into the crystal structure, we solved the co-crystal structure of the SARS-CoV-2 M^{pro}-**Se-1** complex. The complex was prepared the same as with **1** but with overnight incubation at 4 °C. The complex was diluted to a protein concentration of 1 mg/mL and crystallized at 18 °C in a drop size of 1 μ L reservoir, 1.5 μ L protein and 0.5 μ L seed stock against a reservoir solution of 22% PEG 3350, 0.1 M Bis-Tris pH 6.0, 0.3 M NaCl. Crystals were seeded using crystal seeds of the SARS-CoV-2 M^{pro}-**1** crystals. Crystals formed as thin plates after ~4–5 days and were flash frozen without cryoprotection.

Diffraction data were collected at 100 K using the MX2 beamline at the Australian Synchrotron²⁰. Reflections collected were indexed and integrated using XDS²¹ and scaled in Aimless (CCP4)²². The phase problem was overcome by molecular replacement in Phaser MR (CCP4)²³, using PDB ID 7JKV as the search model. The structure was refined by iterative rounds of rebuilding in Coot²⁴, and twin refinement in Refmac^{25, 26}. The crystal was twinned P21 (-h, -k, (k+l)); initially autoindexing as C2221). Data collection and refinement statistics are given in Table S3 in the ESI. The final structure was deposited in the Protein Data Bank (PDB: 7RNW). Omit maps were generated using phenix (with twin refinement (-h, -k, (k+l))²⁷. Polder omit maps²⁸, and composite omit maps (5% omit fraction with refinement)²⁹ were also generated for comparison (Figure S26), with all methods yielding essentially identical omit electron density.

SARS-CoV-2 Infectivity Assays

HEK293-ACE2-TMPRSS2 cells stably expressing human ACE2 and TMPRSS2 were generated as previously described³⁰. A high content fluorescence microscopy approach was used to assess the ability of the cyclic peptide M^{pro} inhibitors to protect cells from SARS-CoV-2 induced cytopathic effects in permissive cells. In brief, the engineered cell line succumbs to viral cytopathic effects after 6 to 18 hours post infection. Cytopathic effects can be enumerated, as cells and their nuclei collapse into large syncytia after 18 hours of viral culture. The remaining cells outside of the syncytia increase in a dose dependent manner the lower the viral titers are and/or if a viral inhibitor is introduced within the culture.

For testing the cyclic peptides, compounds were initially diluted in cell culture medium (DMEM-5% FCS) to make 4x working stock solutions and then serially diluted further in the above media to achieve a 2-fold dilution series. On the day of the assay, HEK293-ACE2-TMPRSS2 cells were trypsinized, stained with NucBlue in suspension and then seeded at 16,000 cells in a volume of 40 μ L of DMEM-5% FCS per well in a 384-well plate (Corning #CLS3985). Diluted compounds (20 μ L) were added to the cells and the plates containing cells and compounds incubated for 1 hour at 37 °C, 5% CO₂. 20 μ L of virus solution at 8x10³ TCID₅₀/mL³¹ was then added to the wells and plates were incubated for a further 24 hours (37 °C, 5% CO₂). Stained cells were then imaged using the InCell 2500 (Cytiva) high throughput microscope, with a 10x 0.45 NA CFI Plan Apo Lambda air objective. Acquired nuclei were counted using InCarta high-content image analysis software (Cytiva) to give a quantitative measure of CPE. Virus inhibition/neutralization was calculated as %N = (D-(1-Q))x100/D, where; "Q" is the value of nuclei in test well divided by the average number of nuclei in untreated uninfected controls, and "D" = 1-Q for the wells infected with virus but untreated with inhibitors. Thus, the average nuclear counts for the infected and uninfected cell controls get defined as 0% and 100% neutralization respectively. To account for cell death due to drug toxicity, cells treated with a given compound alone and without virus were included in each assay. The % neutralization for each compound concentration in infected wells was normalized to % neutralization in wells with equivalent amount of compound but without the virus

to yield the final neutralization values for each condition. Inhibition curves and 50% (EC₅₀) effective concentrations were determined by non-linear regression analysis using GraphPad Prism software (version 9.1.2, GraphPad software, USA).

Cytotoxicity and targeted proteomics on HEK293-ACE2-TMPRSS2 cell line

HEK293-ACE2-TMPRSS2 cells were maintained in Dulbecco's Modified Eagle Medium (DMEM) with 4.5 g/L D-Glucose, L-Glutamine and 110 mg/L sodium pyruvate (Gibco), supplemented with 10% foetal calf serum (Hyclone). Cells were sub-cultured between 70-90% confluency and tested regularly to ensure free of mycoplasma contamination. Cytotoxicity of **1**, **pen-1**, **6** and **pen-6**, was determined by an Alamar Blue HS (Invitrogen) cell viability assay as per manufacturer's instructions. Briefly, 5x10⁴ cells were seeded into wells of a 96-well flat bottom culture plate (Corning) and once adhered, compounds or vehicle control (DMSO) were added at varying concentrations and incubated for 24 hours (37 °C, 5% CO₂). Alamar Blue HS cell viability reagent (Invitrogen) was added and the cells further incubated for 2-3 hours. Relative fluorescent units (RFU) were determined per well at ex/em 560/590 nm (Tecan Infinite M1000 pro plate reader). Increasing RFU is proportional to cell viability.

For targeted proteomics, cells in 6-well plates at 70% confluency were treated with vehicle control (DMSO) or inhibitors at 10 µM. At various time points (performed in triplicate), the cells were washed 3 times with 2 mL DPBS (Gibco), scraped and lysed in 4% SDC buffer (4% sodium deoxycholate, 0.1 M Tris-HCl pH 8.0) then immediately heated to 95 °C for 10 mins before freezing at -30 °C prior to processing for targeted proteomics³². Cell lysates were digested to peptides as described previously. Peptides were analyzed by LC-MS/MS using a data-independent acquisition method as described previously.³³ Extracted ion chromatograms for fragment ions derived from tryptic peptides were plotted using Xcalibur Qual Browser (Thermo Scientific). The area under the curve for each peak was used for quantification.

Cyclic peptide synthesis

General procedure A; Automated Fmoc-Solid-Phase Peptide Synthesis (SPPS) – SYRO I automatic peptide synthesizer (Biotage)

Unless otherwise specified, peptides were synthesized on a 50 µmol scale. Rink amide resin (0.56 mmol g⁻¹, 1 eq.) was treated with a solution of piperidine (40 vol.%, 0.8 mL) in DMF for 3 min, drained, before repeat treatment with piperidine (20 vol.%, 0.8 mL) in DMF for 10 min. The resin was then drained and washed with DMF (4 x 1.2 mL) before addition of a solution of Fmoc-amino acid (200 µmol, 4 eq.) and Oxyma (4.4 eq.) in DMF (400 µL), followed by a solution of *N-N'*-diisopropylcarbodiimide (4 eq.) in DMF (400 µL). The resin was then agitated at 75 °C for 15 min or 50 °C for 30 min as specified (coupling of Fmoc-His(Trt)-OH and Fmoc-Cys(Trt)-OH were reacted at 50 °C for 30 min in all instances). The resin was then drained and a repeat treatment of the coupling conditions was conducted. The resin was then washed with DMF (4 x 1.2 mL) before being treated with a solution of 5 vol.% Ac₂O and 10 vol.% *i*-Pr₂NEt in DMF (1.6 mL) and agitated for 5 min to cap unreacted peptide N-termini. The resin was then drained and washed with DMF (4 x 1.6 mL). Iterative cycles of this process were repeated until complete

peptide elongation was achieved after which the resin was washed with DMF (4 x 5 mL) and CH₂Cl₂ (5 x 5 mL).

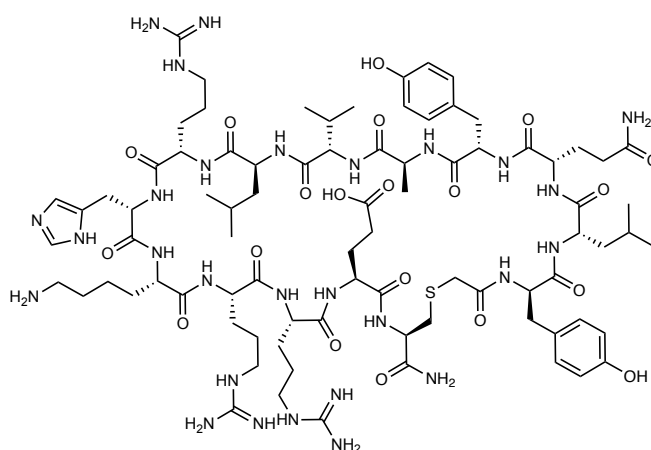
General procedure B; Cyclisation (CH₃CN:H₂O)

The peptide was dissolved in 1:1 v/v CH₃CN:H₂O (5 mM) in the presence of *i*-Pr₂NEt (2.5 vol.%) and incubated for 1 h to facilitate thioether or selenoether cyclization.

General procedure C; Cyclisation (DMSO)

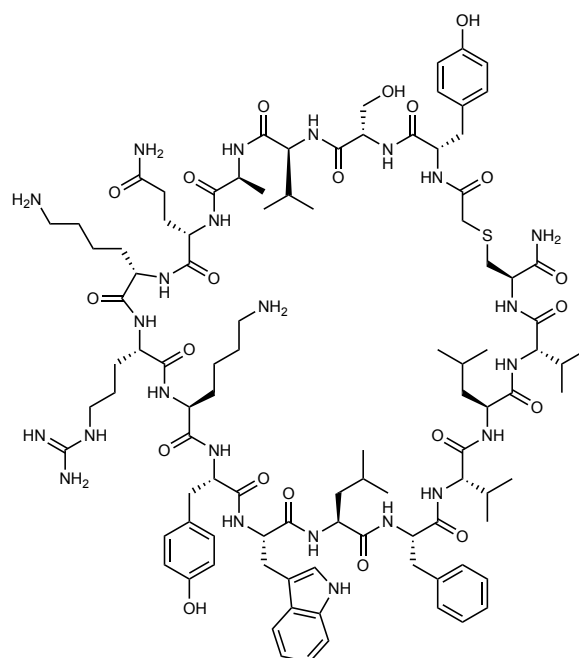
The peptide was dissolved in DMSO (5-10 mM) in the presence of *i*-Pr₂NEt (2.5 vol.%) and incubated for 1 h to facilitate thioether cyclization.

1:



The peptide (50 μmol) was synthesized by general procedure **A** at 75 °C (Oxyma Pure was omitted from the terminal coupling of chloroacetic acid). The peptide was then cleaved from resin by treatment with 87.5:5:5:2.5 v/v/v/v trifluoroacetic acid/triisopropylsilane/H₂O/EDT for 3 h. The cleave solution was collected, dried to ~1 mL under N₂ flow and the peptide product precipitated from Et₂O (30 mL) and collected by centrifugation. The crude linear peptide was then purified by preparative RP-HPLC (0 vol.% CH₃CN + 0.1 vol.% TFA for 5 min, then 0-40 vol.% CH₃CN + 0.1 vol.% TFA over 80 min, 35 mL/min, XBridge® C8, 300 Å, 30 x 150 mm). Fractions containing the linear peptide were combined and lyophilized. The lyophilized peptide was then cyclized by general procedure **B**. The reaction was concentrated under N₂ flow before being purified by preparative HPLC (0 vol.% CH₃CN + 0.1 vol.% TFA for 5 min, then 0-30 vol.% CH₃CN + 0.1 vol.% TFA over 80 min, 35 mL/min, XBridge® C8, 300 Å, 30 x 150 mm) to afford **1** as a white solid (12.6 mg, 10%). **R_t** 214nm: 21.93 min. (1 to 40 vol.% CH₃CN+ 0.1 vol.% TFA over 30 min). **LR-MS (+ESI)**: m/z = 1874.60 [M+H]⁺, 937.95 [M+2H]²⁺, 625.60 [M+3H]³⁺, 469.45 [M+4H]⁴⁺.

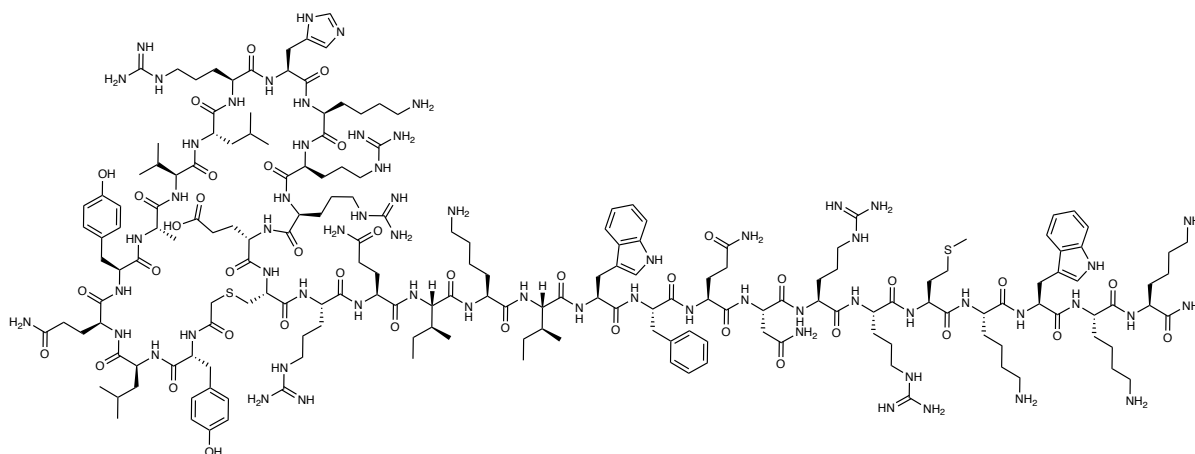
4.



The peptide (50 μmol) was synthesized by general procedure **A** at 75 $^{\circ}\text{C}$, with the exception that K6, R7 and K9 were subjected to a third treatment at the amino acid coupling step. The peptide was then cleaved from resin with 85:5:5:2.5:2.5 v/v/v/v/v TFA/TIS/ H_2O /phenol/EDT for 2 h. The cleave solution was collected, dried to ~ 1 mL under N_2 flow and the peptide product precipitated from Et_2O over dry ice (2 x 40 mL) and collected by centrifugation. The crude peptide was then lyophilized and purified by preparative RP-HPLC (0 vol.% CH_3CN + 0.1 vol.% formic acid for 5 min, then 0-50 vol.% CH_3CN + 0.1 vol.% formic acid over 60 min). The linear peptide was then cyclized by general procedure **B**. The cyclic peptide solution was then dried under N_2 flow and purified by semi-preparative RP-HPLC (0 vol.% CH_3CN + 0.1 vol.% TFA acid for 5 min, then 0-50 vol.% CH_3CN + 0.1 vol.% TFA over 80 min) to afford **4** as a white amorphous solid (1.0 mg, 0.8%). $R_{\text{t}214\text{nm}}$: 19.15 min. (1 to 80 vol.% CH_3CN + 0.1 %vol TFA over 30 min). **LR-MS (+ESI)**: $m/z = 1021.95$ $[\text{M}+2\text{H}]^{2+}$, 681.70 $[\text{M}+3\text{H}]^{3+}$.

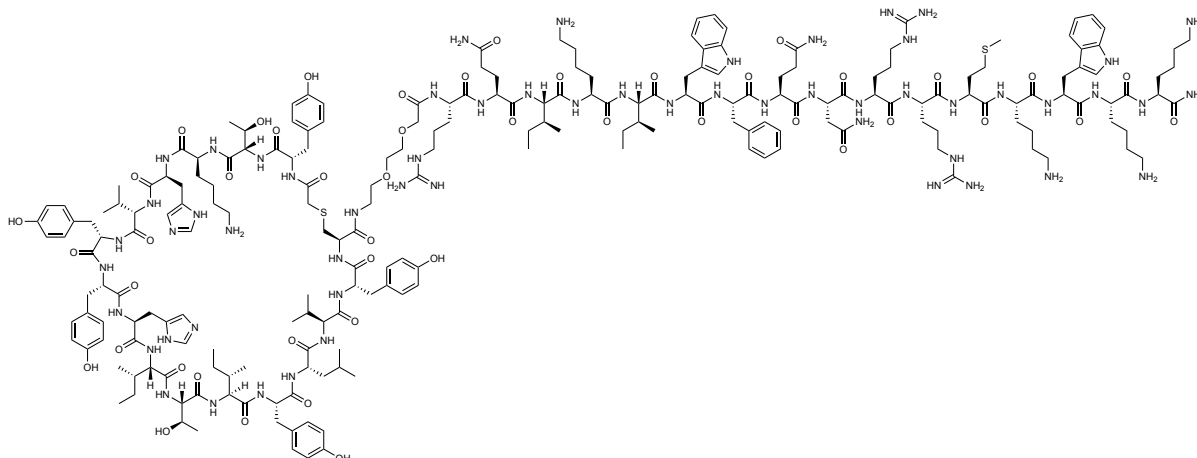
collected by centrifugation. The peptide was then cyclized by general procedure **B** before being concentrated by N₂ flow and purified by preparative RP-HPLC (0 vol.% CH₃CN + 0.1 vol.% TFA for 5 min, then 5–45 vol.% CH₃CN + 0.1 vol.% TFA over 60 min) to afford **8** as a white solid (26.9 mg, 25%). **R_t 214nm**: 16.71 min. (1 to 80 vol.% CH₃CN + 0.1 %vol TFA over 30 min). **LR-MS (+ESI)**: *m/z* = 1033.30 [M+2H]²⁺.

Pen-1.



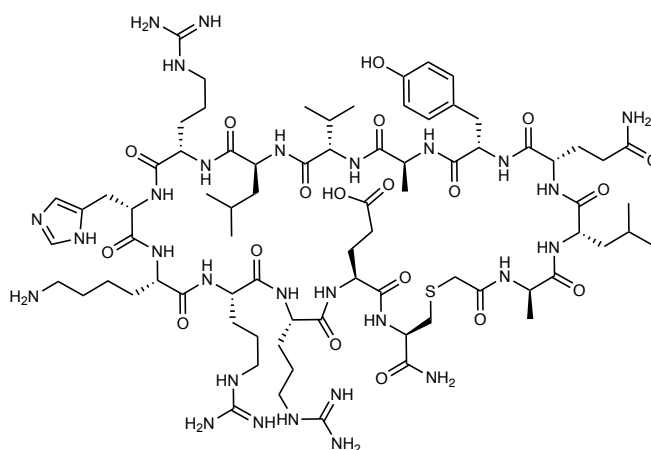
The peptide (25 μmol) was synthesized by general procedure **A** (Oxyma Pure was omitted from the terminal coupling of chloroacetic acid). The peptide was then cleaved from resin by treatment with 87.5:5:5:2.5 v/v/v/v trifluoroacetic acid/triisopropylsilane/H₂O/EDT for 3 h. The cleave solution was collected, dried to ~1 mL under N₂ flow and the peptide product precipitated from Et₂O (2 x 40 mL) and collected by centrifugation. The crude peptide was then purified by preparative RP-HPLC (0 vol.% CH₃CN + 0.1 vol.% TFA for 5 min, then 0–40 vol.% CH₃CN + 0.1 vol.% TFA over 80 min, 35 mL/min, XBridge® C8, 300 Å, 30 x 150 mm). The peptide was then cyclized by general procedure **B** with the addition of TCEP (2.5 mg, 10 μmol) and concentrated under N₂ flow before purification by preparative RP-HPLC (0 vol.% CH₃CN + 0.1 vol.% TFA for 5 min, then 5–30 vol.% CH₃CN + 0.1 vol.% TFA over 80 min, 15 mL/min, XBridge® C18, 300 Å, 19 x 150 mm) to afford **Pen-1** as a white solid (5.1 mg, 3%). **R_t 214nm**: 24.16 min. (1 to 40 vol.% CH₃CN+ 0.1 %vol TFA over 30 min). **LR-MS (+ESI)**: *m/z* = 1368.35 [M+3H]³⁺, 1026.50 [M+4H]⁴⁺, 821.45 [M+5H]⁵⁺, 684.70 [M+6H]⁶⁺, 587.05 [M+7H]⁷⁺, 513.80 [M+8H]⁸⁺.

Pen-6



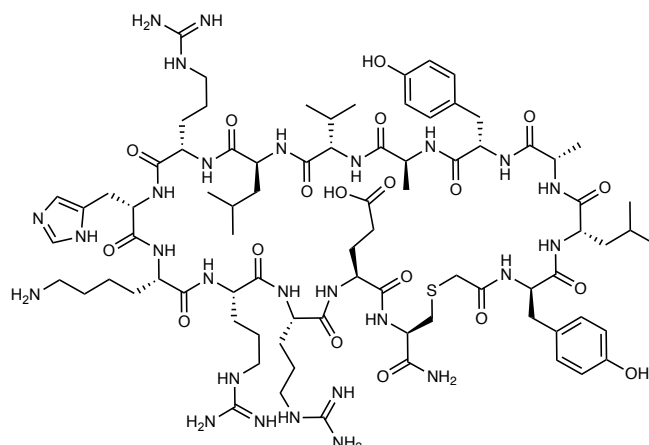
The peptide (12.5 μmol) was synthesized by general procedure **A**. The peptide was then cleaved from resin by treatment with 90:5:5 v/v/v trifluoroacetic acid/triisopropylsilane/ H_2O for 1.5 h, after which the cleave solution was collected, dried to ~ 1 mL under N_2 flow and the peptide product precipitated from Et_2O (30 mL) and collected by centrifugation. The crude peptide was then cyclized by general procedure **C** before being purified by preparative RP-HPLC (0 vol.% CH_3CN + 0.1 vol.% TFA for 5 min, then 0-40 vol.% CH_3CN + 0.1 vol.% TFA over 40 min, 38 mL/min, XBridge[®] C8, 300 \AA , 30 x 150 mm) to afford **Pen-6** as a white amorphous solid (2.31 mg, 3.3%). $R_{t214\text{nm}}$: 20.64 min. (1 to 60 vol.% CH_3CN + 0.1 %vol TFA over 30 min). **LR-MS (+ESI)**: m/z = 1498.0 $[\text{M}+3\text{H}]^{3+}$, 1123.9 $[\text{M}+4\text{H}]^{4+}$, 899.3 $[\text{M}+5\text{H}]^{5+}$, 749.6 $[\text{M}+6\text{H}]^{6+}$, 642.7 $[\text{M}+7\text{H}]^{7+}$.

1-y1a



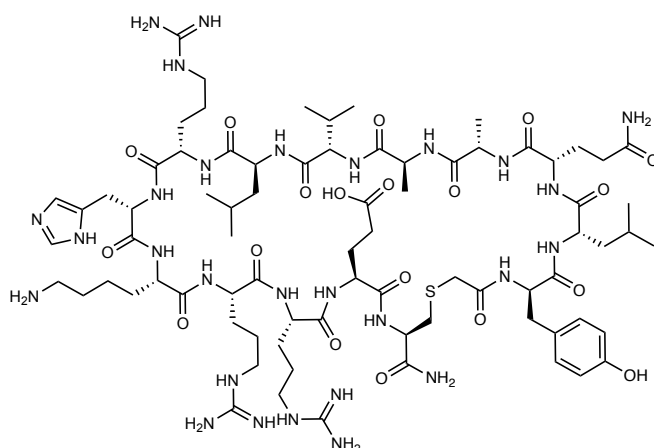
The peptide (50 μmol) was synthesized by general procedure **A** at 50 $^\circ\text{C}$ (Oxyma Pure was omitted from the terminal coupling of chloroacetic acid). The peptide was then cleaved from resin by treatment with 87.5:5:5:2.5 v/v/v/v trifluoroacetic acid/triisopropylsilane/ H_2O /EDT for 2 h. The cleave solution was collected, dried to ~ 1 mL under N_2 flow and the peptide product precipitated from Et_2O (2 x 20 mL) and collected by centrifugation. The crude peptide was then purified by RP-HPLC (100% H_2O with 0.1 vol.% TFA over 5 min then 0 to 30 vol.% CH_3CN in H_2O with 0.1 vol.% TFA over 40 min XBridge[®] C8, 300

1-Q3A



The peptide (50 μmol) was synthesized by general procedure **A** at 50 °C (Oxyma Pure omitted from the terminal coupling of chloroacetic acid). The peptide was then cleaved from resin by treatment with 87.5:5:5:2.5 v/v/v/v trifluoroacetic acid/trisopropylsilane/H₂O/EDT for 2 h. The cleave solution was collected, dried to \sim 1 mL under N₂ flow and the peptide product precipitated from Et₂O (2 x 30 mL) and collected by centrifugation. The crude peptide was then cyclized by general procedure **B** before being concentrated under N₂ flow and purified by preparative RP-HPLC (0 vol.% CH₃CN + 0.1 vol.% formic acid for 5 min, then 0-30 vol.% CH₃CN + 0.1 vol.% formic acid over 80 min, 15 mL/min, XBridge® C18, 300 Å, 19 x 150 mm) to afford **1** as a white solid (5.2 mg, 5%). **R_t 214nm**: 23.41 min, (1 to 40 vol.% CH₃CN+ 0.1 vol.% TFA over 30 min). **LR-MS (+ESI)**: $m/z = 1817.55 [M+H]^+$, 909.35 $[M+2H]^{2+}$, 606.65 $[M+3H]^{3+}$, 455.20 $[M+4H]^{4+}$.

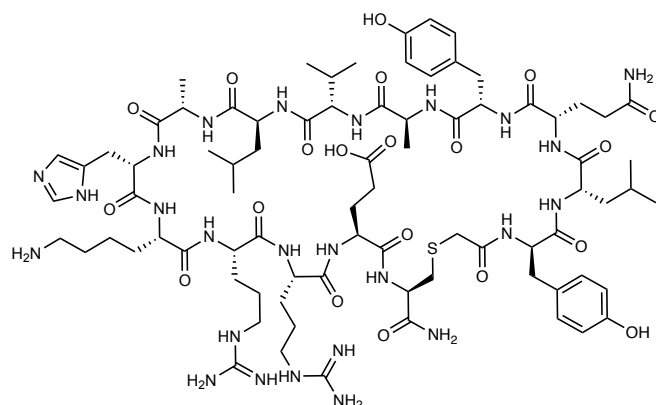
1-Y4A



The peptide (50 μmol) was synthesized by general procedure **A** at 50 °C (Oxyma Pure omitted from the terminal coupling of chloroacetic acid). The peptide was then cleaved from resin by treatment with 87.5:5:5:2.5 v/v/v/v trifluoroacetic acid/trisopropylsilane/H₂O/EDT for 2 h. The cleave solution was collected, dried to \sim 1 mL under N₂ flow and the peptide product precipitated from Et₂O (2 x 20 mL) and collected by centrifugation. The crude peptide was then purified by preparative RP-HPLC (0 vol.%

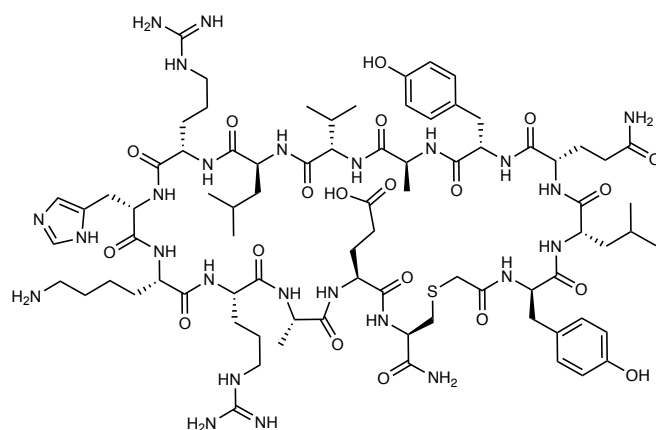
CH₃CN + 0.1 vol.% TFA for 5 min, then 0-40 vol.% CH₃CN + 0.1 vol.% TFA over 60 min). The peptide was then cyclized by general procedure **B** before being lyophilized and purified by preparative RP-HPLC (0 vol.% CH₃CN + 0.1 vol.% TFA for 5 min, then 5-35 vol.% CH₃CN + 0.1 vol.% TFA over 60 min) to afford **1** as a white solid (6.7 mg, 5%). R_{t214nm} : 20.84 min. (1 to 40 vol.% CH₃CN+ 0.1 %vol TFA over 30 min). **LR-MS (+ESI)**: $m/z = 1782.45 [M+H]^+$, 891.80 $[M+2H]^{2+}$.

1-R8A



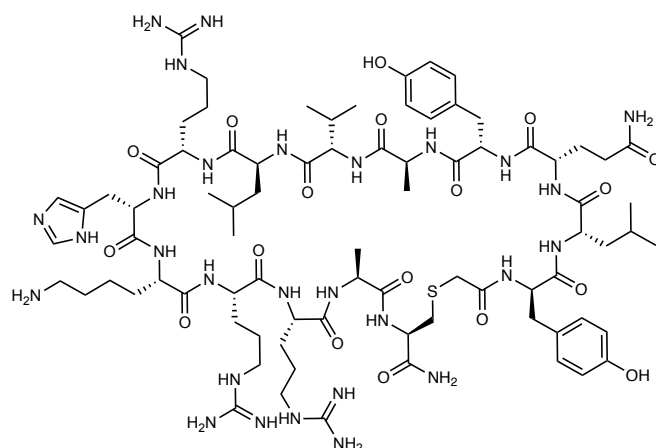
The peptide (50 μ mol) was synthesized by general procedure **A** (Oxyma Pure was omitted from the terminal coupling of chloroacetic acid). The peptide was then cleaved from resin by treatment with 87.5:5:5:2.5 v/v/v/v trifluoroacetic acid/trisopropylsilane/H₂O/EDT for 2 h. The cleave solution was collected, dried to \sim 1 mL under N₂ flow and the peptide product precipitated from Et₂O (2 x 40 mL) and collected by centrifugation. The crude peptide was then purified by preparative RP-HPLC (0 vol.% CH₃CN + 0.1 vol.% TFA for 5 min, then 5-30 vol.% CH₃CN + 0.1 vol.% TFA over 60 min). Fractions containing the linear peptide were combined and lyophilized. The peptide was then cyclized by general procedure **B**. The reaction was concentrated under N₂ flow before being purified by preparative RP-HPLC (0 vol.% CH₃CN + 0.1 vol.% TFA for 5 min, then 8-30 vol.% CH₃CN + 0.1 vol.% TFA over 60 min, 15 mL/min, XBridge® C18, 300 Å, 19 x 150 mm) to afford **1** as a white solid (12.0 mg, 10%). R_{t214nm} : 22.51 min. (1 to 40 vol.% CH₃CN+ 0.1 vol.% TFA over 30 min). **LR-MS (+ESI)**: $m/z = 1789.50 [M+H]^+$, 895.35 $[M+2H]^{2+}$, 597.25 $[M+3H]^{3+}$, 448.25 $[M+4H]^{4+}$.

1-R12A



The peptide (50 μ mol) was synthesized by general procedure **A** (Oxyma Pure was omitted from the terminal coupling of chloroacetic acid). The peptide was then cleaved from resin by treatment with 87.5:5:5:2.5 v/v/v/v trifluoroacetic acid/trisopropylsilane/H₂O/EDT for 2 h. The cleave solution was collected, dried to \sim 1 mL under N₂ flow and the peptide product precipitated from Et₂O (2 x 40 mL) and collected by centrifugation. The crude peptide was then purified by preparative RP-HPLC (0 vol.% CH₃CN + 0.1 vol.% TFA for 5 min, then 5-30 vol.% CH₃CN + 0.1 vol.% TFA over 60 min). Fractions containing the linear peptide were combined and lyophilized. The peptide was then cyclized by general procedure **B**. The reaction was concentrated under N₂ flow before being purified by preparative RP-HPLC (0 vol.% CH₃CN + 0.1 vol.% TFA for 5 min, then 5-25 vol.% CH₃CN + 0.1 vol.% TFA over 60 min) to afford **1** as a white solid (16.3 mg, 14%). $R_{t\ 214nm}$: 22.20 min. (1 to 40 vol.% CH₃CN+ 0.1 %vol TFA over 30 min). **LR-MS (+ESI)**: m/z = 1789.35 [M+H]⁺, 895.25 [M+2H]²⁺, 597.20 [M+3H]³⁺, 448.15 [M+4H]⁴⁺.

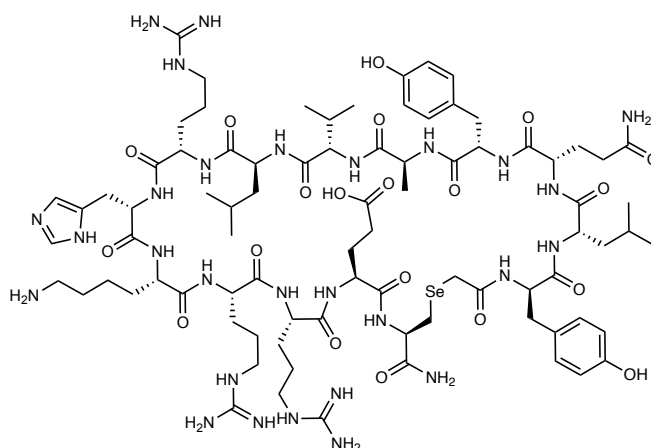
1-E13A



The peptide (50 μ mol) was synthesized by general procedure **A** at 75 $^{\circ}$ C (Oxyma Pure omitted from the terminal coupling of chloroacetic acid). The peptide was then cleaved from resin with 87.5:5:5:2.5 v/v/v/v TFA/trisopropylsilane/H₂O/EDT (5 mL, 2 h). The cleave solution was collected, dried to \sim 1 mL under N₂ flow and the peptide product precipitated from Et₂O over dry ice (2 x 40 mL) and collected by centrifugation. The peptide was then purified by preparative RP-HPLC (0 vol.% CH₃CN + 0.1 vol.% TFA for 5 min, then 5-25 vol.% CH₃CN + 0.1 vol.% TFA over 60 min). Fractions containing the linear peptide

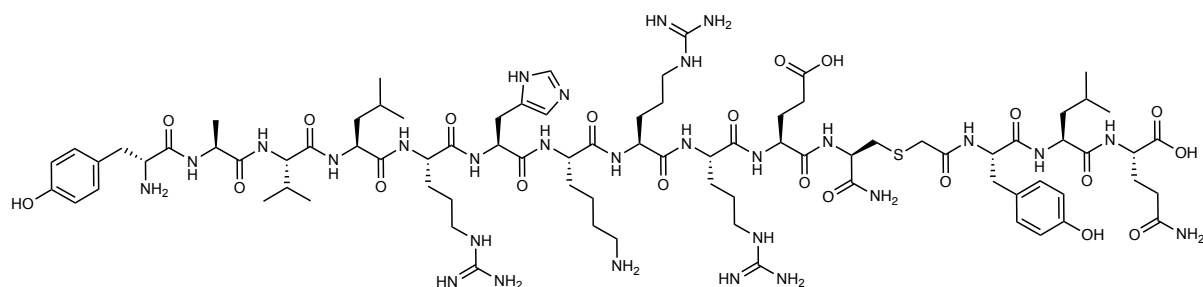
were combined and lyophilized. The lyophilized peptide was then cyclized by general procedure **B** before being dried under N₂ flow and purified by preparative RP-HPLC (0 vol% CH₃CN + 0.1 vol% formic acid for 5 min, then 5-30 vol% CH₃CN + 0.1 vol% formic acid over 60 min, 15 mL/min, XBridge® C18, 300 Å, 19 x 150 mm). The appropriate fractions were combined and lyophilized to afford **1-E13A** as a white amorphous solid (7.0 mg, 6%). **R_t214nm**: 21.88 min. (1 to 40 vol% CH₃CN+ 0.1 %vol TFA over 30 min, 1 mL/min, 40 °C, XBridge® BEH C18, 4.6 x 250 mm, 300 Å, 5 μM). **LR-MS (+ESI)**: m/z = 1816.55 [M+H]⁺, 908.90 [M+2H]²⁺, 606.35 [M+3H]³⁺, 454.95 [M+4H]⁴⁺.

Se-1



Rink Amide resin (40 μmol, 0.488 mmol.g⁻¹) was treated with a solution of 20 vol.% piperidine in DMF (3 mL) for 2 x 5 min, then washed with DMF (5 x 4 mL), CH₂Cl₂ (5 x 4 mL) and DMF (5 x 4 mL) before Fmoc-Sec(PMB)-OH (51 mg, 100 μmol) was loaded in the presence of *N,N'*-diisopropylcarbodiimide (15.6 μL, 100 μmol) and Oxyma Pure (14.2 mg, 100 μmol). The resin was then washed with DMF (5 x 4 mL) CH₂Cl₂ (5 x 4 mL) and DMF (5 x 4 mL) before treatment with 5 vol.% Ac₂O with 10 vol.% *i*-Pr₂NEt in DMF for 5 min followed by washing with DMF (5 x 4 mL), CH₂Cl₂ (5 x 4 mL) and DMF (5 x 4 mL). The remainder of the peptide was then synthesized by general procedure **A** at 50 °C (Oxyma Pure was omitted from the terminal coupling of chloroacetic acid). The peptide was then cleaved from resin by treatment with 87.5:5:5:2.5 v/v/v/v trifluoroacetic acid/triisopropylsilane/H₂O/EDT for 2 h. The cleave solution was collected, dried to ~1 mL under N₂ flow and the peptide product precipitated from Et₂O (2 x 40 mL) and collected by centrifugation. The crude peptide was then purified by preparative RP-HPLC (0 vol.% CH₃CN + 0.1 vol.% TFA for 5 min, then 0-30 vol.% CH₃CN + 0.1 vol.% TFA over 60 min). Fractions containing the linear peptide were combined and lyophilized. The peptide was then cyclized by general procedure **B** in the presence of TCEP (10 mM). The reaction was lyophilized before being purified by RP-HPLC (0 vol.% CH₃CN + 0.1 vol.% TFA for 5 min, then 0-40 vol.% CH₃CN + 0.1 vol.% TFA over 60 min) to afford **1** as a white solid (6.2 mg, 6%). **R_t214nm**: 22.23 min. (1 to 40 vol.% CH₃CN+ 0.1 vol.% TFA over 30 min). **LR-MS (+ESI)**: m/z = 961.40 [M+2H]²⁺, 641.25 [M+3H]³⁺, 481.20 [M+4H]⁴⁺.

Authentic standard of cleaved 1



The peptide was synthesized in two fragments:

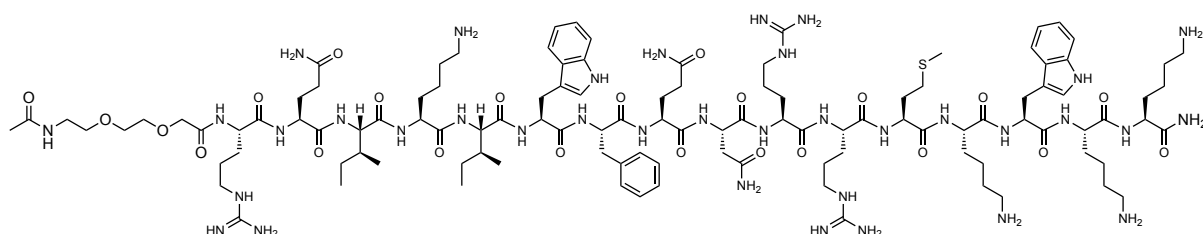
Fragment 1: The sequence YAVLRHKRREC was synthesized by general procedure **A** at 50 °C. The resin-bound peptide was washed with DMF (3 x 4 mL), DCM (3 x 4 mL) and DMF (3 x 4 mL), prior to Fmoc-deprotection of the N-terminus with 20 vol.% piperidine in DMF (4 mL, 2 x 10 min, rt.). The resin-bound peptide was washed with DMF (3 x 4 mL) and DCM (5 x 4 mL), then cleaved from bead with TFA/TIS/H₂O/EDT (87.5/5/5/2.5 vol.%, 5 mL, 2 h, rt). The cleave solution was collected, dried to ~1 mL under N₂ flow and the peptide product precipitated from Et₂O over dry ice (2 x 40 mL) and collected by centrifugation. The peptide was then purified by preparative RP-HPLC (0 vol.% CH₃CN + 0.1 vol.% TFA for 5 min, then 0-40 vol.% CH₃CN + 0.1 vol.% TFA over 60 min). Fractions containing the linear peptide were combined and lyophilized to afford **Fragment 1** as a white solid (45.0 mg, 40%).

Fragment 2: 2-chlorotriylchloride resin (Mimotopes, 50 μmol, 1.12 mmol g⁻¹) was loaded with Fmoc-Gln(Trt)-OH (8 equiv.) and *i*-Pr₂NEt (8 equiv) for 16 h before being drained and treated with 17:2:1 v/v/v CH₂Cl₂:MeOH:*i*-Pr₂NEt (5 mL) for 30 mins. The resin was then washed with DMF (4 x 5 mL), CH₂Cl₂ (4 x 5 mL) and DMF (4 x 5 mL). The resin was then treated with a solution of piperidine (20 vol.%) in DMF (2 x 5 mL, 5 min each). The resin was then washed with DMF (4 x 5 mL), CH₂Cl₂ (4 x 5 mL) and DMF (4 x 5 mL). The sequence IAc-yLQ-OH was then elongated by coupling Fmoc-amino acid (200 μmol), *N*-*N*'-diisopropylcarbodiimide (31.2 μL, 200 μmol) and Oxyma Pure (28.4 mg) in DMF (4 mL, 2 h, rt.). Following each coupling, the resin-bound peptide treated with 10 vol.% Ac₂O/pyridine (2 x 5 min, rt.), washed, and then treated with 20 vol.% piperidine in DMF (2 x 10 min). Iodoacetic acid (37 mg, 200 μmol) was then coupled *N*-*N*'-diisopropylcarbodiimide (31.2 μL, 200 μmol) and Oxyma Pure (28.4 mg) in DMF (4 mL, 2 h, rt.). The resin-bound peptide was washed with DMF (3 x 4 mL) and DCM (5 x 4 mL), before resin cleavage with 90:5:5 v/v/v TFA/TIS/H₂O (5 mL, 2 h, rt). The cleave solution was collected, dried to ~1 mL under N₂ flow and the peptide product precipitated from Et₂O over dry ice (2 x 20 mL) and collected by centrifugation. The crude peptide pellet was then air dried and used without further purification.

Authentic standard of cleaved 1: **Fragment 1** (1.0 eq., 11.4 mg, 5.39 μmol) and **Fragment 2** (1.2 eq., 3.9 mg, 6.61 μmol) were dissolved in 1:1 v/v CH₃CN/H₂O (1 mL) and *i*-Pr₂NEt (5 vol.%) added. The reaction was stirred for 1 h at rt. The product was then isolated by preparative RP-HPLC (0 vol.% CH₃CN + 0.1 vol.% TFA for 5 min, then 0-40 vol.% CH₃CN + 0.1 vol.% TFA over 80 min, 15 mL/min,

XBridge® C18, 300 Å, 19 x 150 mm). The appropriate fractions were combined and lyophilized to afford the product as a white solid (4.65 mg, 33%). R_{t214nm} : 14.61 min. (1 to 50 vol.% CH₃CN/H₂O + 0.1 vol.% formic acid over 30 min, 60 °C) **LR-MS (+ESI)**: m/z = 946.90 [M+2H]²⁺, 631.60 [M+3H]³⁺, 473.95 [M+4H]⁴⁺.

Ac-PEG₂-Penetratin



The peptide (25 μmol) was synthesized by general procedure **A** at 75 °C. The peptide was then cleaved from resin with 90:5:5 v/v/v TFA/triisopropylsilane/H₂O (5 mL, 2 h). The cleave solution was collected, dried to ~1 mL under N₂ flow and the peptide product precipitated from Et₂O over dry ice (2 x 40 mL) and collected by centrifugation. The peptide was then purified by preparative RP-HPLC (0 vol% CH₃CN + 0.1 vol% TFA for 5 min, then 0-40 vol% CH₃CN + 0.1 vol% TFA over 40 min). The appropriate fractions were combined and lyophilized to afford **Ac-PEG₂-Penetratin** as a white amorphous solid (18.2 mg, 45%). R_{t214nm} : 18.97 min. (1 to 50 vol% CH₃CN+ 0.1 %vol TFA over 30 min, 1 mL/min, 40 °C, XBridge® BEH C18, 4.6 x 250 mm, 300 Å, 5 μM). **LR-MS (+ESI)**: m/z = 1217.4 [M+2H]²⁺, 811.85 [M+3H]³⁺, 609.0 [M+4H]⁴⁺, 487.35 [M+5H]⁵⁺, 406.25 [M+6H]⁶⁺.

Supplementary Figures

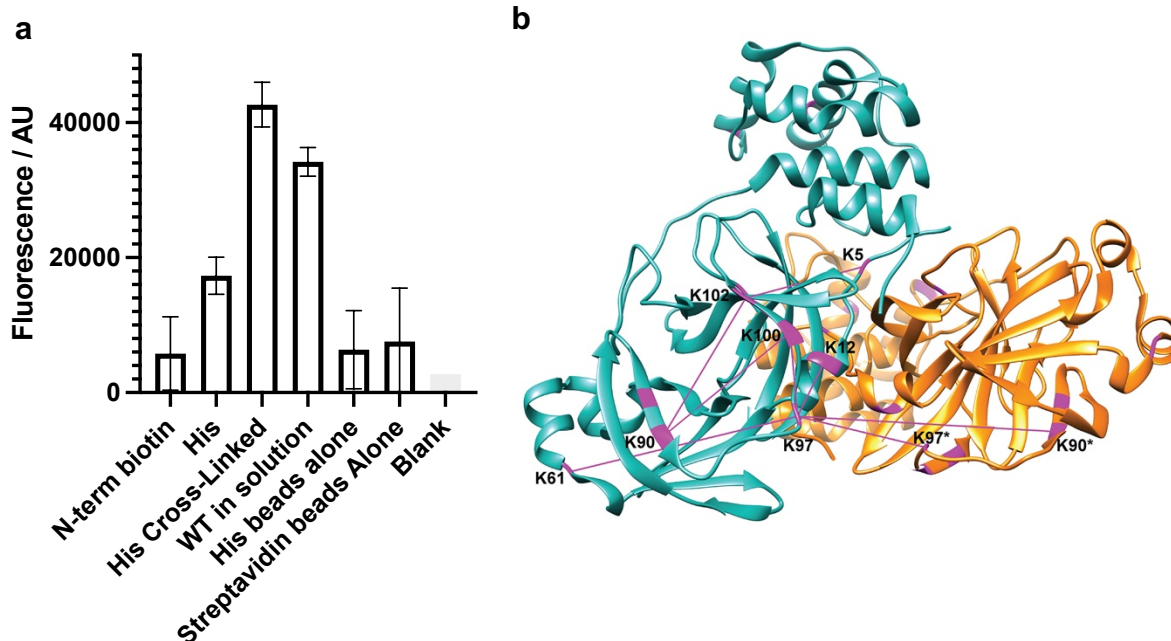
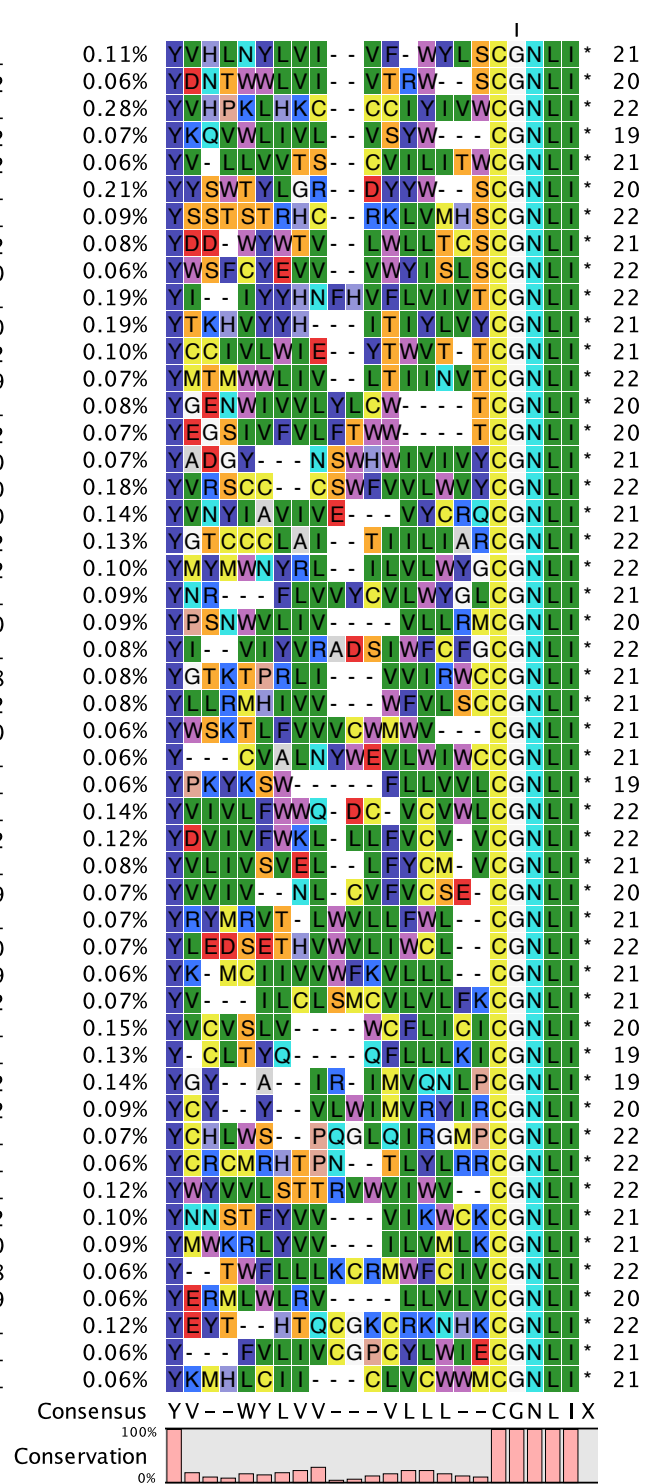
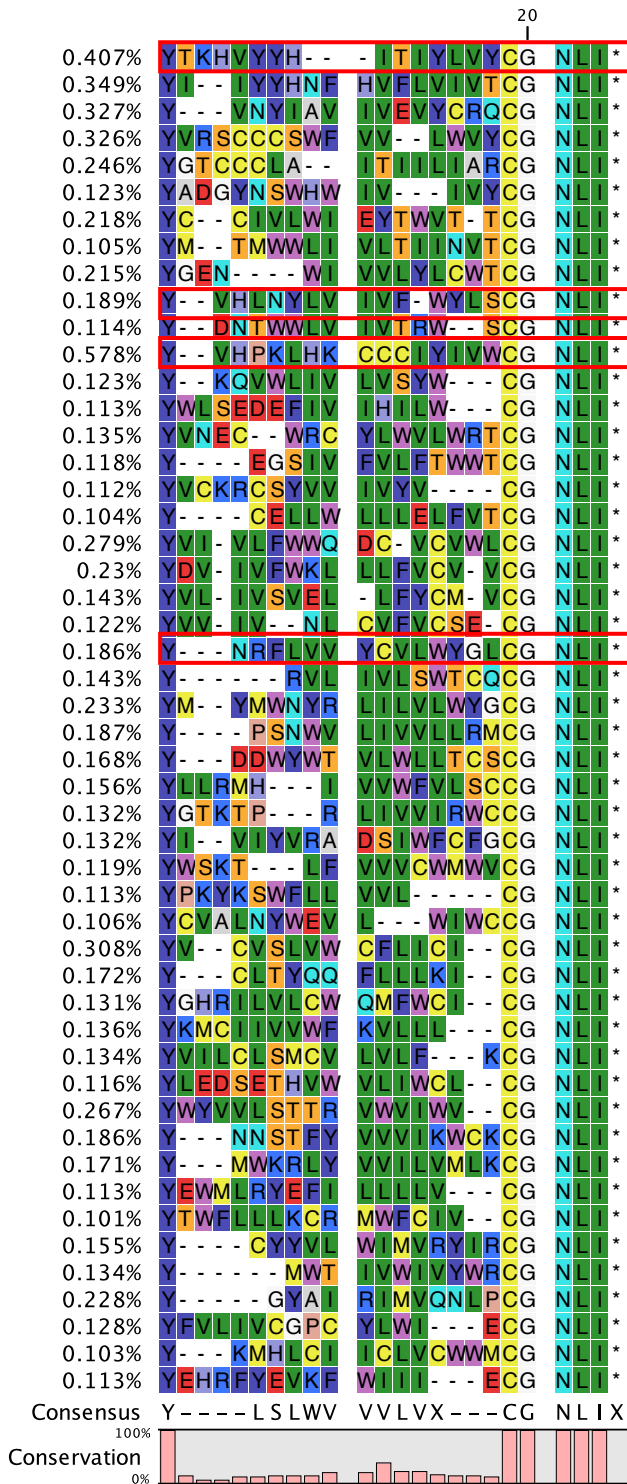


Fig. S1. a Catalytic activity of different SARS-CoV-2 M^{pro} constructs including: N-terminally biotinylated M^{pro} immobilized to Streptavidin Dynabeads™ (N-term biotin), C-terminally His-tagged M^{pro} immobilized onto Co²⁺-NTA Dynabeads™ (His), DSG cross-linked and C-terminally His-tagged M^{pro} immobilized onto Co²⁺-NTA Dynabeads™ (His Cross-Linked), wild-type M^{pro} in solution (WT in solution) All experiments were performed with 25 nM M^{pro} and 20 μM FRET substrate (DABCYL)-KTS AVLQ↓SGFRKM-E(EDANS)-NH₂ (Mimotopes, Australia) with incubation at 37 °C for 15 min. **b** Identification of DSG crosslinking sites in SARS-CoV-2 M^{pro} was performed after trypsin digestion by mass spectrometry using the Byonic search engine (Protein Metrics). Crosslinks <30 Å are displayed on the dimeric structure of SARS-CoV-2 M^{pro} (PDB: 6Y2E) as purple lines connecting lysine residues (all shown in purple on ribbon) using UCSF Chimera.³⁴ All intramolecular crosslinks are shown only on one monomer (cyan) with residue numbers indicated. Intermolecular crosslinks are shown with linked lysines in the second monomer (orange) indicated by an asterisk.

**N-chloroacetyl-L-tyrosine initiated
Library 1 - Round 9**
Total number of reads: 177428

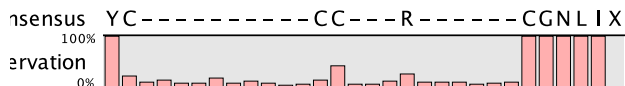
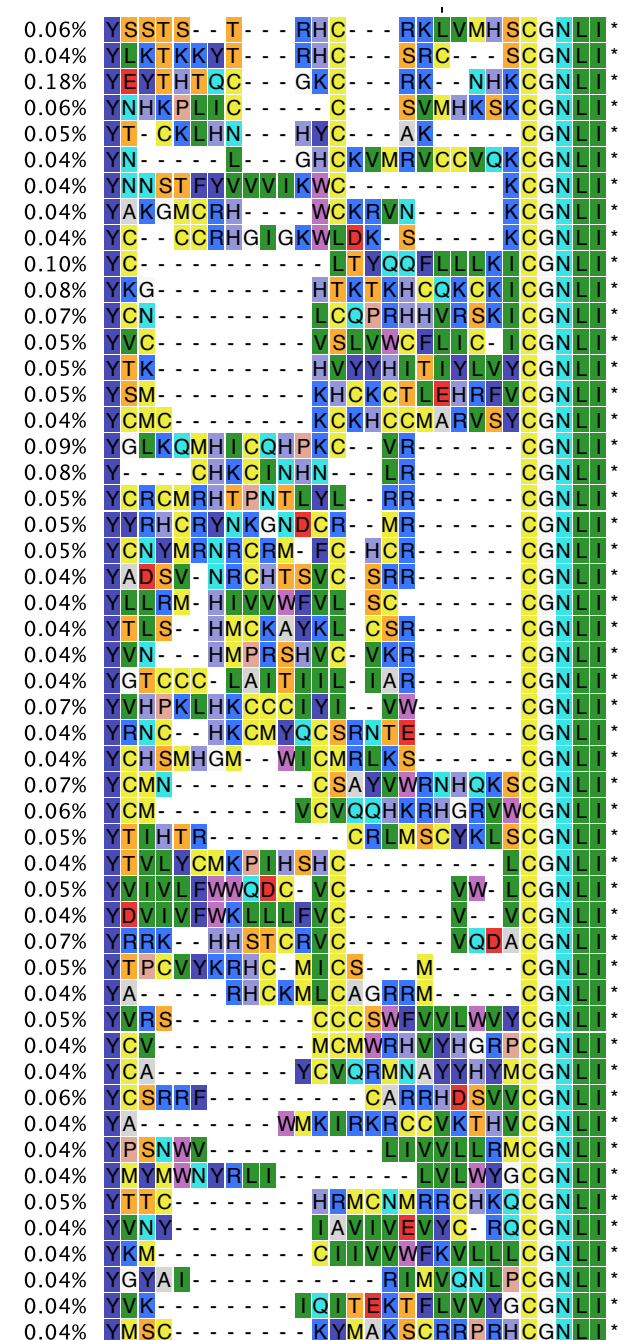
**N-chloroacetyl-L-tyrosine initiated
Library 1 - Round 8**
Total number of reads: 250591



N-chloroacetyl-L-tyrosine initiated

Library 1 – Round 7

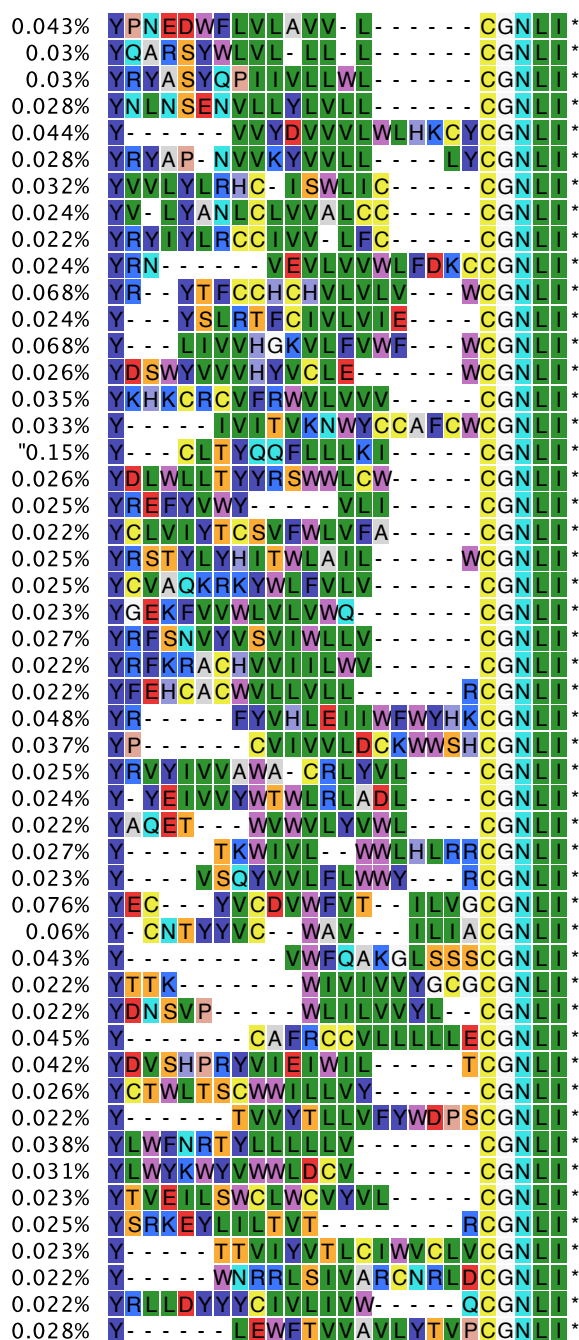
Total number of reads: 180386



N-chloroacetyl-L-tyrosine initiated

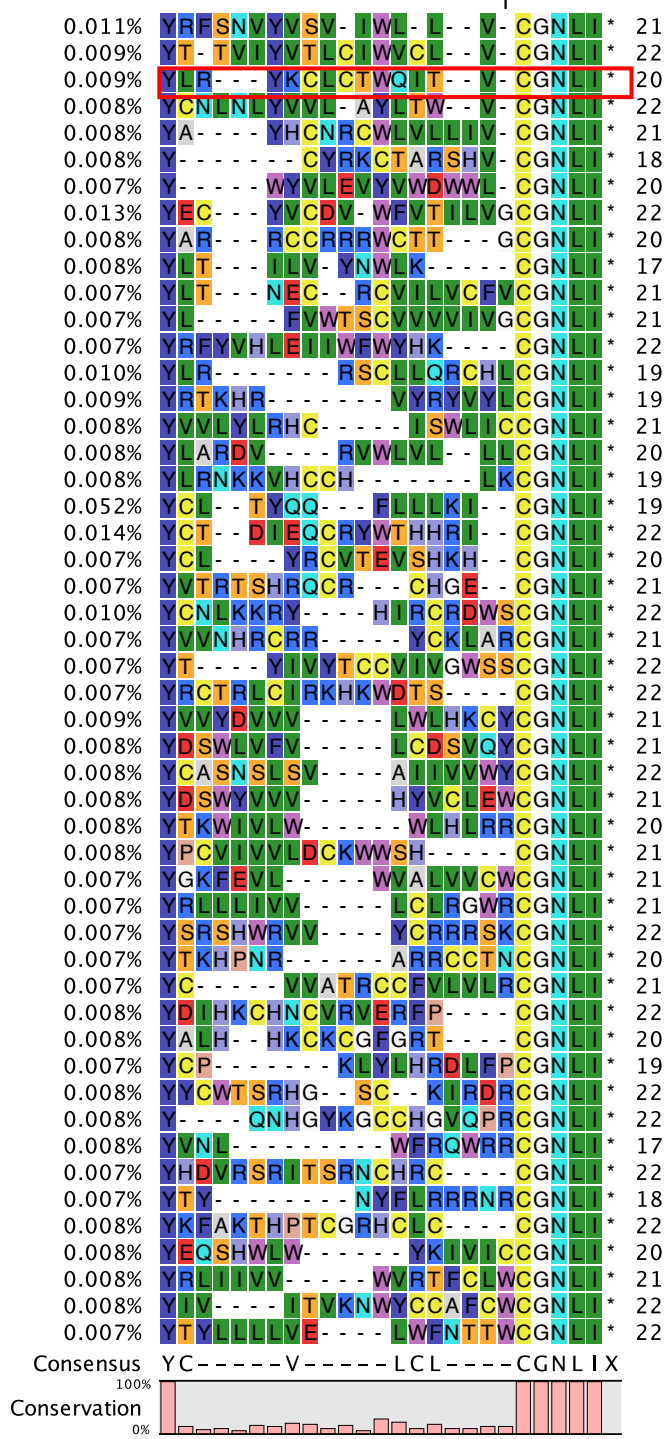
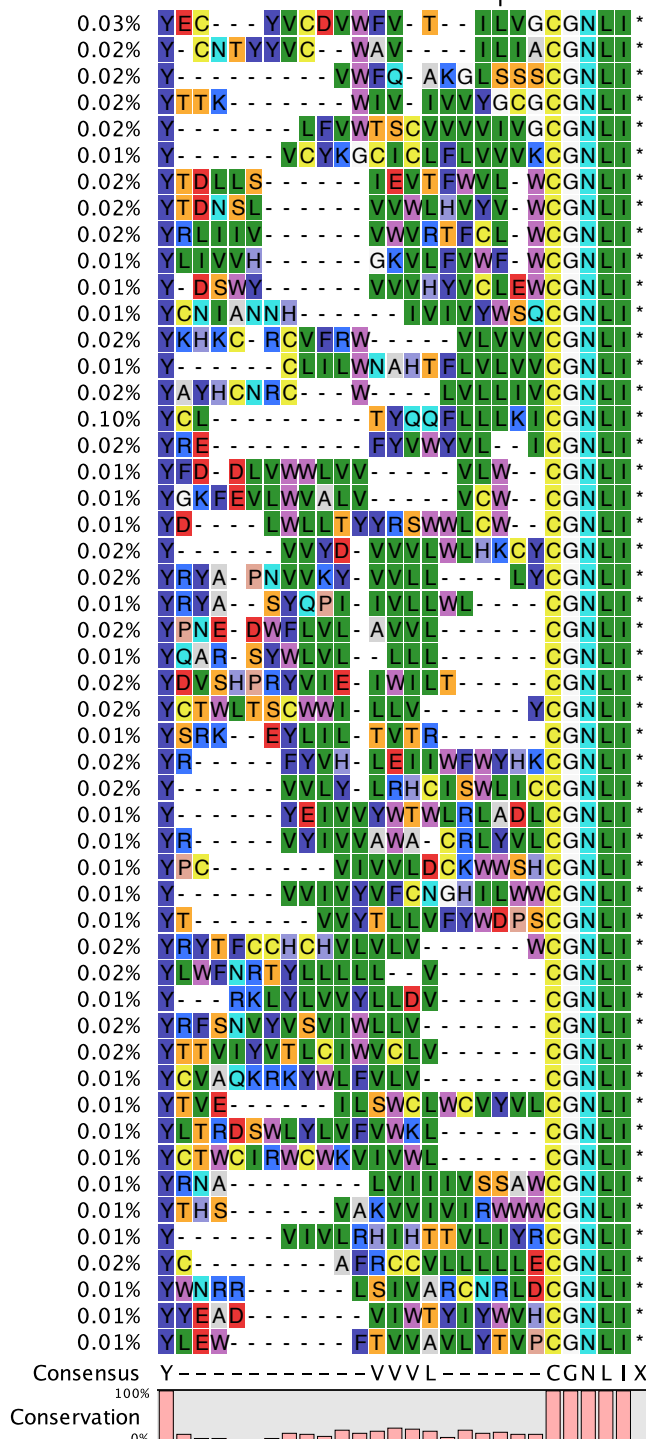
Library 2 – Round 9

Total number of reads: 165529



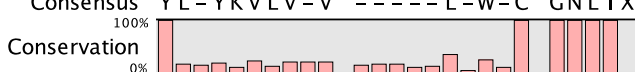
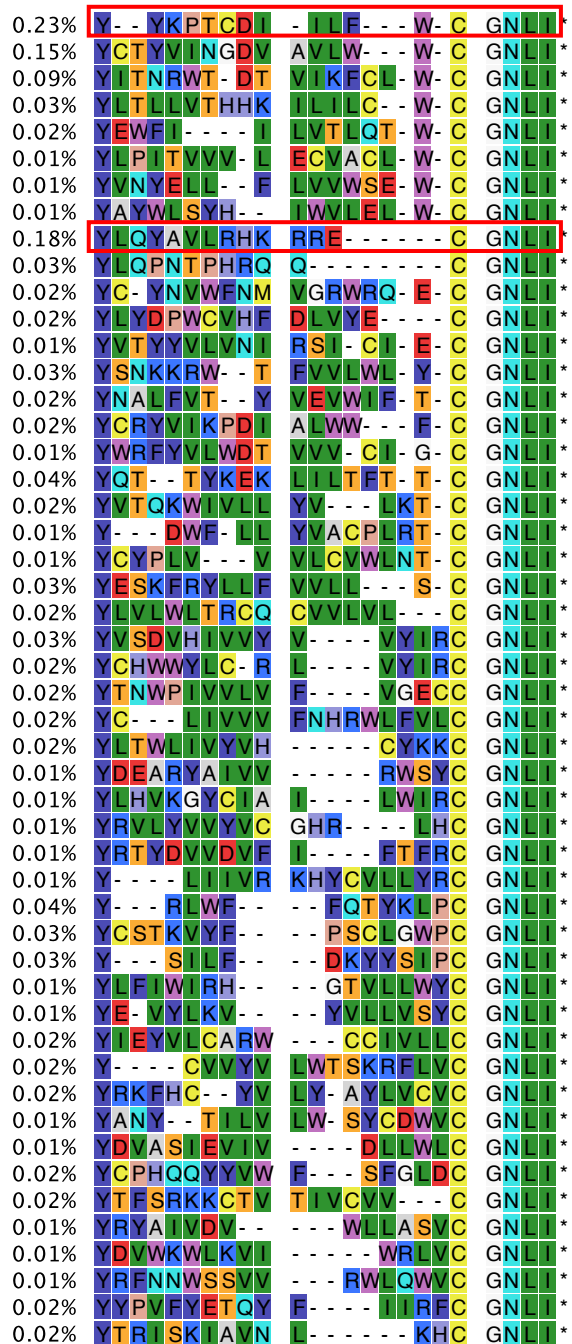
**N-chloroacetyl-L-tyrosine initiated
Library 2 – Round 8**
Total number of reads: 185590

**N-chloroacetyl-L-tyrosine initiated
Library 2 - Round 7**
Total number of reads: 131603



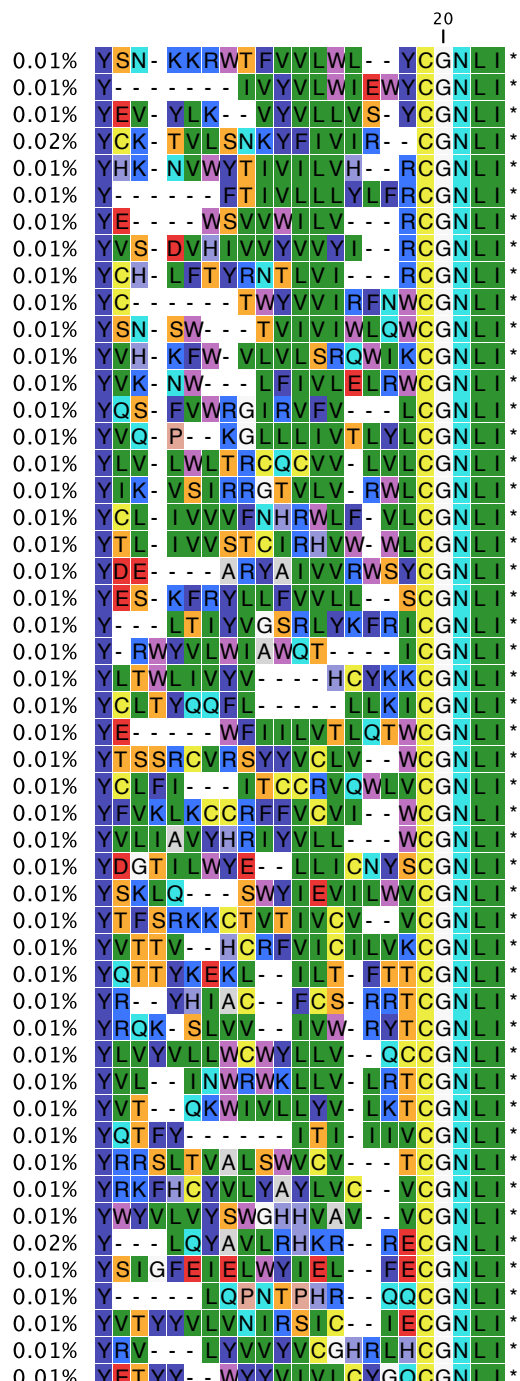
**N-chloroacetyl-D-tyrosine initiated
Round 9**

Total number of reads: 161193



**N-chloroacetyl-D-tyrosine initiated
Round 8**

Total number of reads: 207939



***N*-chloroacetyl- D-tyrosine initiated
Round 7**

Total number of reads: 226931

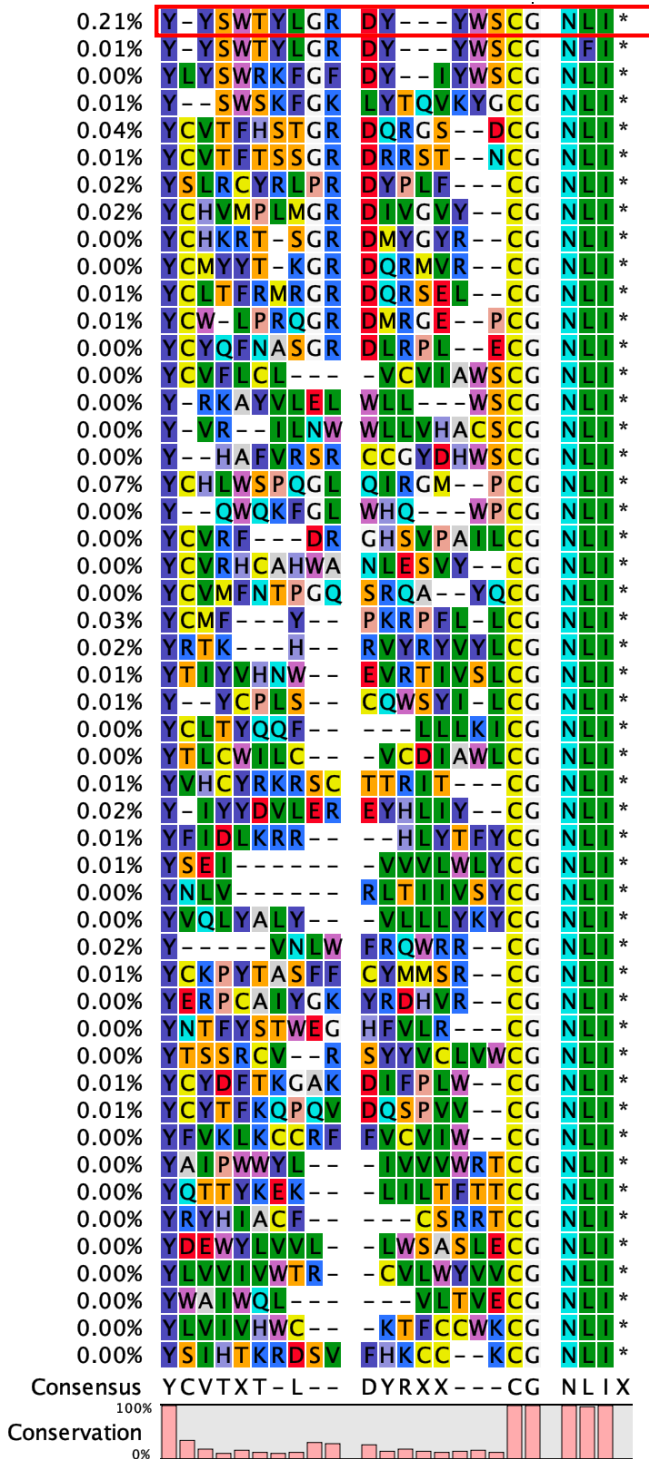


Fig. S2. Top 50 sequences for each selection based on percentage enrichment in the final library after rounds 7 – 9, along with the corresponding total number of peptides captured (reads). Peptides selected for synthesis and evaluation are highlighted with red boxes. NB: Peptides were selected based on relative abundance or the presence of canonical LQ or WQ M^{Pro} recognition motifs.

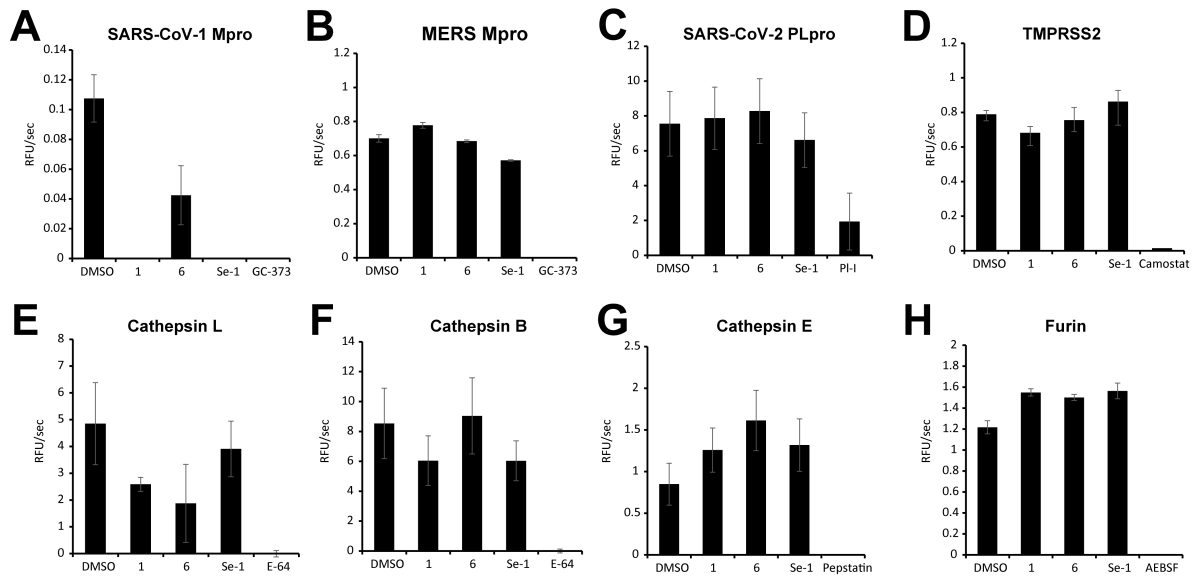


Fig. S3: Evaluating inhibition of key viral and host proteases. DMSO stocks of Peptide **1**, **6** and **Se-1** (10 mM) were diluted to 20 μ M in appropriate assay buffer and incubated with the following enzymes for 15 minutes, 100 nM SARS-CoV-1 Mpro, 100 mM MERS Mpro, 100 nM SARS-CoV-2 PLpro, 6 nM TMPRSS2, 1 nM Cathepsin L, 1 nM Cathepsin B, 2 nM Cathepsin E and 3.75 nM of Furin. The reaction was initiated by addition of substrate.

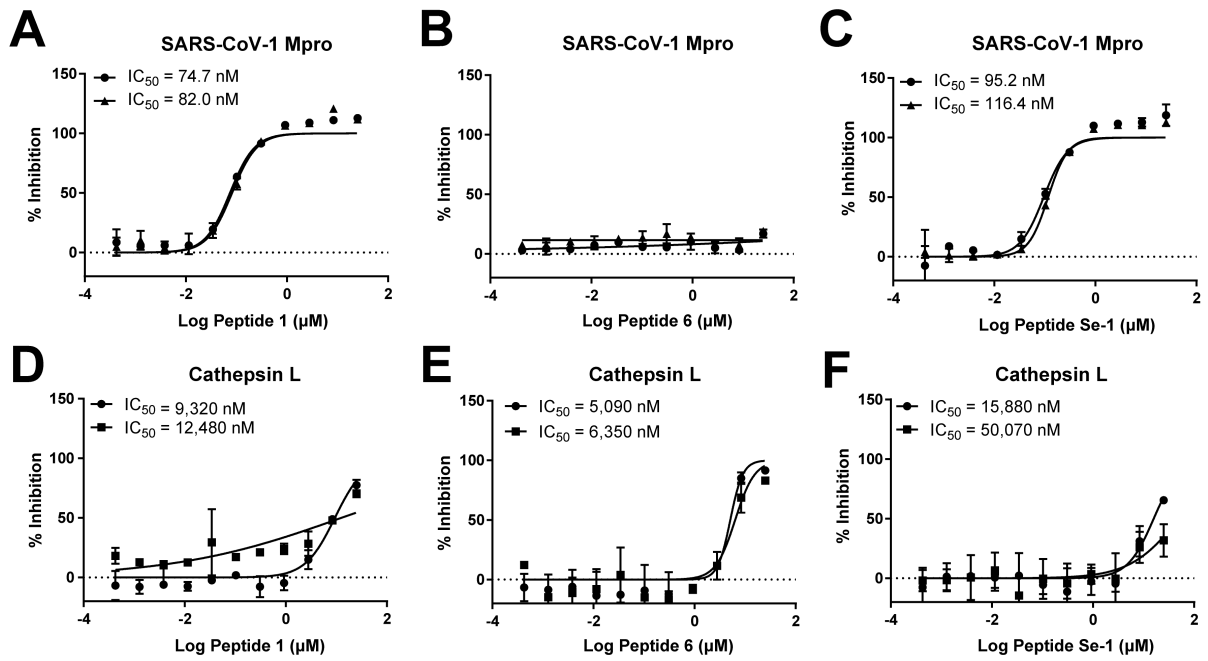
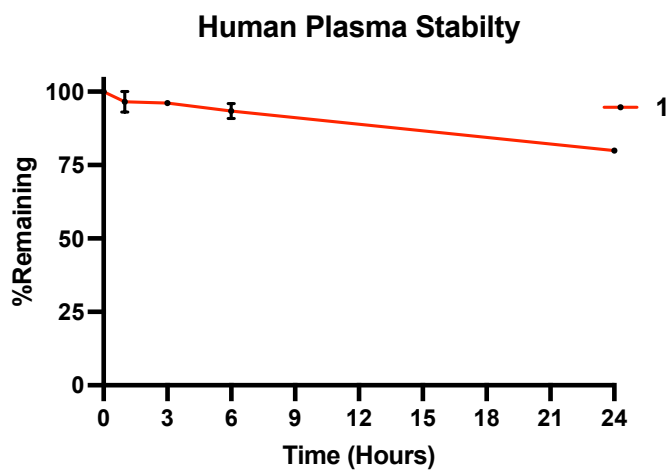
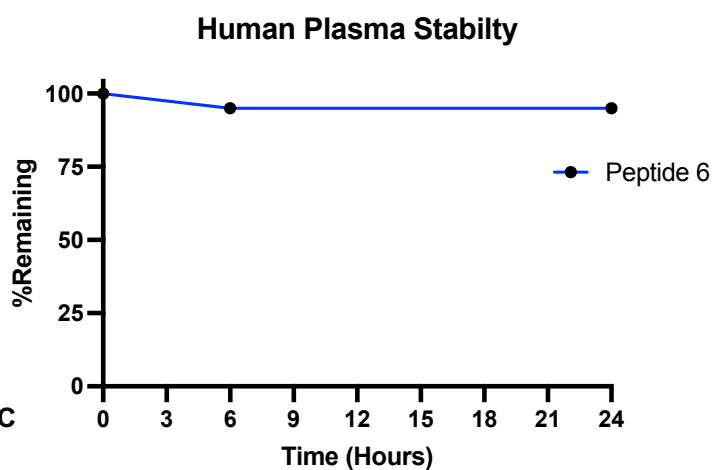


Fig. S4: Calculation of IC₅₀ for SARS-CoV-1 and Cathepsin L. Peptide 1, 6 and Se-1 were evaluated for inhibition in a dose response study with SARS-CoV-1 and Cathepsin L. Two independent assays were performed, both with triplicate wells. Activity in each well was normalized to the DMSO control (0% Inhibition).

A



B



C

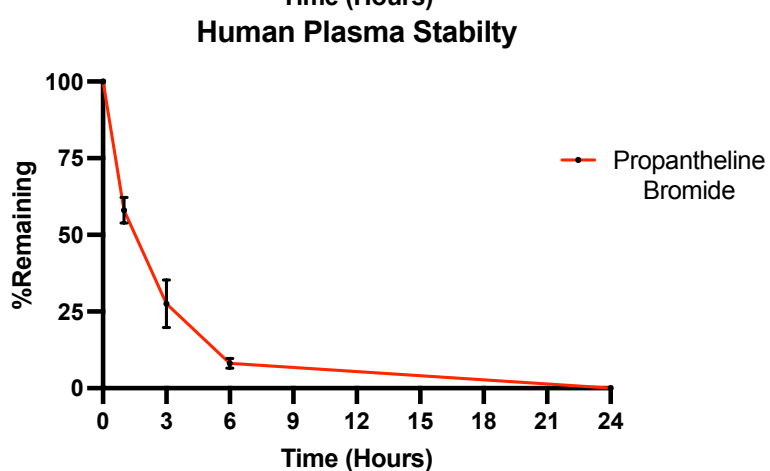
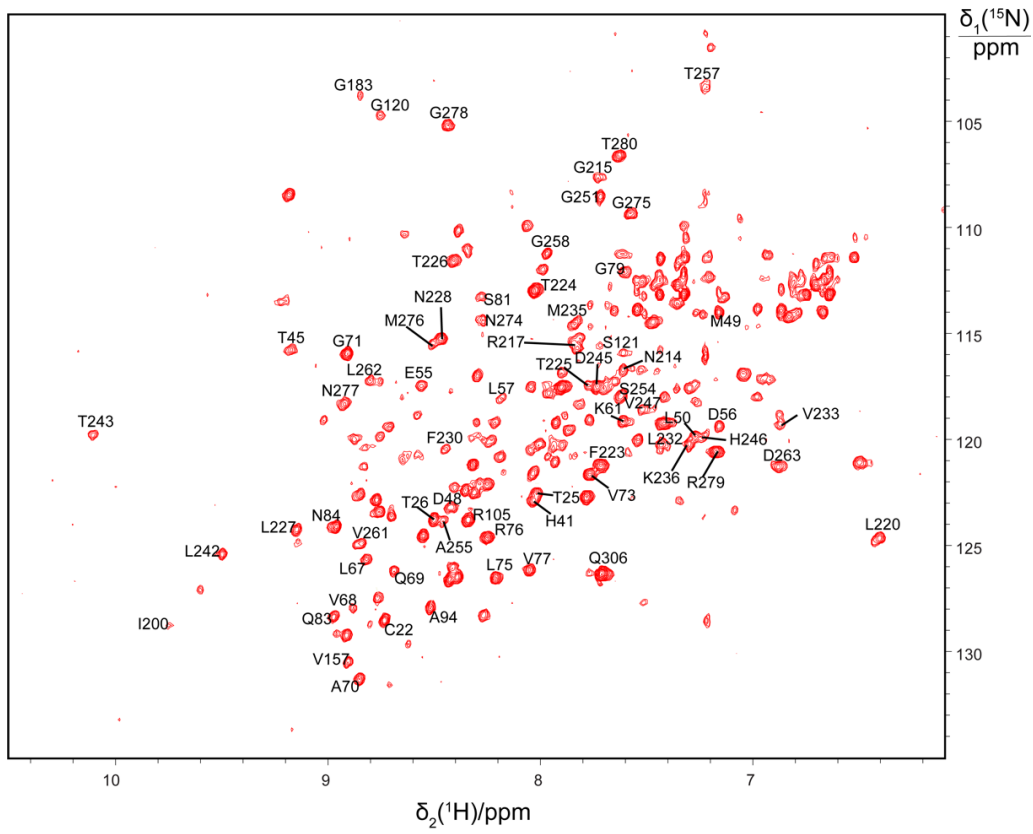
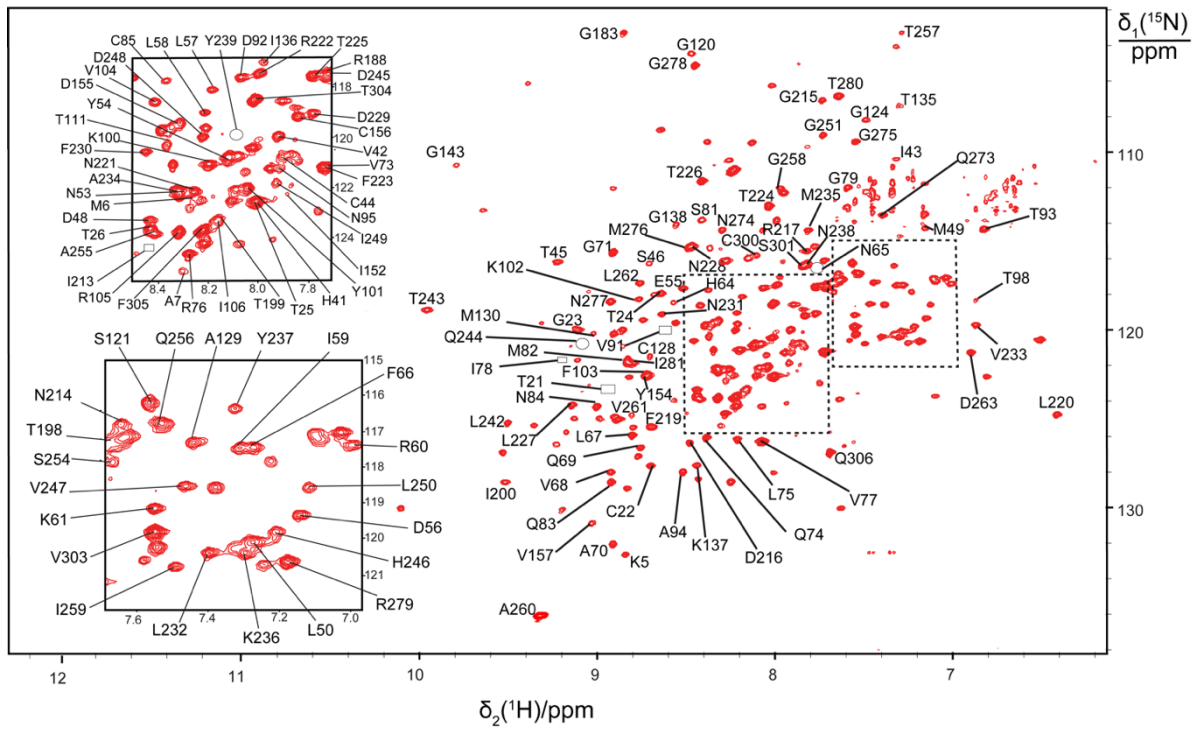


Fig. S5. Stability of 1 and 6 in human plasma as determined by UHPLC-MS. A Plasma stability of 1 over 24 h. **B** Plasma stability of 6 over 24 h. **C** Plasma stability of the positive control, proprantheline bromide, over 24 h.

a**b**

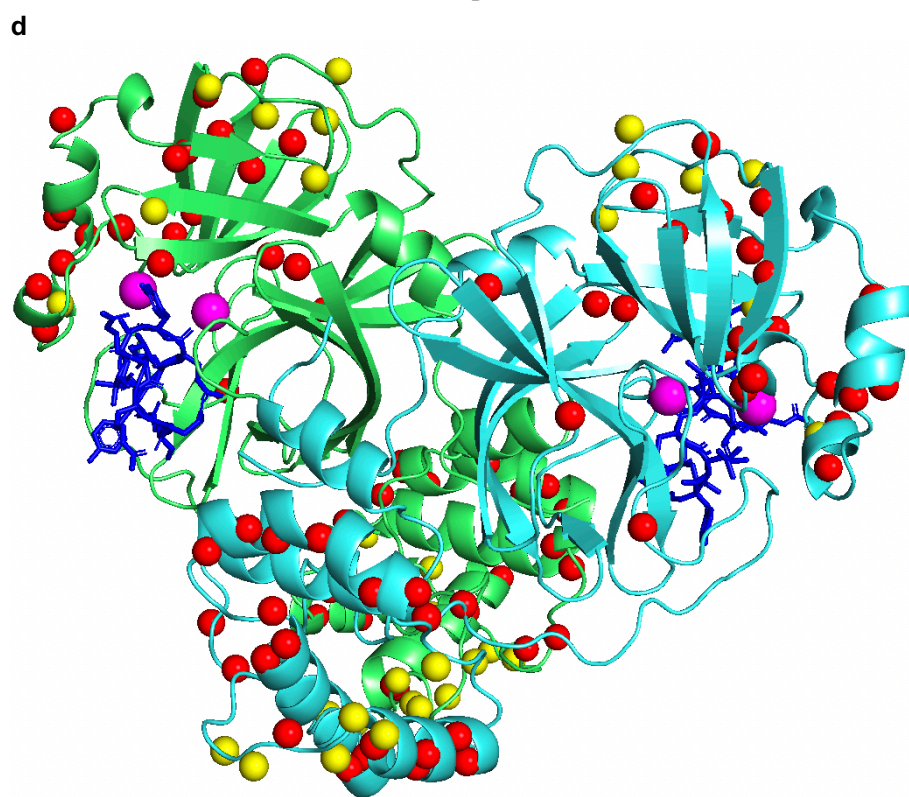
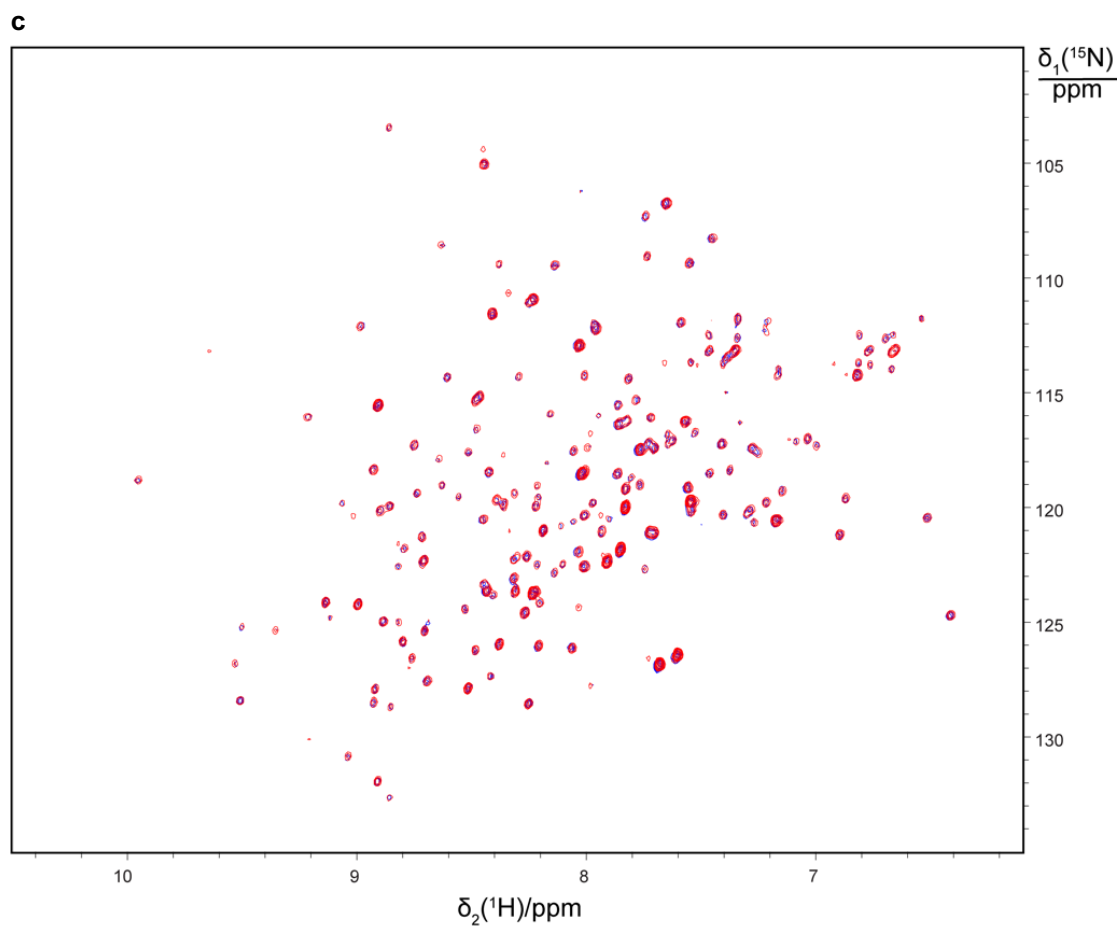


Fig. S6. a Projection onto the ^{15}N - ^1H plane of 3D TROSY-HNCO spectra recorded of wild-type M^{Pro} . Assignments are shown for peaks that could be assigned by comparison with the assignments

made in the monomeric M^{pro} R298A mutant. **b** [¹⁵N,¹H]-TROSY spectrum of a 0.3 mM solution of uniformly ¹⁵N-labelled M^{pro} R298A recorded at 25 °C ($t_{1\max} = 82$ ms, $t_{2\max} = 142$ ms, total recording time 2.2 h). The peaks are labelled with the residue type and amino acid sequence number of the assignments made. Some cross-peaks were observed and assigned in 3D NMR spectra or in [¹⁵N,¹H]-HSQC spectra of selectively ¹⁵N-labelled samples, but not observed in the TROSY spectrum shown here. Their positions are marked by symbols identifying the location and the spectrum where they were observed: ○ peak found in TROSY-HNCA or TROSY-HNCO spectrum; □ peak found in [¹⁵N,¹H]-HSQC spectrum of selectively ¹⁵N-labelled samples. **c** Projection onto the ¹⁵N-¹H plane of 3D TROSY-HNCO spectra recorded of 0.3 mM solutions of ¹⁵N/¹³C/²H-labelled M^{pro} R298A. Two projections are superimposed, recorded of samples without (blue contours) and with equimolar inhibitor (red contours). The spectrum recorded in the presence of inhibitor superimposes almost perfectly the spectrum without inhibitor, indicating that the inhibitor fails to bind and cause any spectral changes. **d** Crystal structure (PDB ID: 7RNW) of the dimer of wild-type M^{pro} showing the location of backbone amide protons which changed in the NMR spectra upon titration with the inhibitor. Red spheres indicate amides with significant changes in chemical shift or intensity in the presence of inhibitor. Yellow spheres indicate amides remaining unchanged in the presence of inhibitor. The locations of the active site residues His41 and Cys145 are highlighted in magenta and the inhibitor **Se-1** in blue.

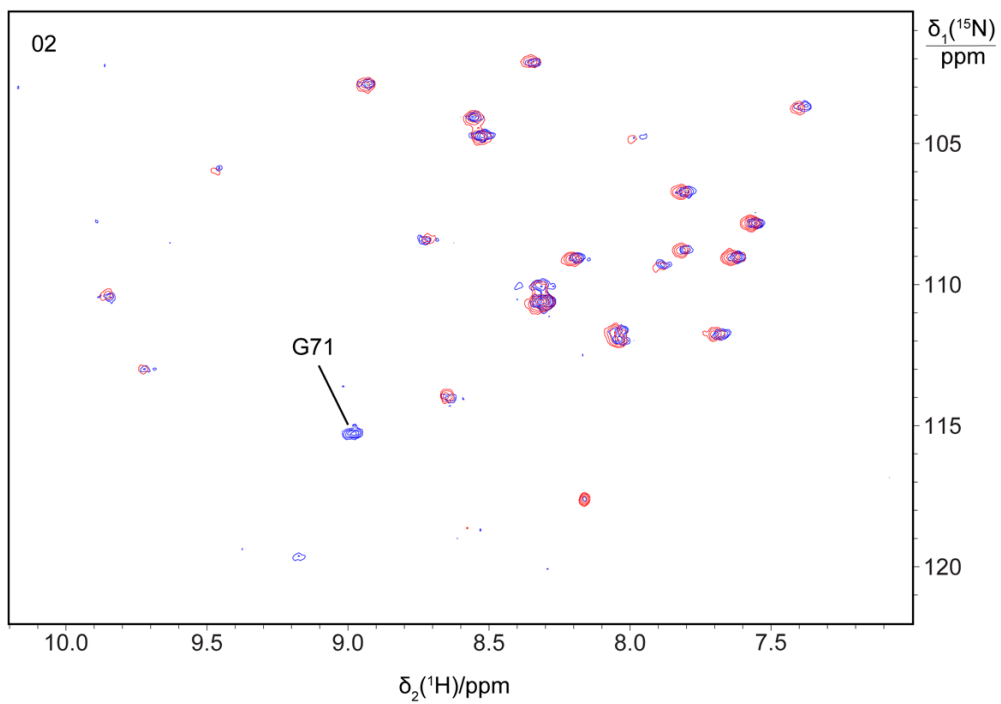
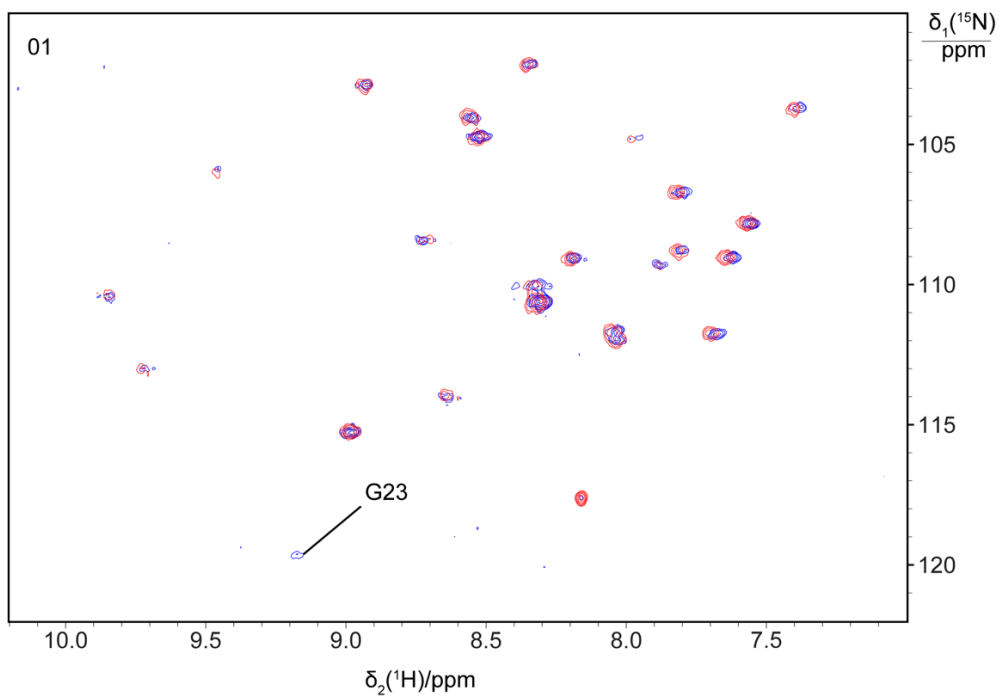
Table S1. Number of specific resonance assignments made in [¹⁵N, ¹H]-HSQC spectra by site-directed mutagenesis.

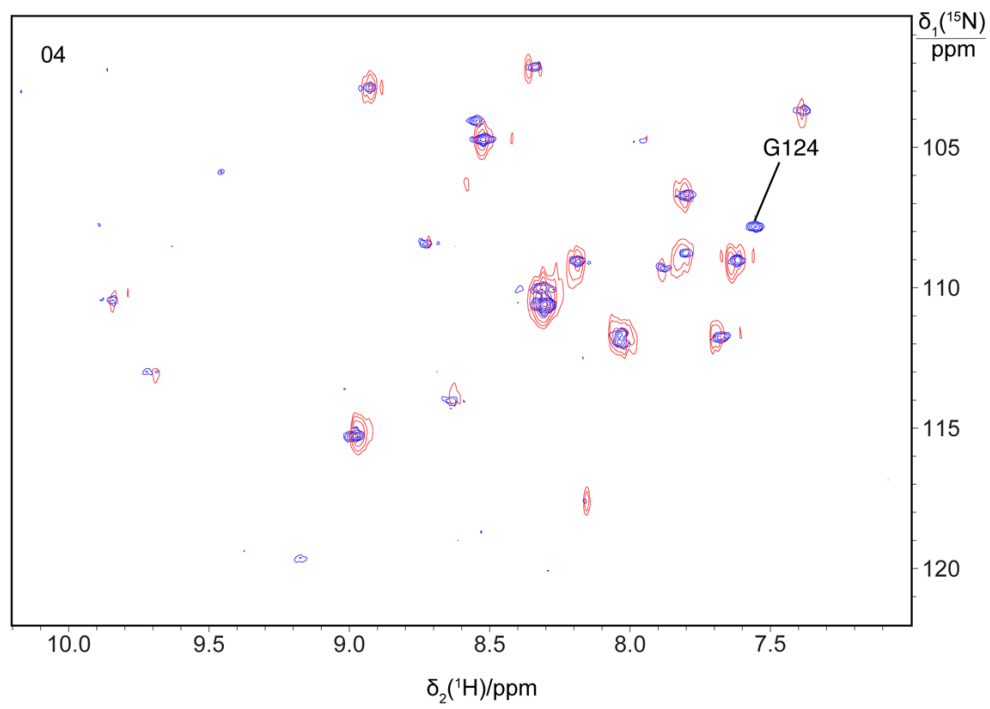
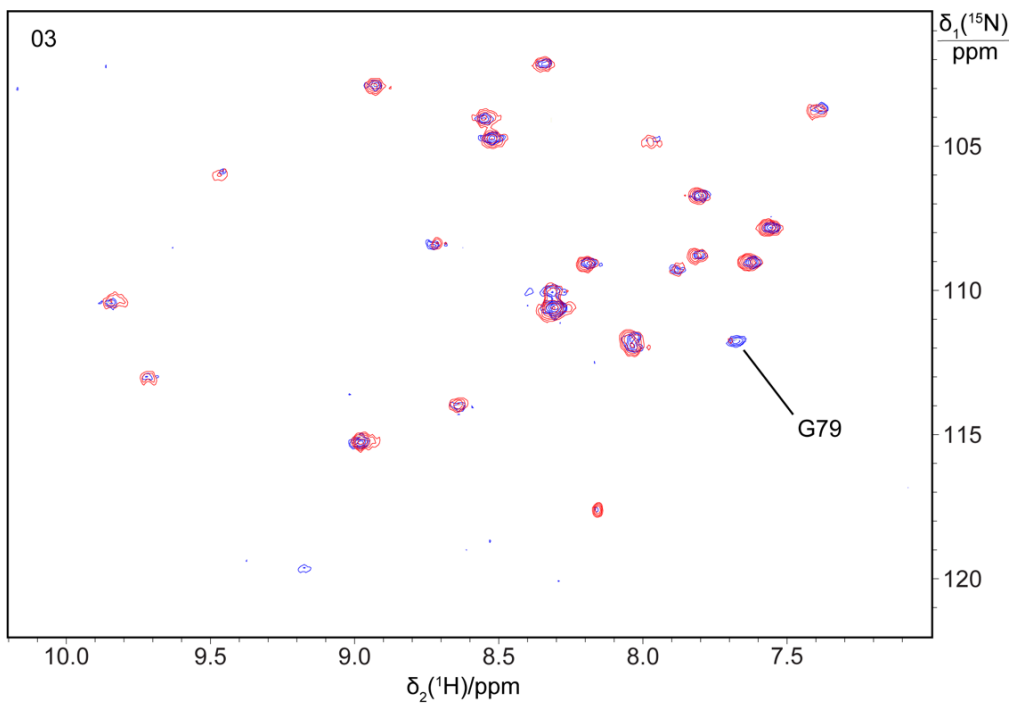
Residue type	Mutated to	Number of mutants made	Peaks assigned
glycine	alanine	19	8
threonine	serine	11	8
isoleucine	valine	6	4
valine	isoleucine	9	5
leucine	alanine	11	6
lysine	arginine	7	3
cysteine	serine	5	3
methionine	alanine	5	2
serine	alanine	6	1
alanine	glycine	4	0
arginine	lysine	2	1

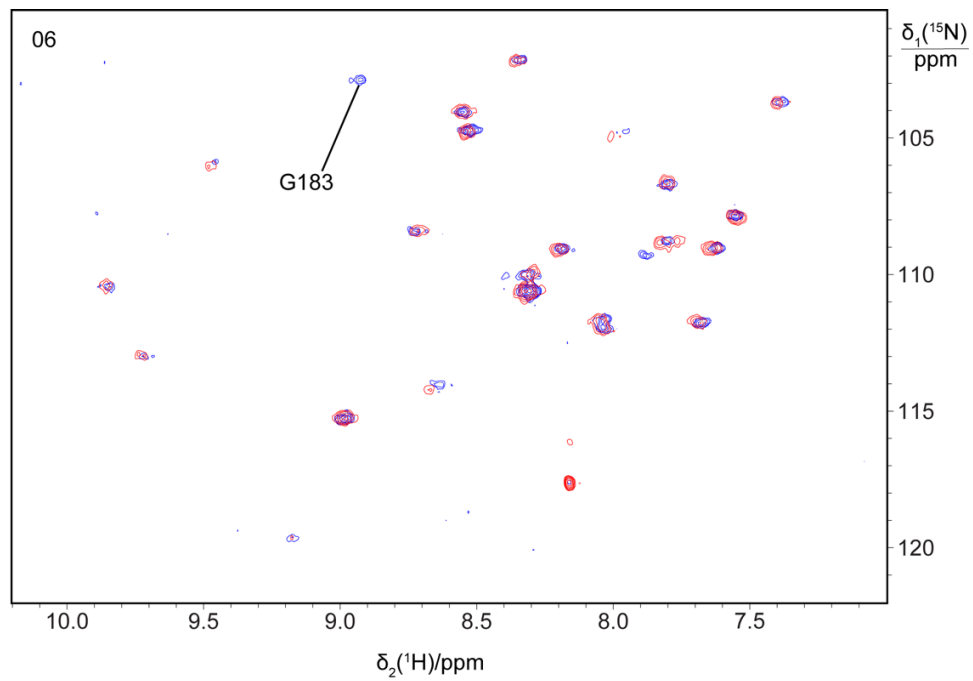
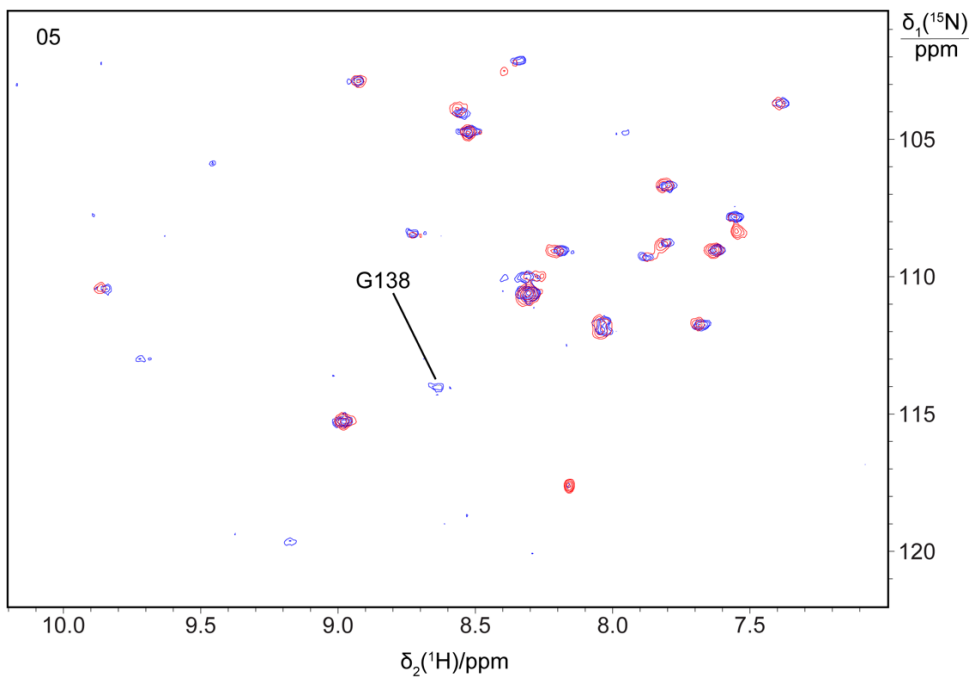
Table S2. Compilation of [¹⁵N, ¹H]-HSQC spectra recorded of selectively ¹⁵N-labelled samples of M^{pro} R298A and mutants enabling specific resonance assignments.^a

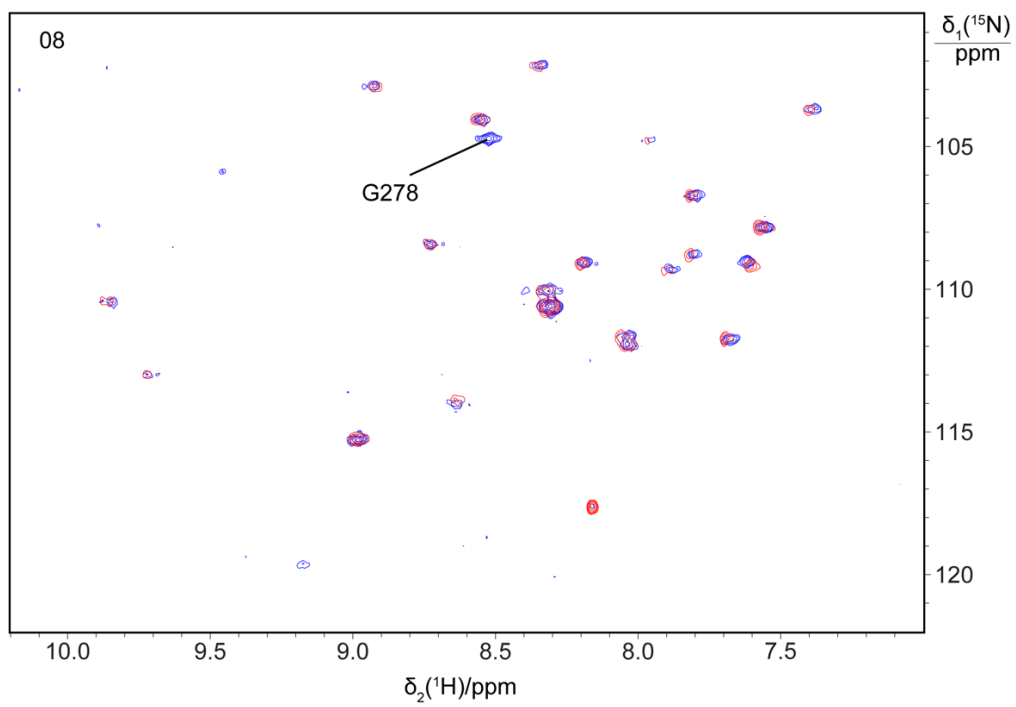
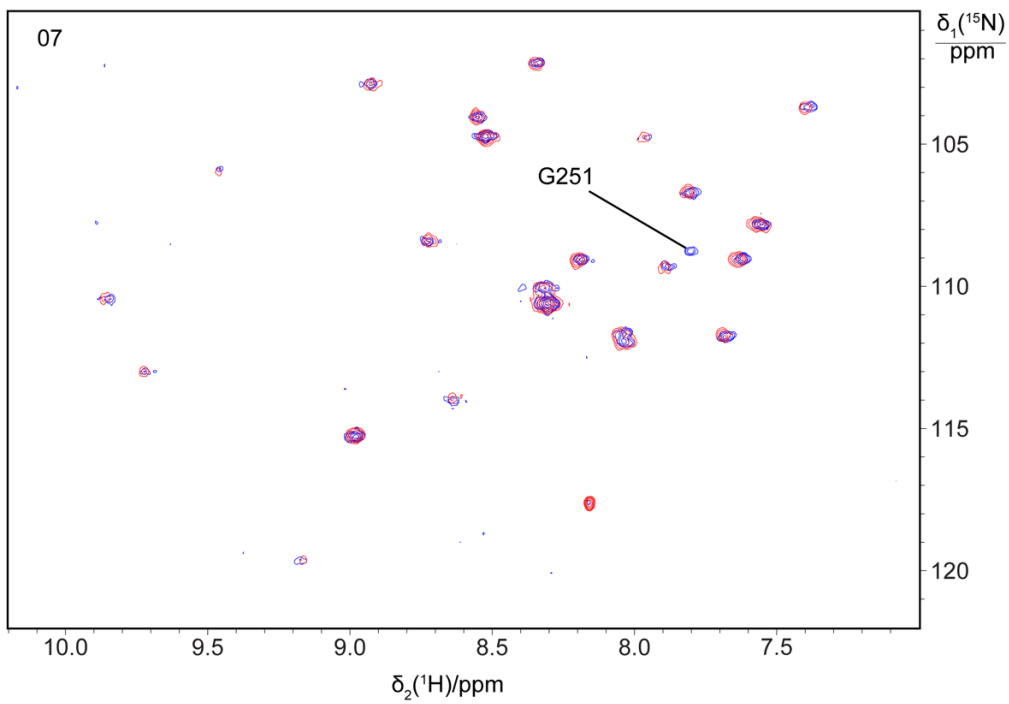
Panel of Supplementary Figure 4	Residue type	Sequence number	Total recording time / h
01	glycine	23	1.3
02	glycine	71	1.3
03	glycine	79	1.3
04	glycine	124	1.3
05	glycine	138	1.3
06	glycine	183	2.7
07	glycine	251	1.3
08	glycine	278	2.7
09	threonine	21	1.3
10	threonine	24	1.3
11	threonine	25	1.3
12	threonine	45	1.3
13	threonine	93	1.3
14	threonine	98	2.7
15	threonine	111	1.3
16	threonine	199	1.3
17	isoleucine	59	1.3
18	isoleucine	78	1.3
19	isoleucine	106	1.3
20	isoleucine	200	1.3
21	valine	68	1.3
22	valine	73	1.3
23	valine	77	1.3
24	valine	91	1.3
25	valine	104	1.3
26	leucine	50	10.6
27	leucine	58	13.3
28	leucine	67	1.3
29	leucine	75	1.3
30	leucine	220	1.3
31	leucine	232	1.3
32	lysine	100	7.3
33	lysine	102	2.7
34	lysine	137	7.3
35	cysteine	85	5.3
36	cysteine	128	1.3
37	cysteine	156	1.3
38	methionine	6	1.3
39	methionine	276	2.7
40	serine	46	1.3
41	arginine	188	5.0

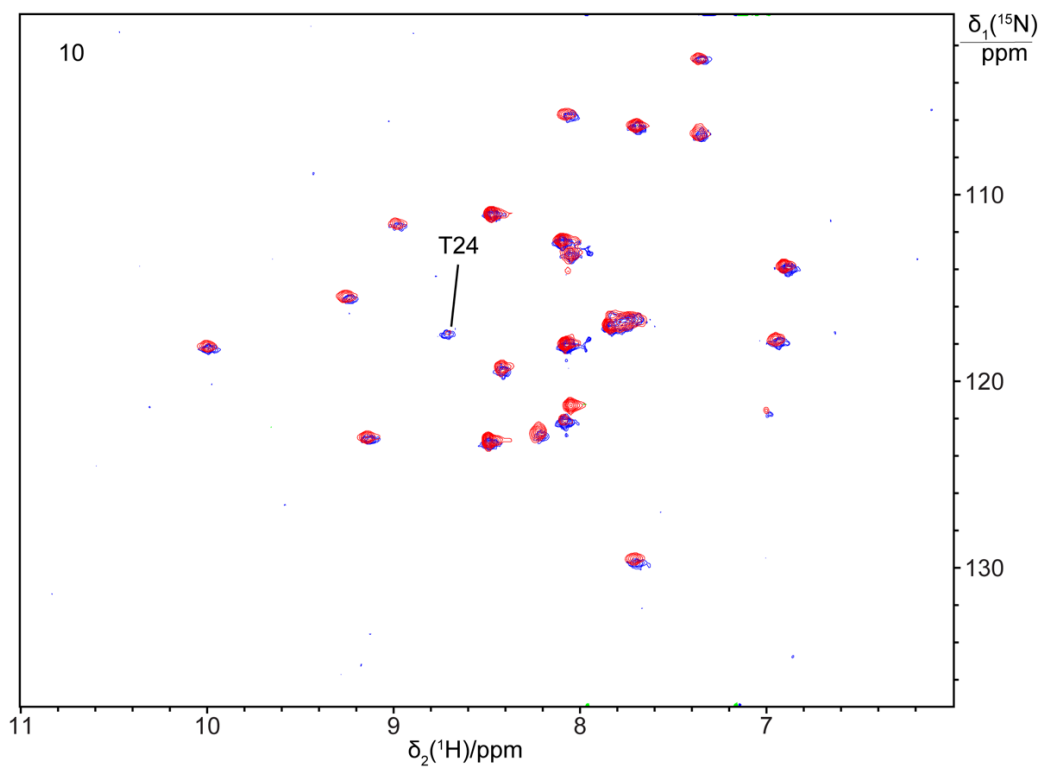
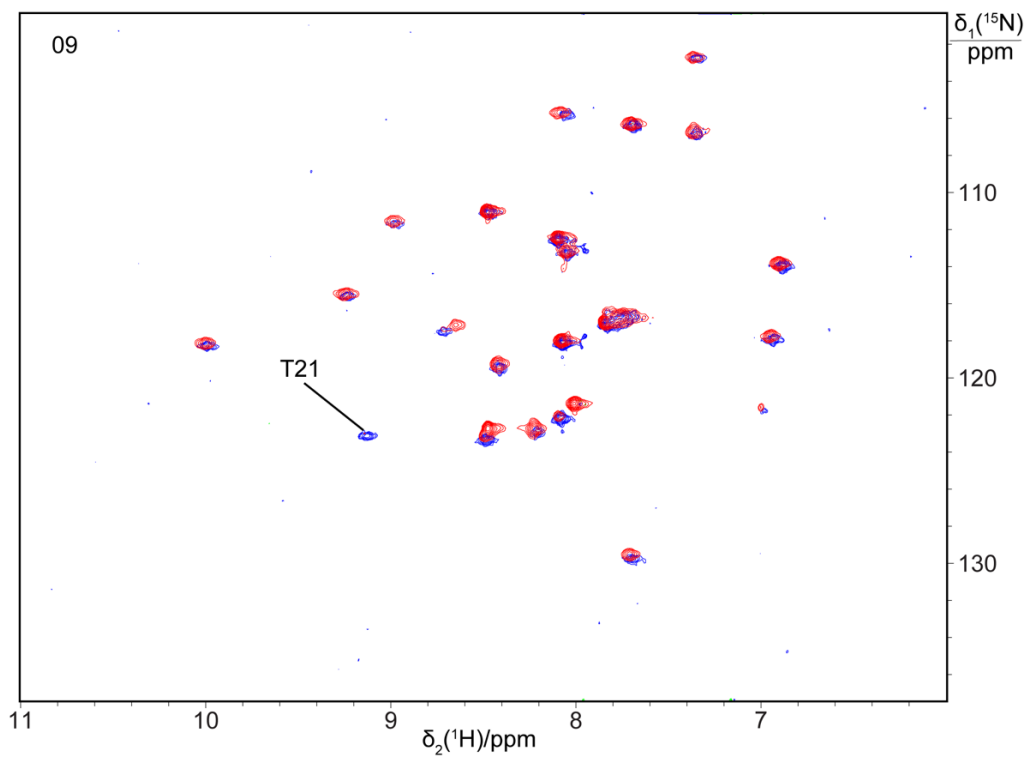
^a The table columns refer to the number of the spectrum, the residue type labelled with ¹⁵N, the amino acid sequence number of the assignment made and the total recording time of the spectrum. The individual spectra are shown in Supplementary Figure S7 below.

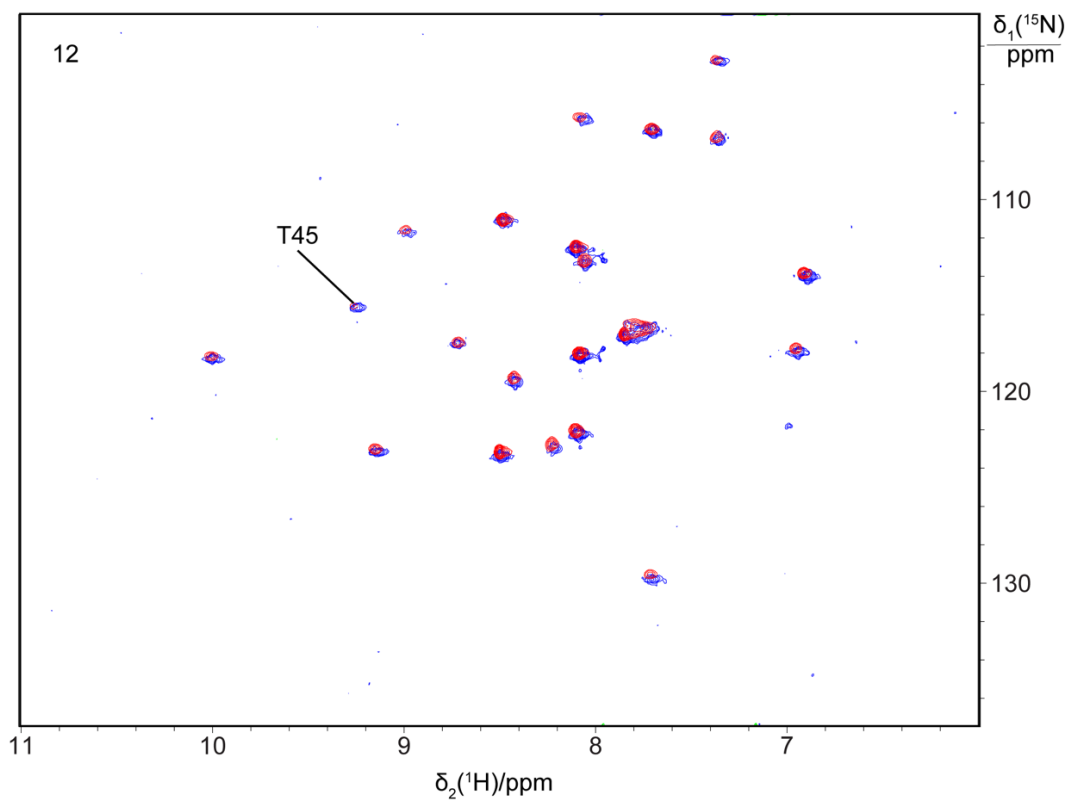
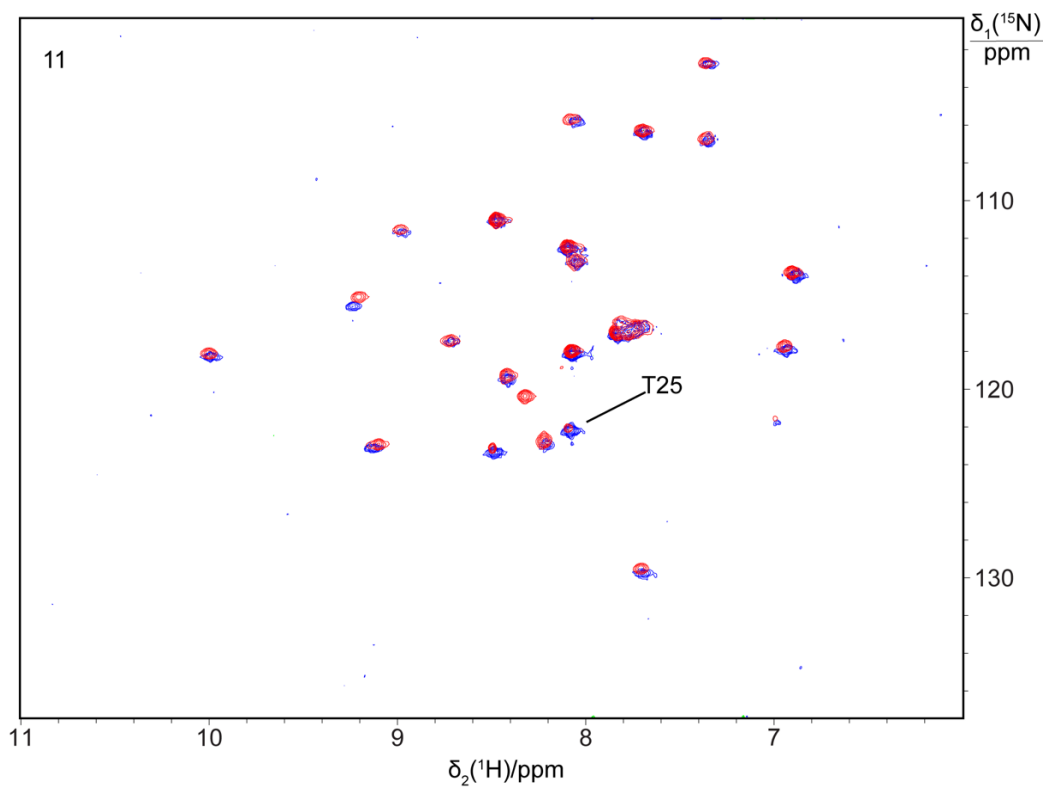


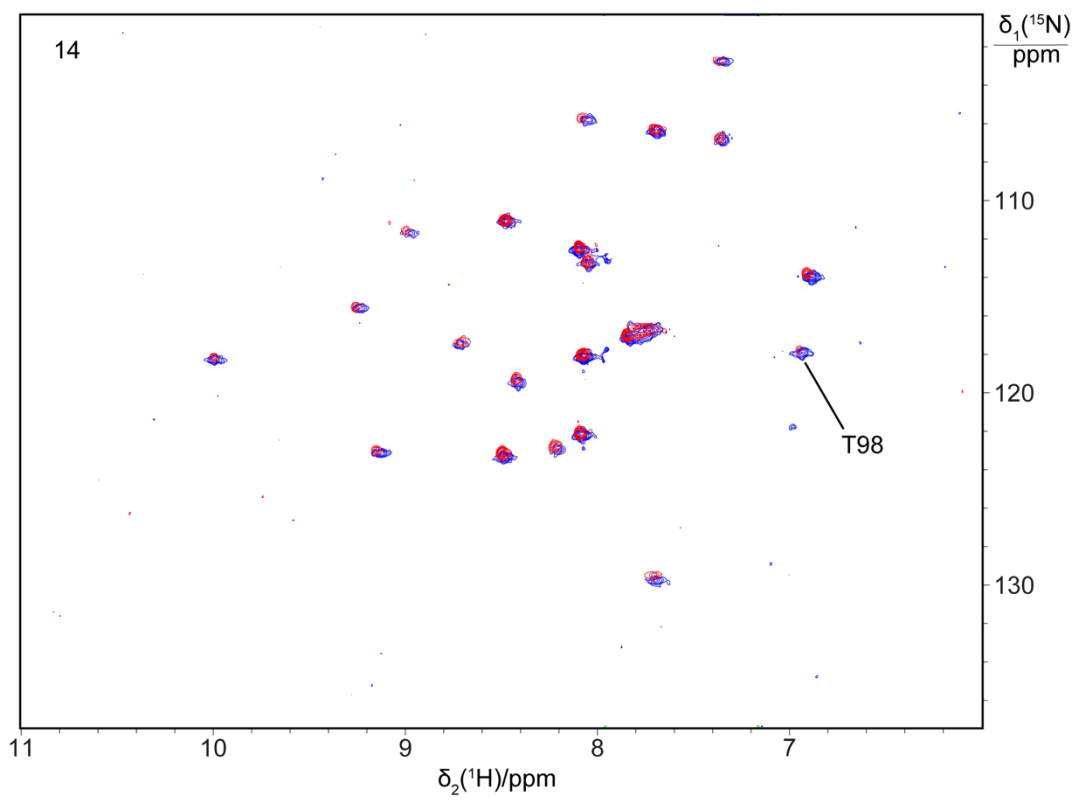
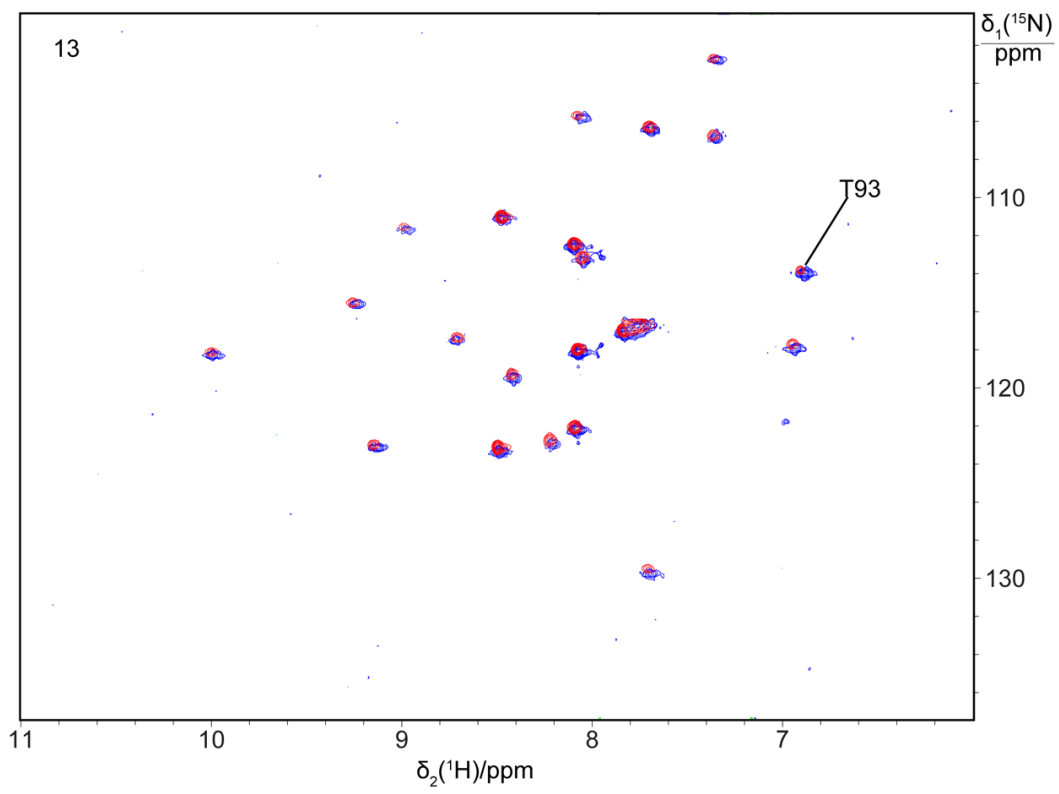


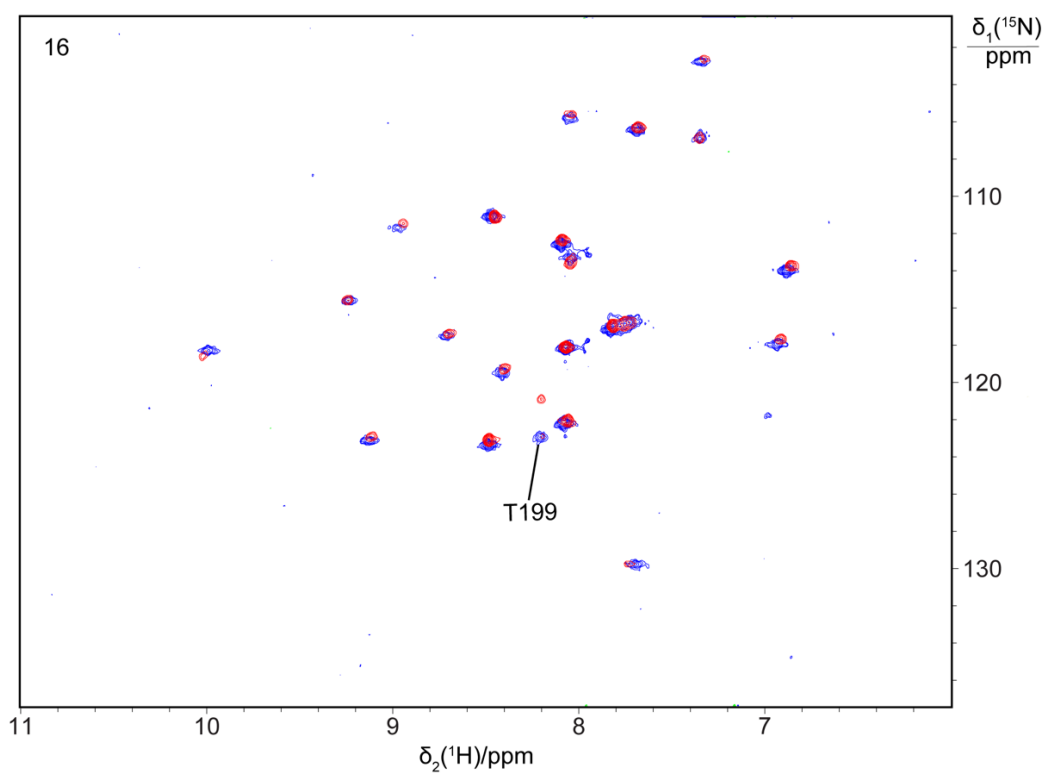
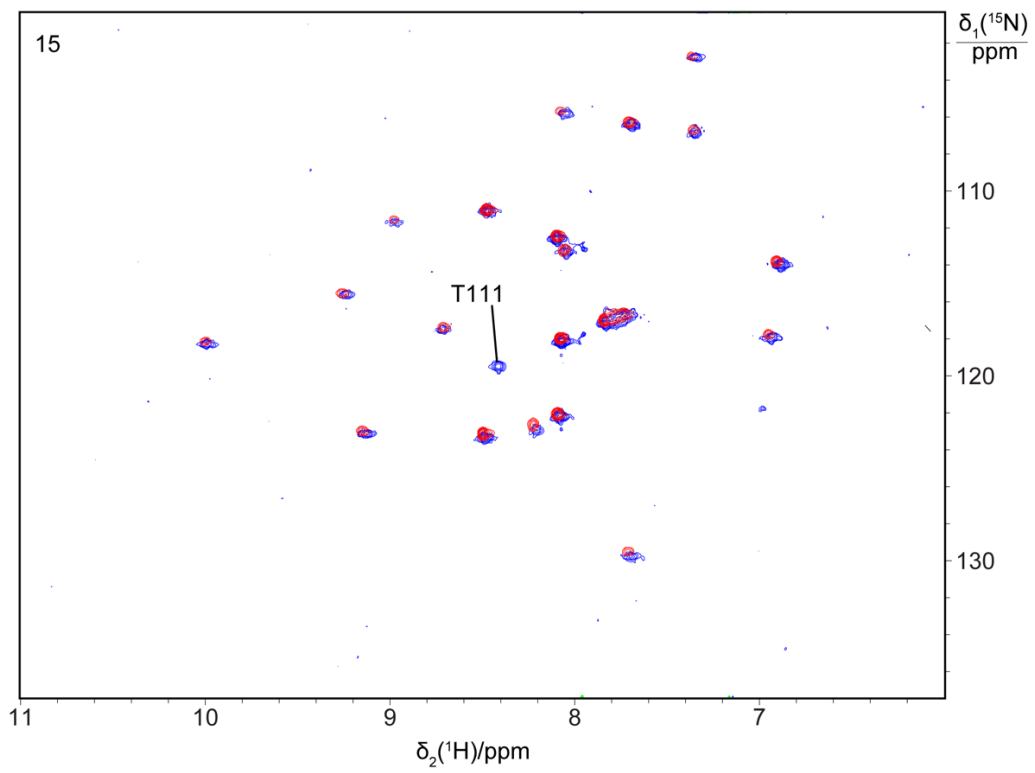


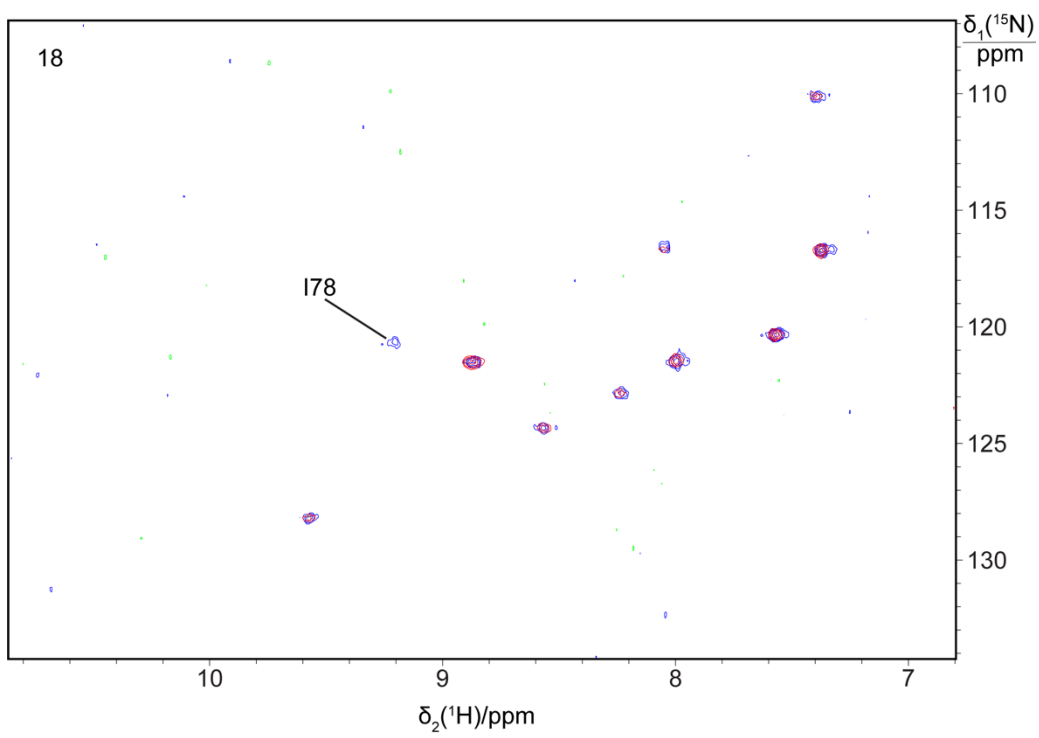
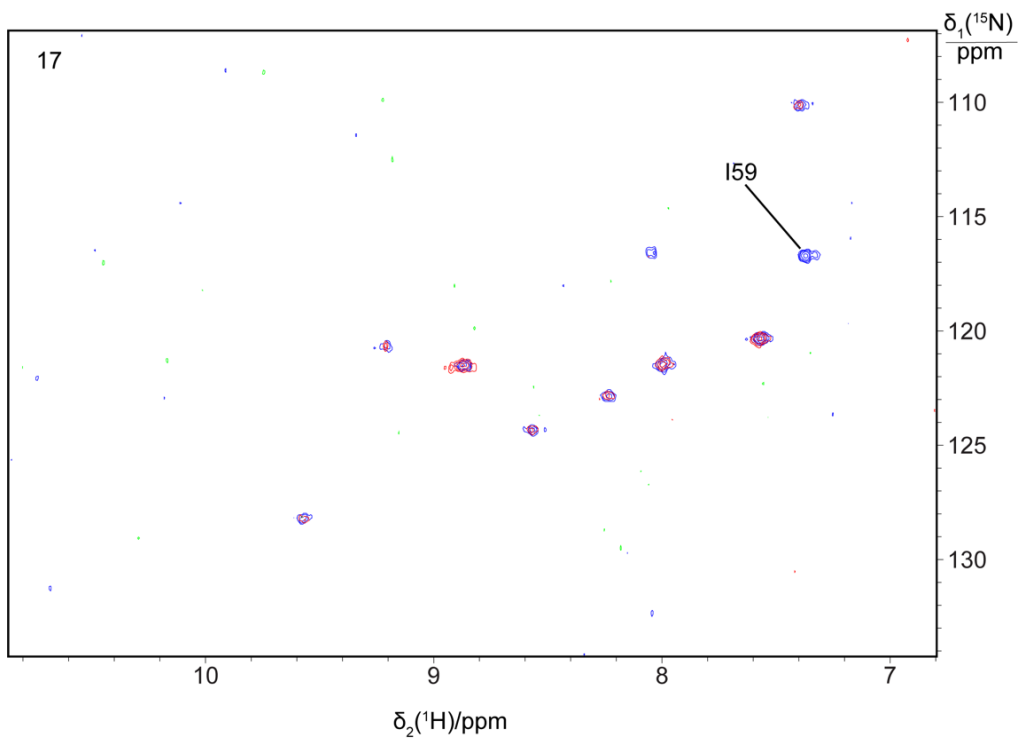


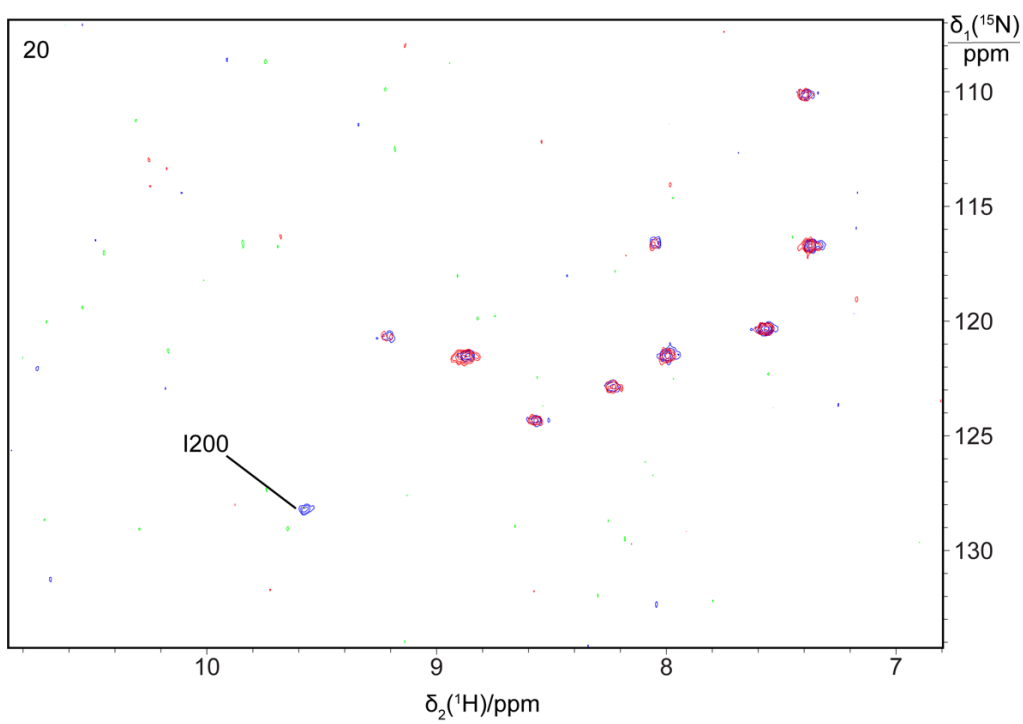
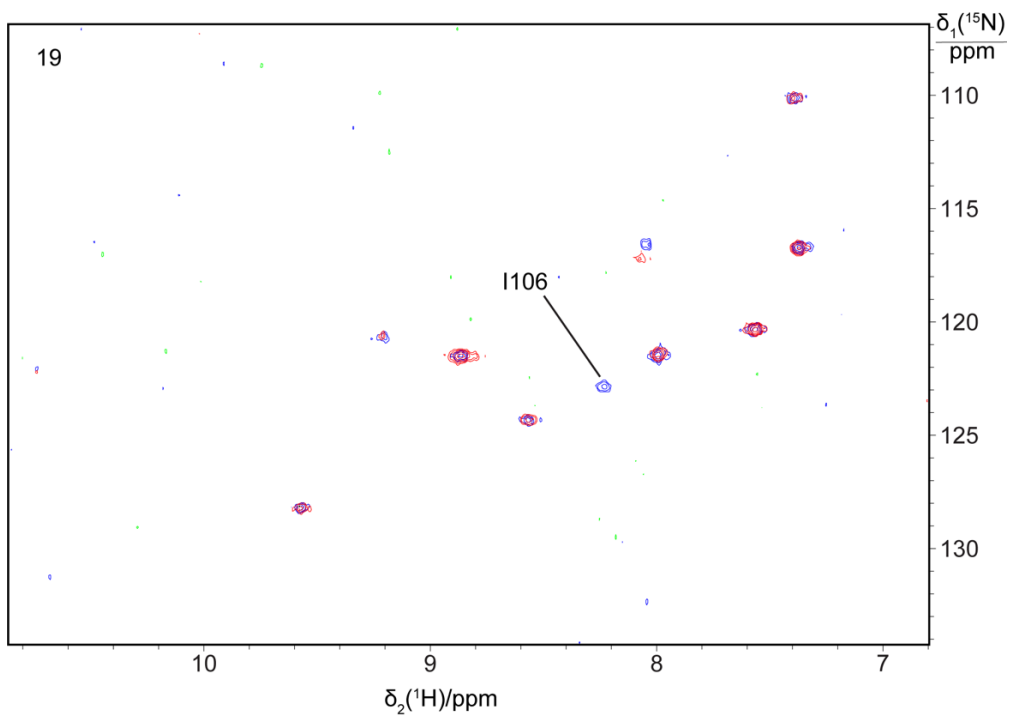


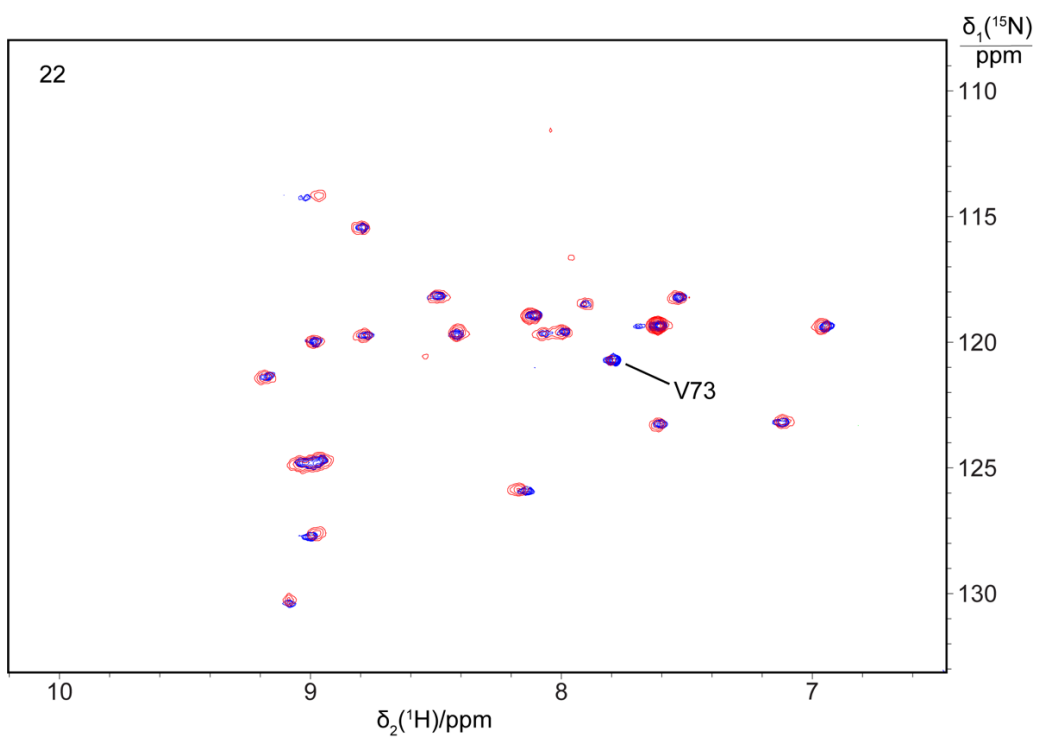
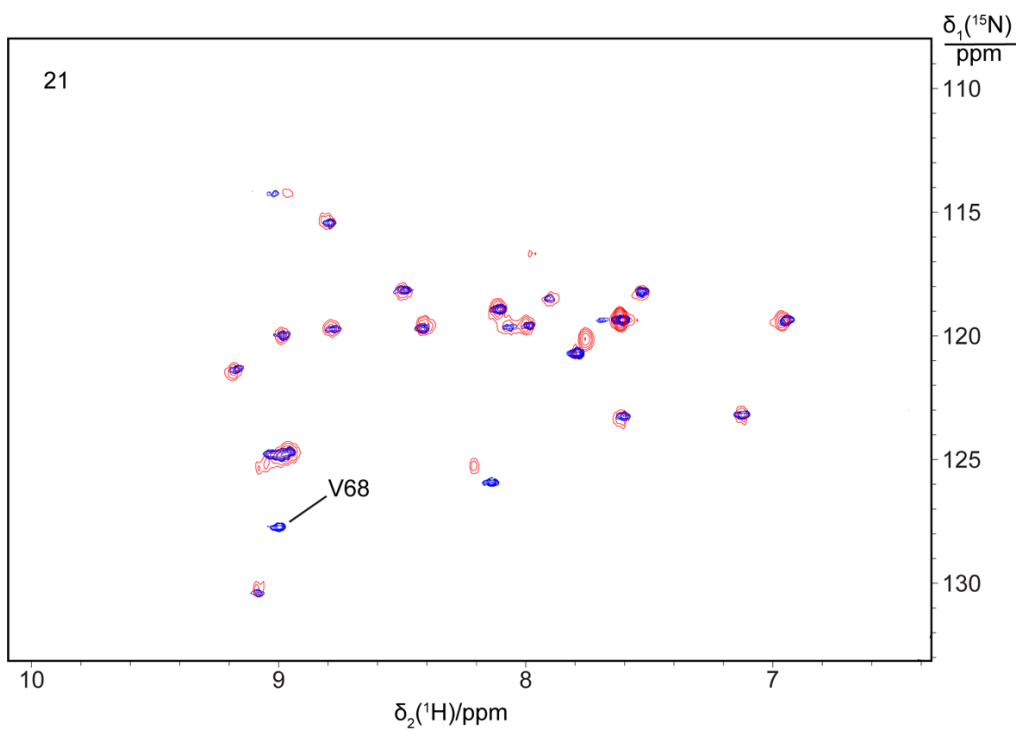


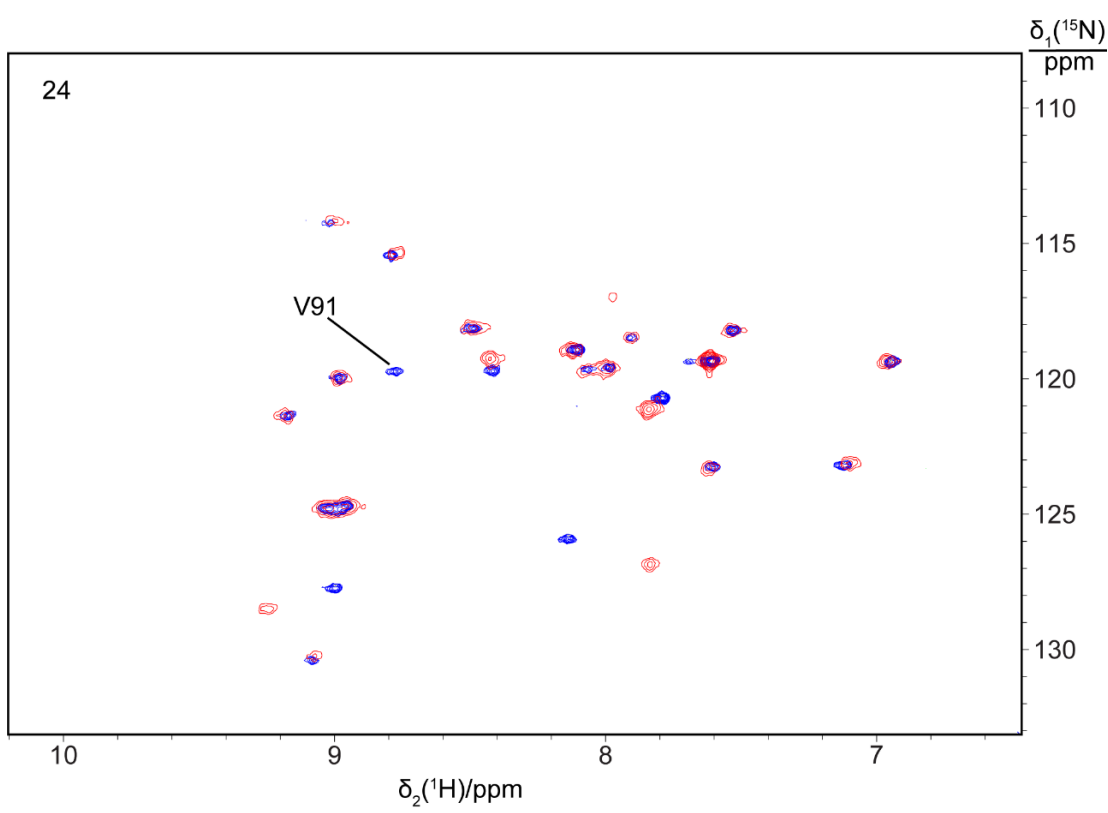
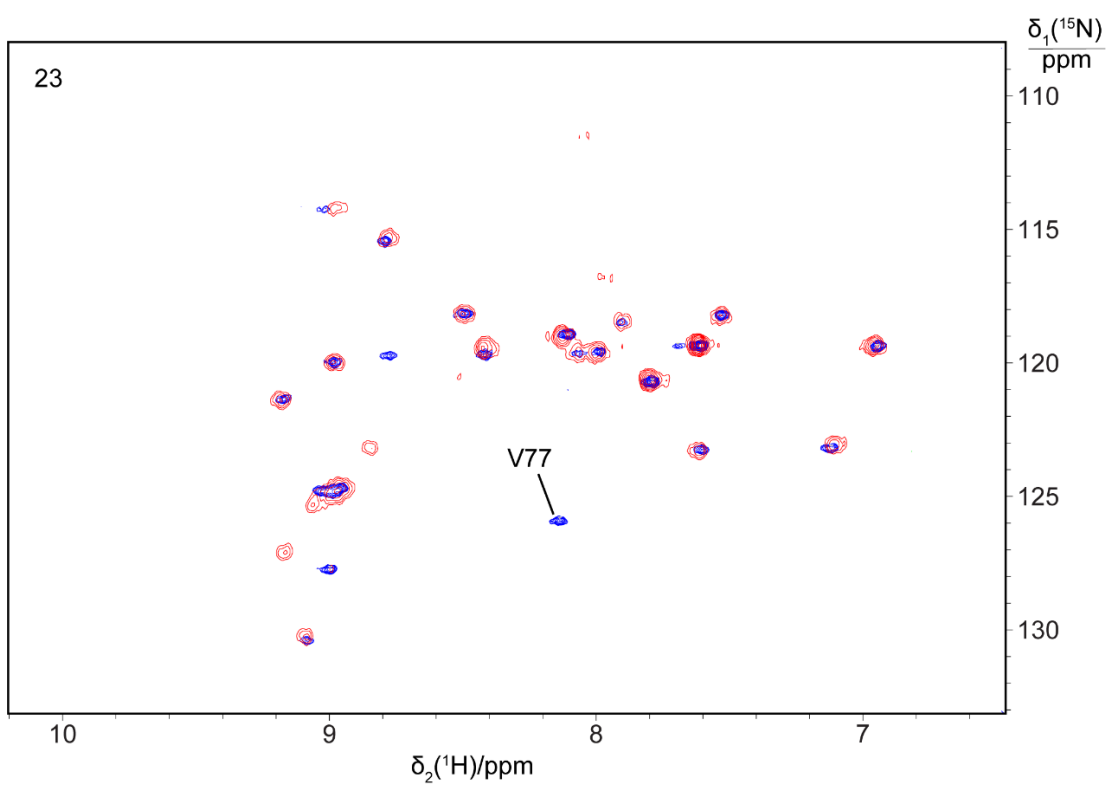


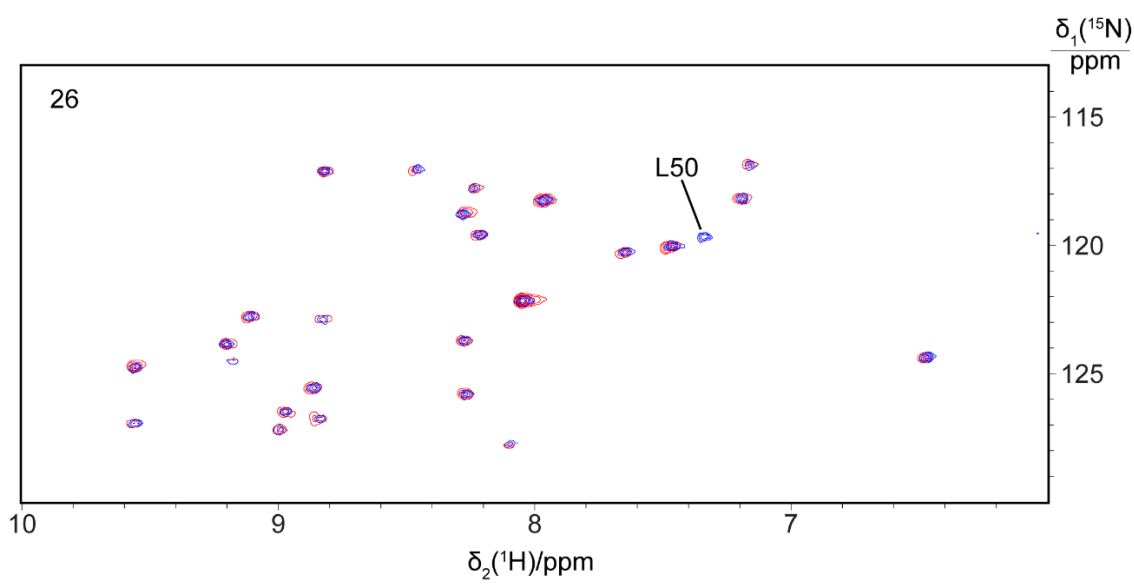
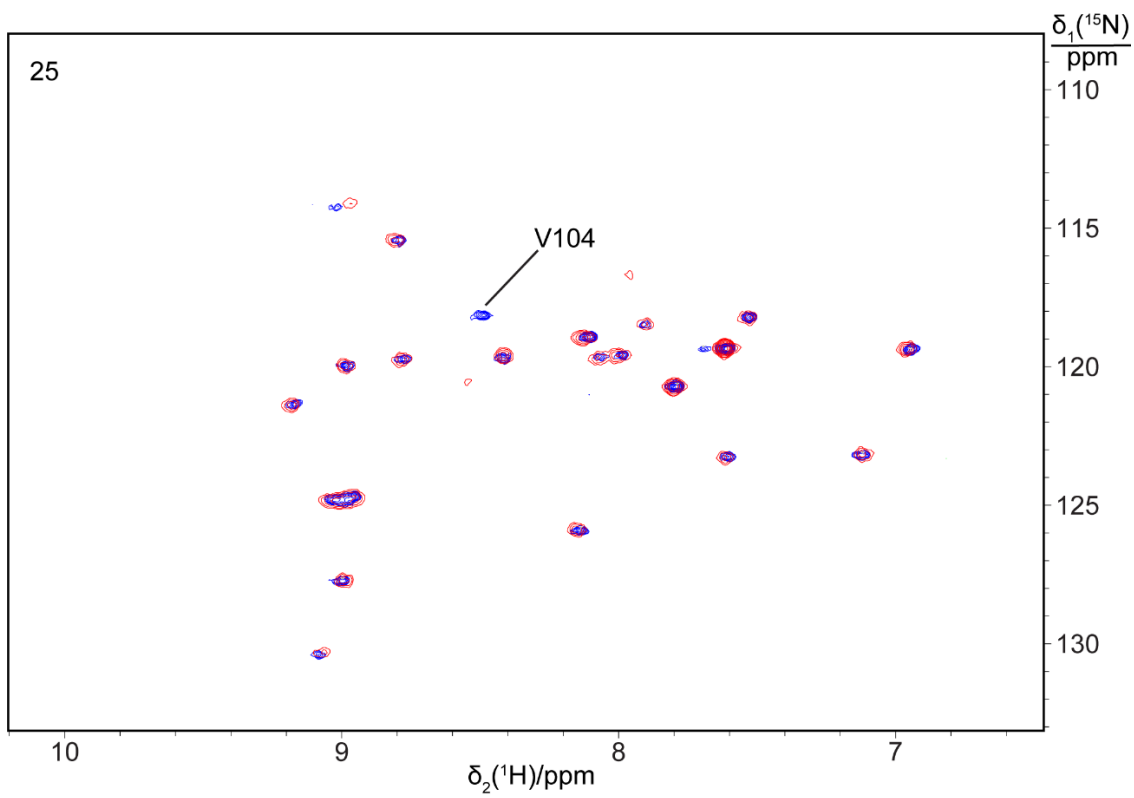


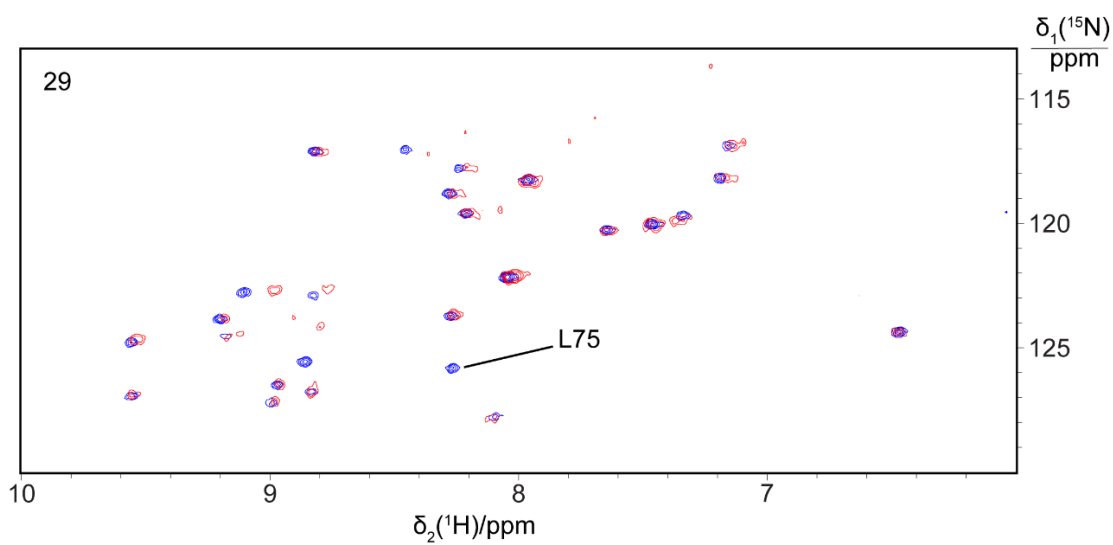
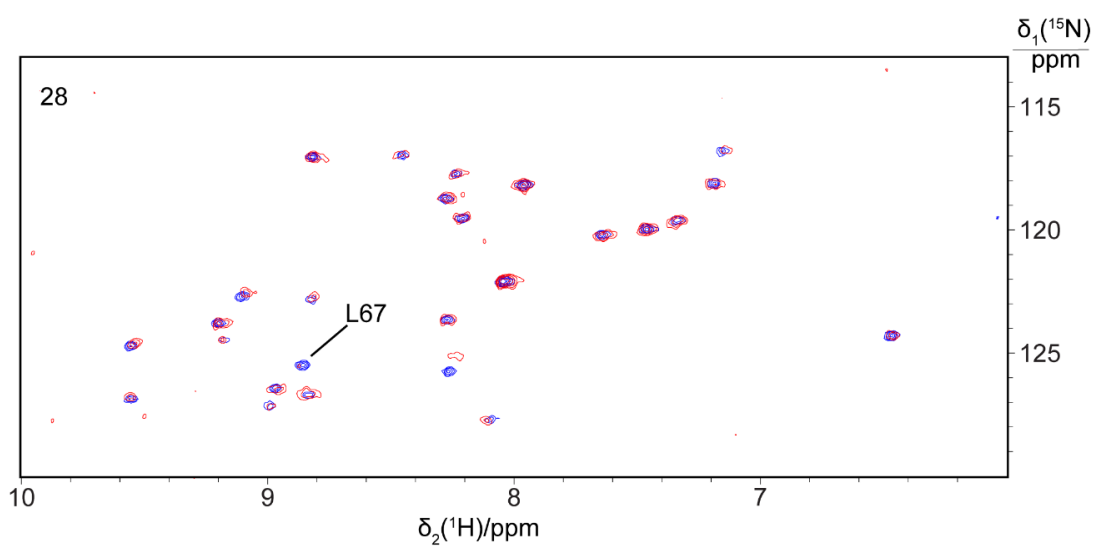
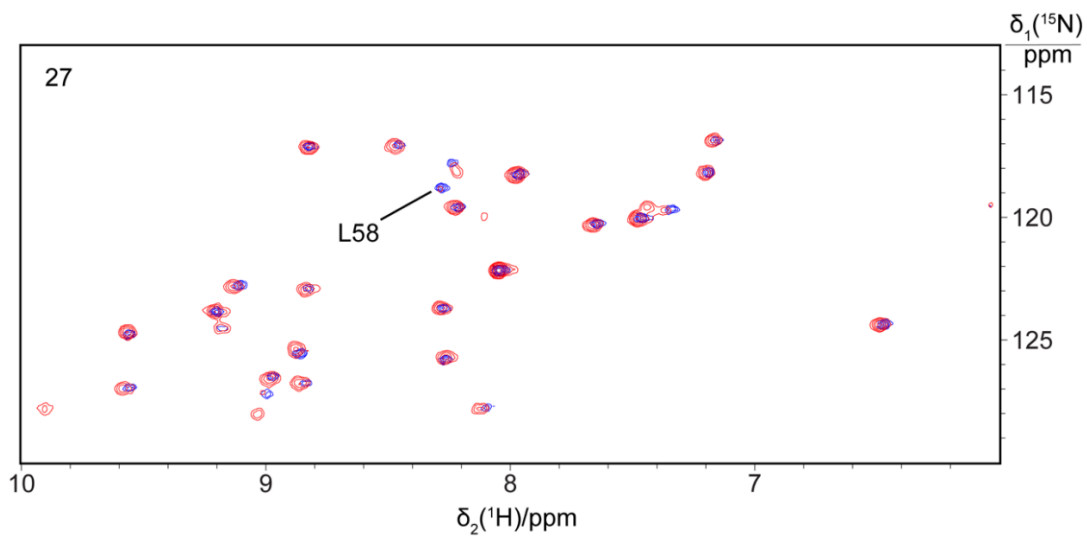


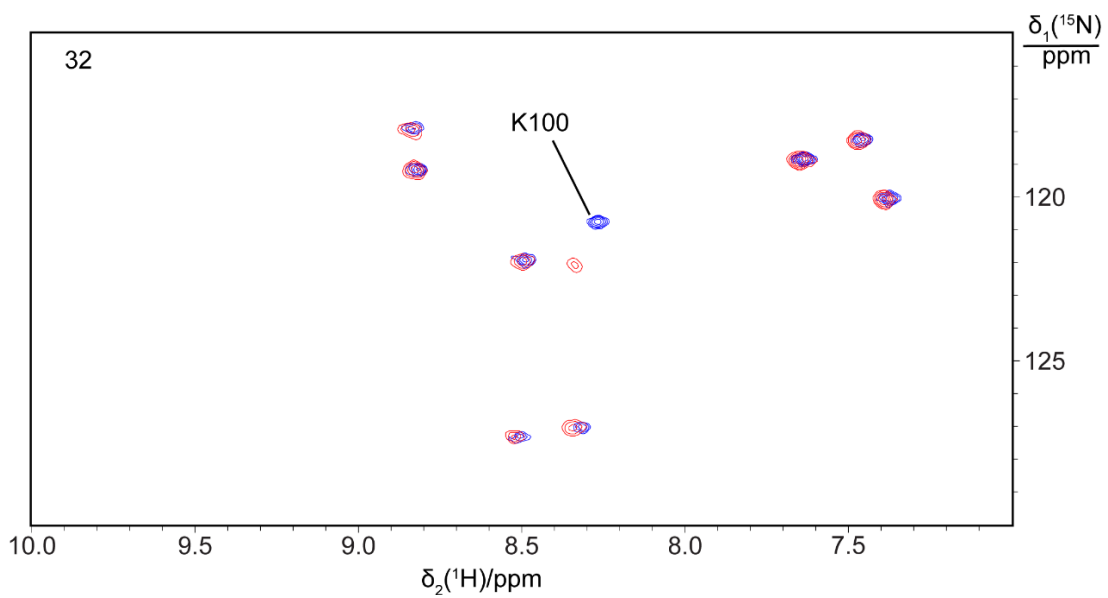
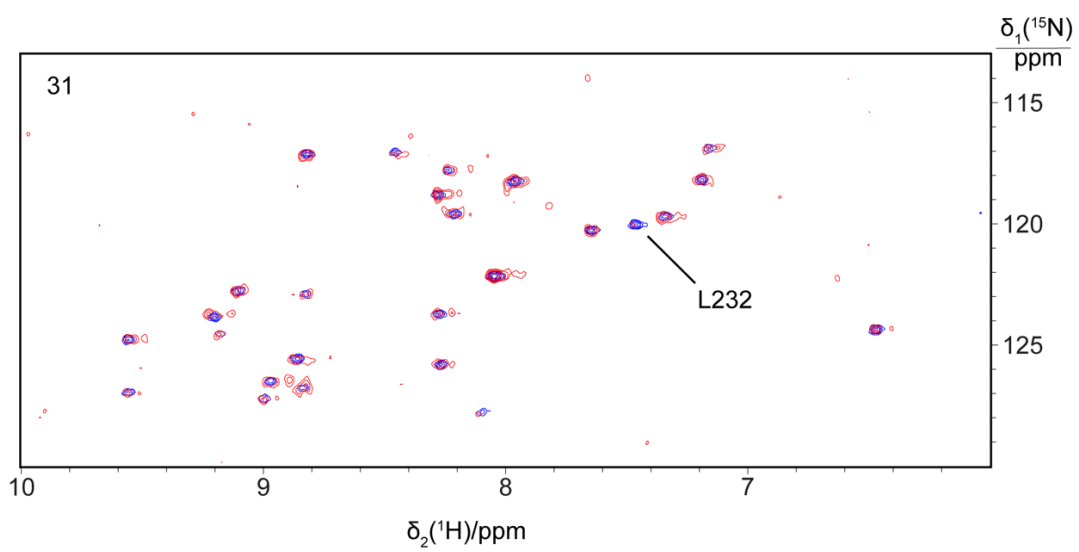
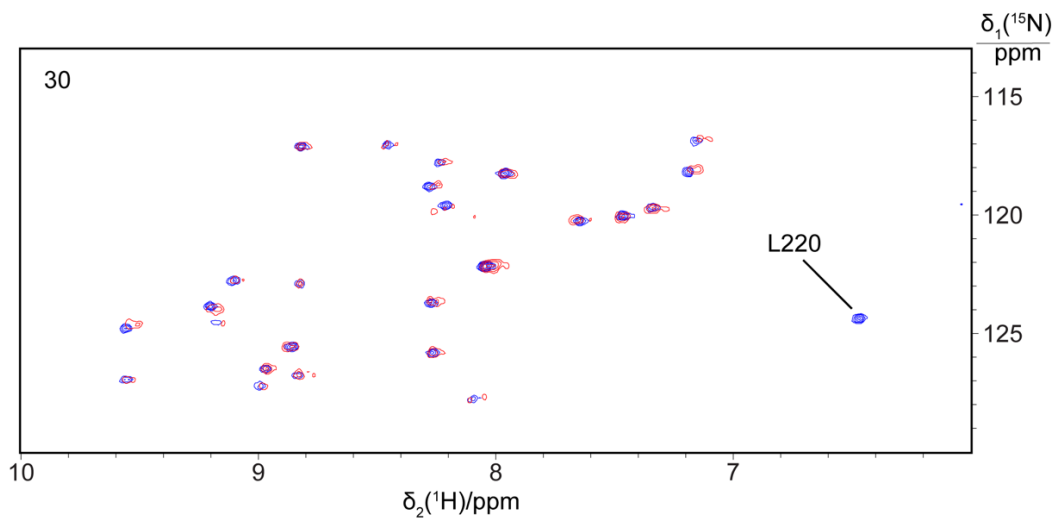


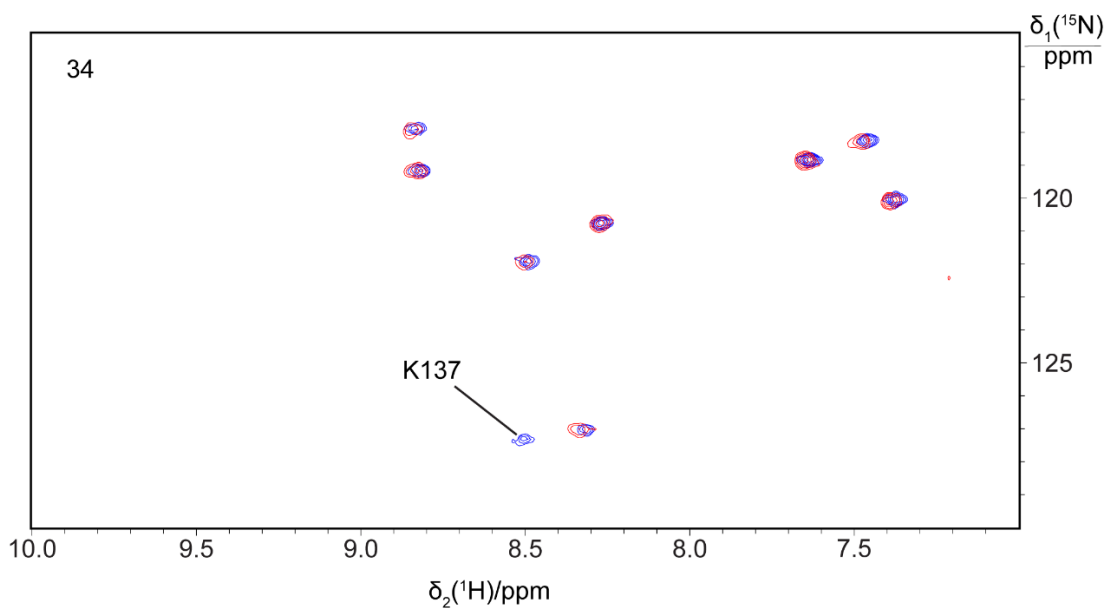
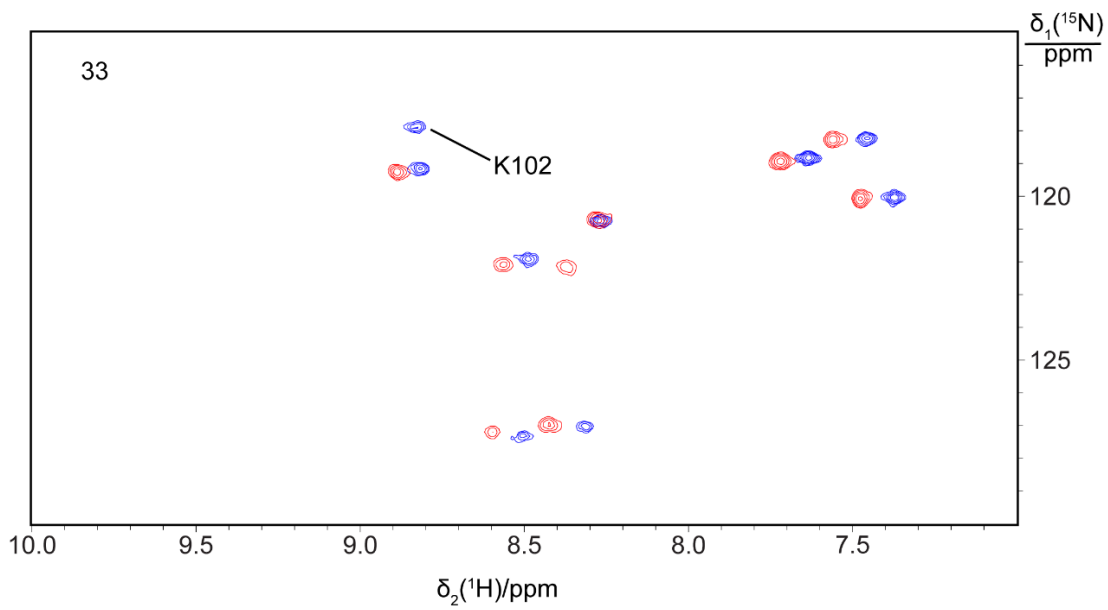


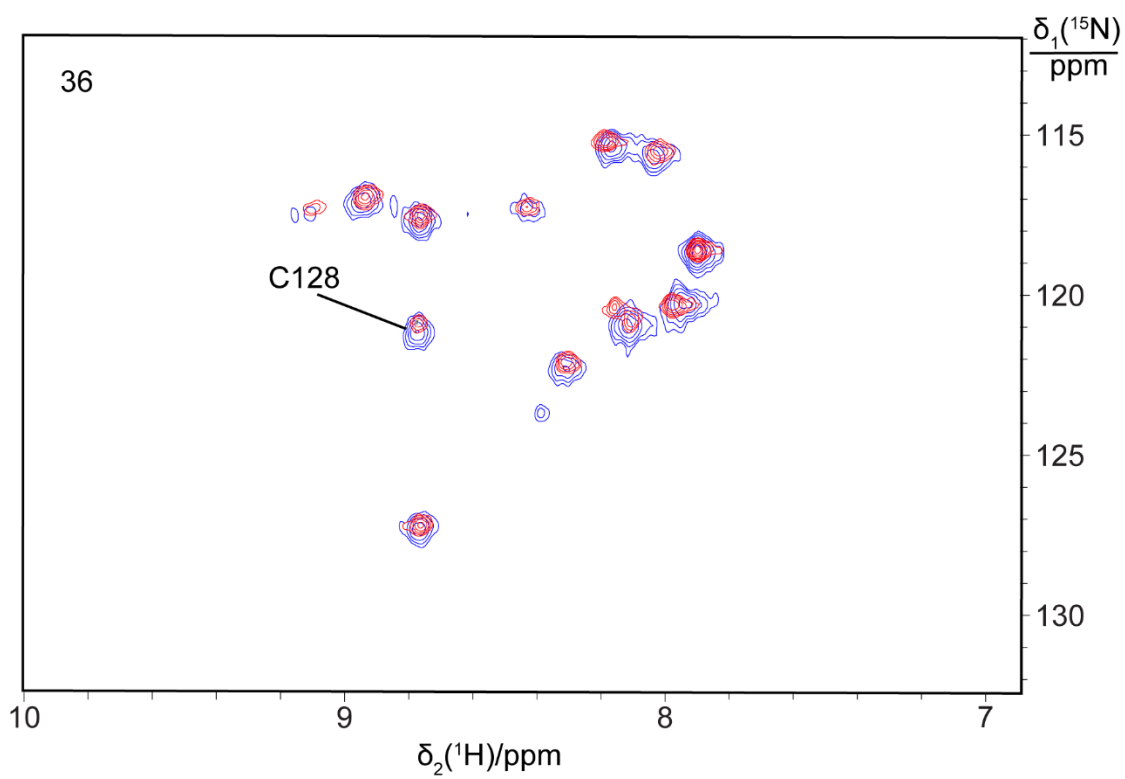
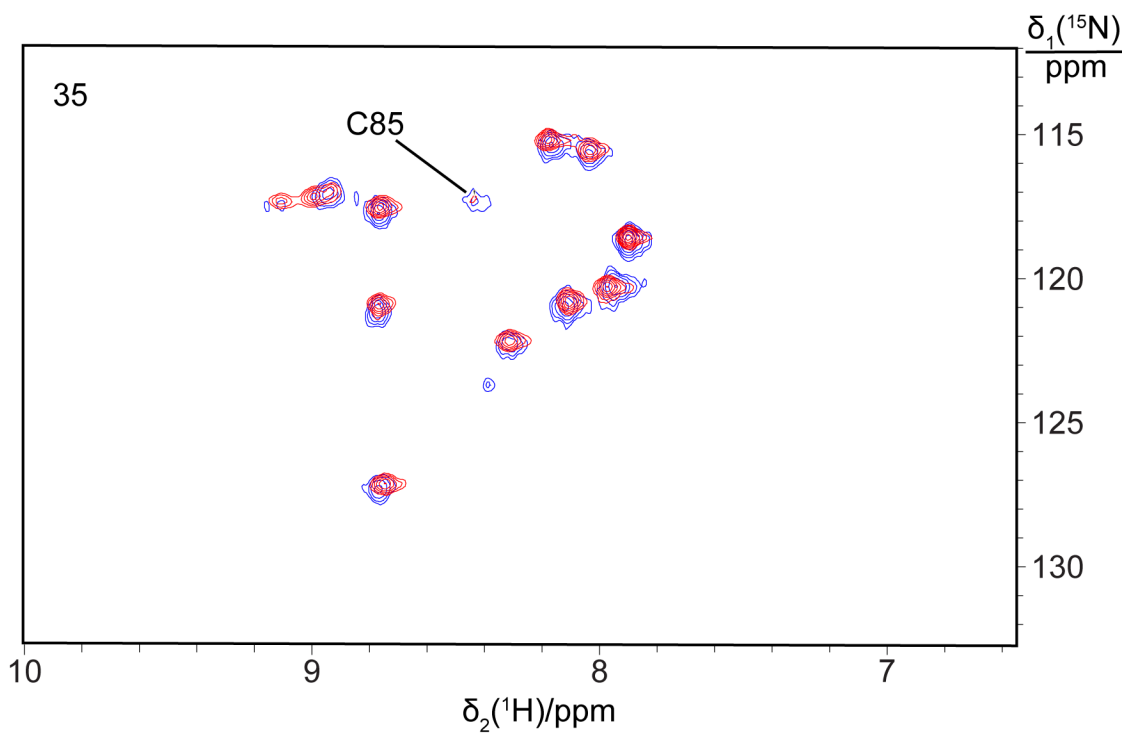


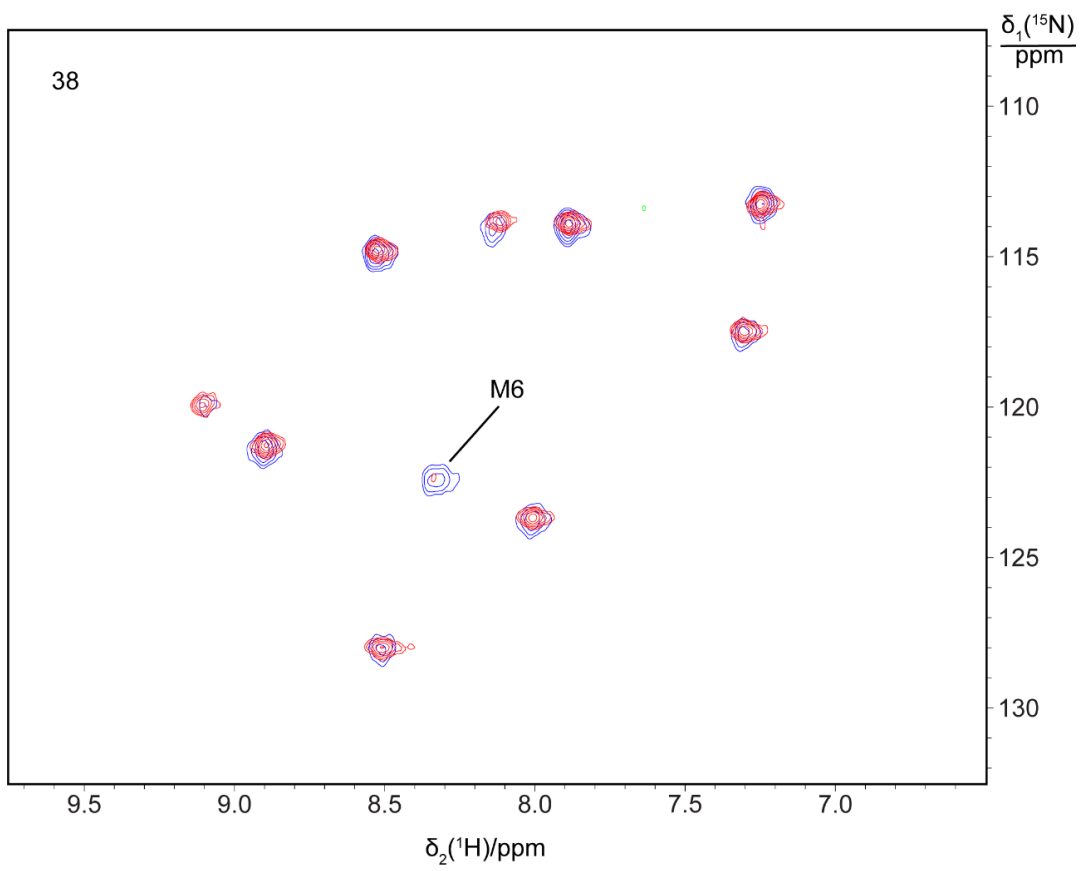
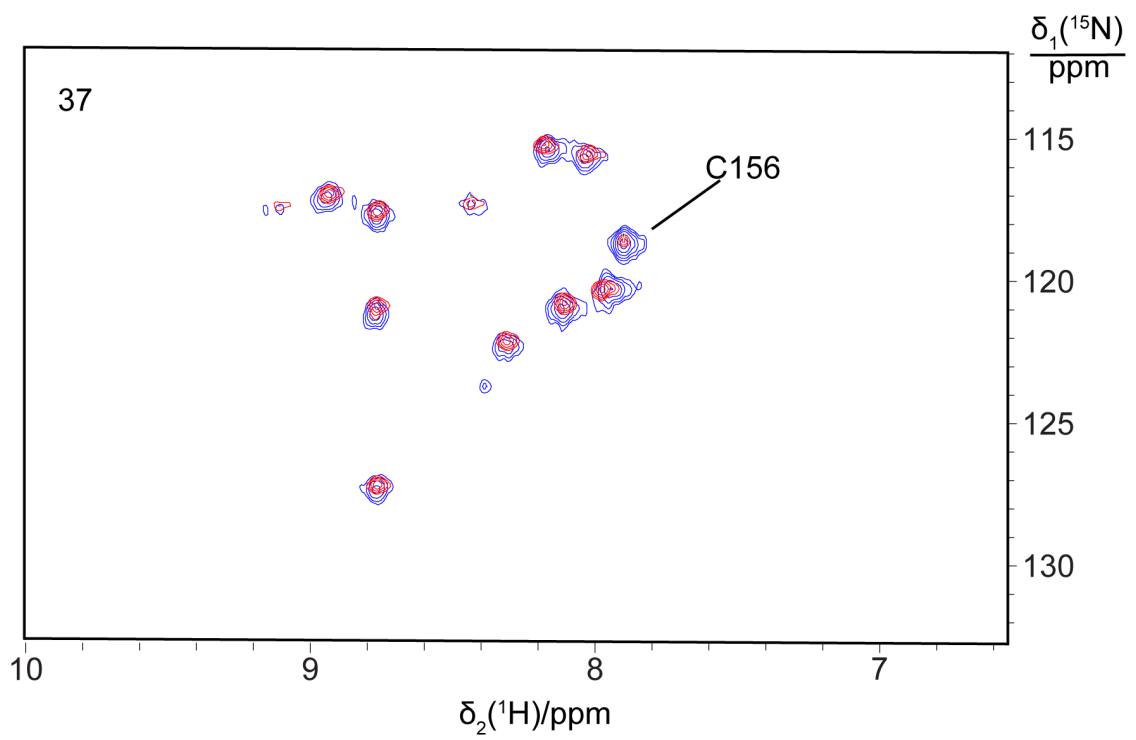


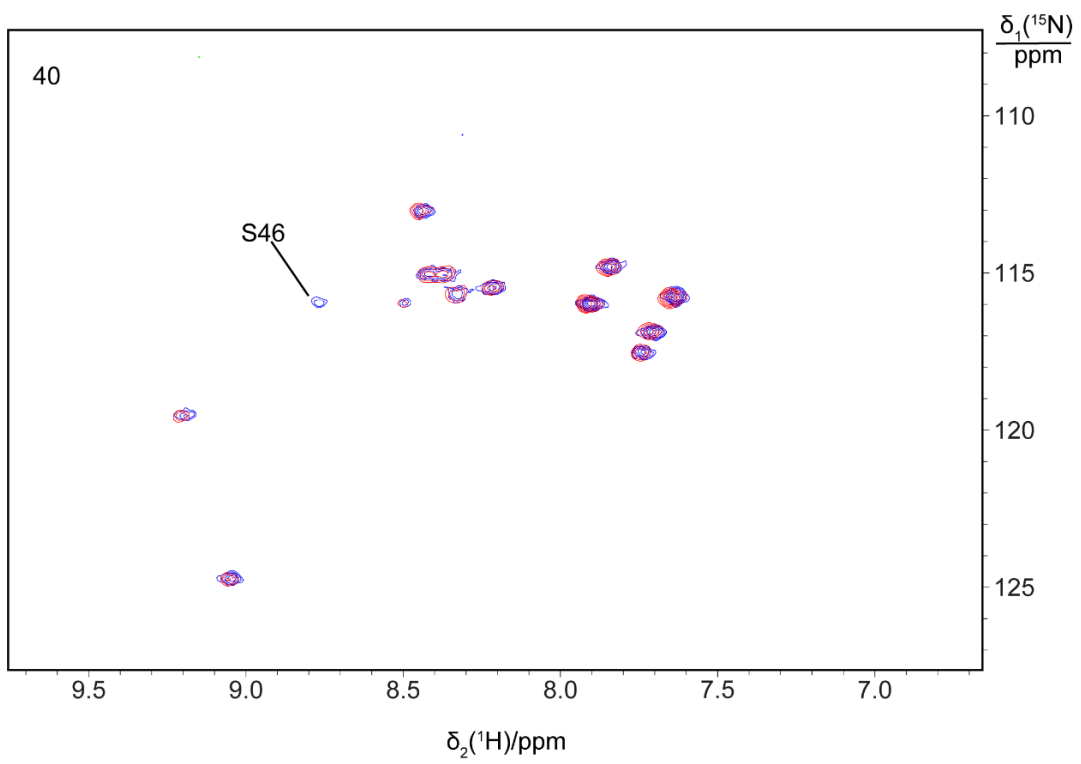
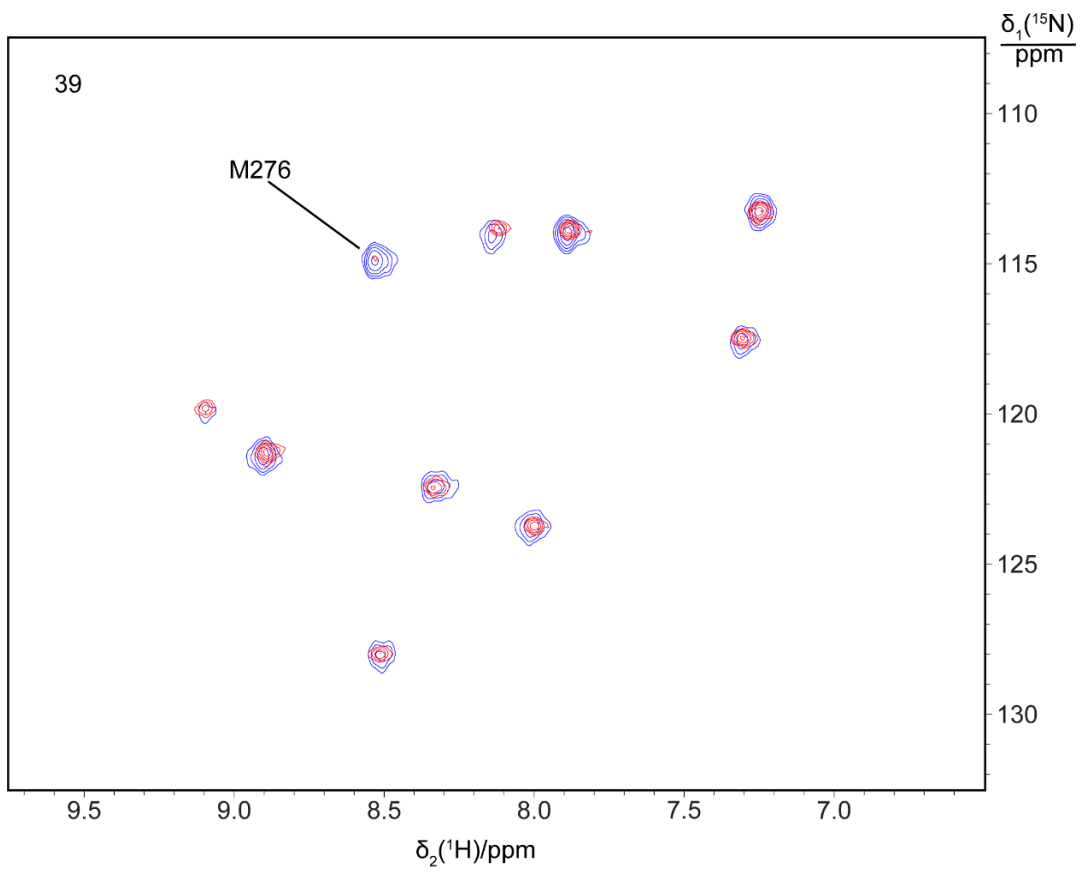












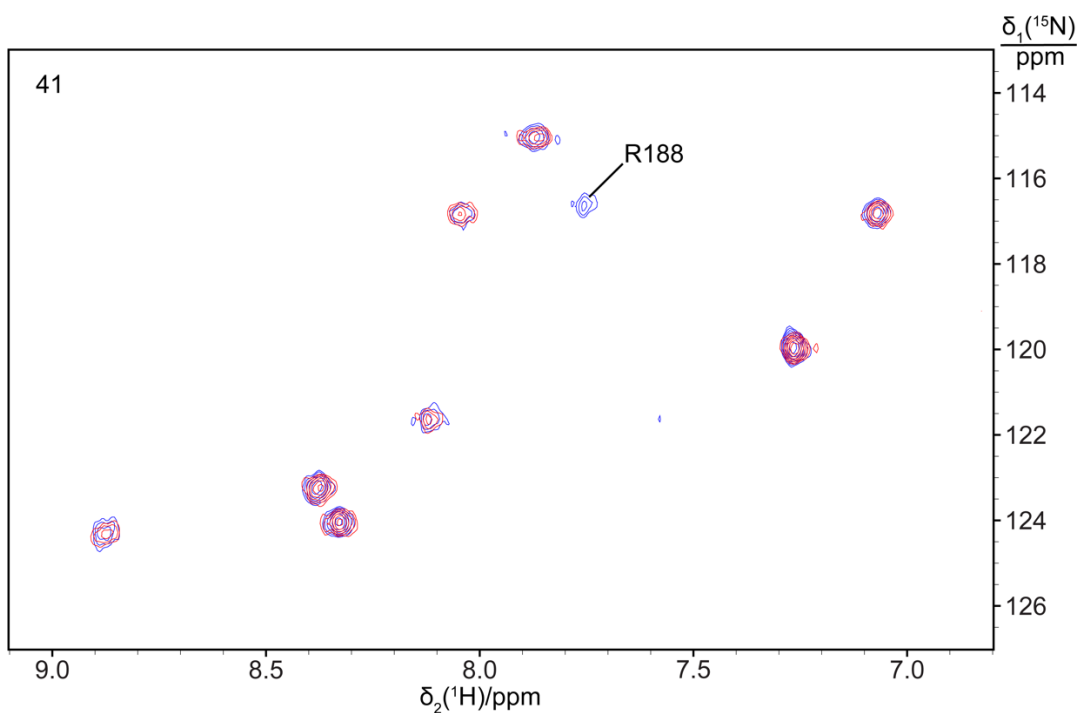


Fig. S7. [^{15}N , ^1H]-HSQC spectra recorded of selectively ^{15}N -labelled samples of M^{pro} R298A and mutants enabling specific resonance assignments. The spectra show superimpositions of the selectively labelled samples (blue) and the corresponding samples with a site-specific mutation (red). The panel numbers refer to Table S2, which reports the amino acid type labelled with ^{15}N and the mutation site. The residue types installed by the mutations are specified in Table S1. The sequence-specific resonance assignment made with each mutation is indicated in the spectra.

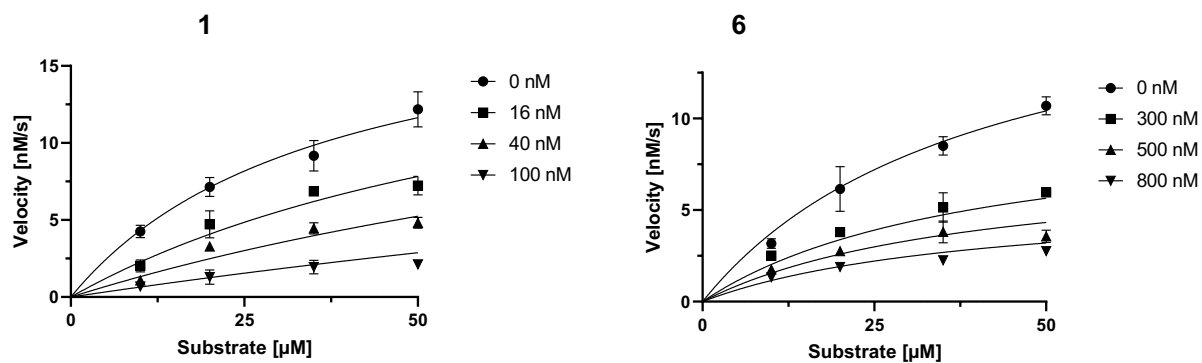


Fig. S8. Michaelis-Menten saturation curves of SARS-CoV-2 M^{Pro} in the presence of range of concentrations of cyclic peptide inhibitors 1 and 6.

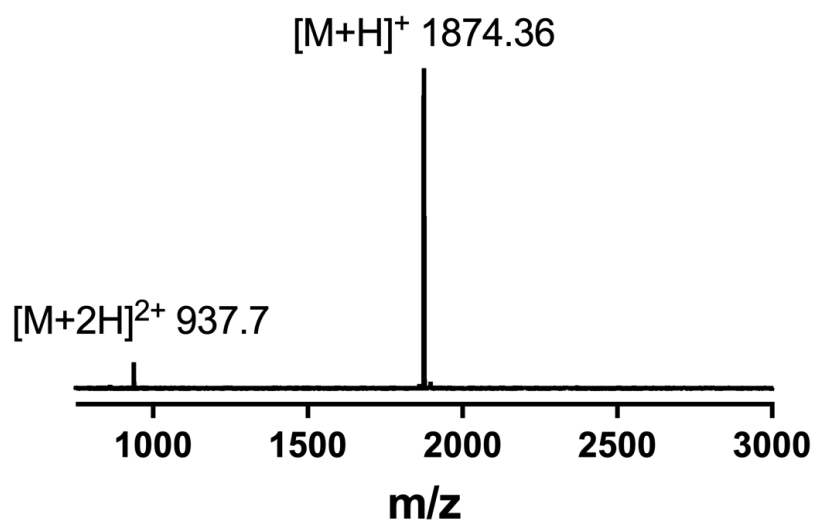


Fig. S9. Monitoring of the cleavage of cyclic peptide inhibitor 1 with SARS-CoV-2 M^{PRO} for 5 h. Negligible cleavage was observed after incubation of 1 after incubation with M^{PRO} for 5 h.

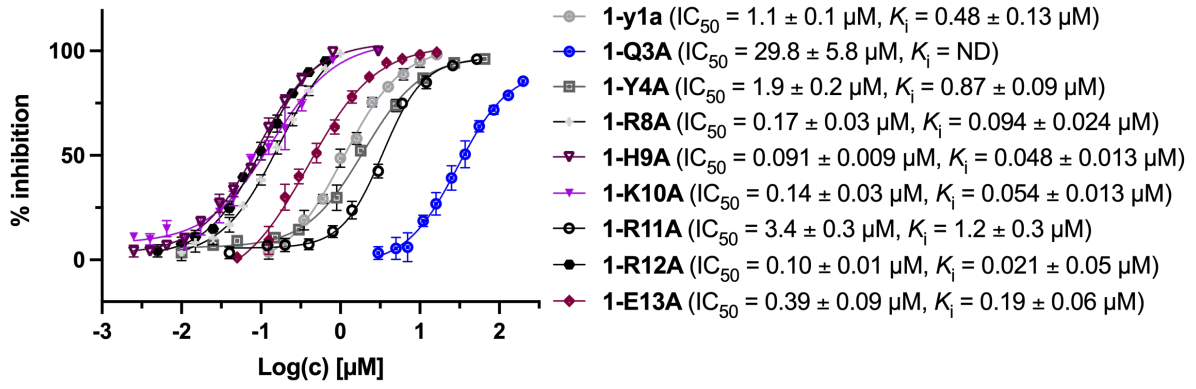


Fig. S11. Dose response curves for single site alanine mutants of lead cyclic peptide 1 against SARS-CoV-2 M^{pro}.

Peptide	Structure	IC ₅₀ (μM)
1-Sec		0.056 ± 0.005

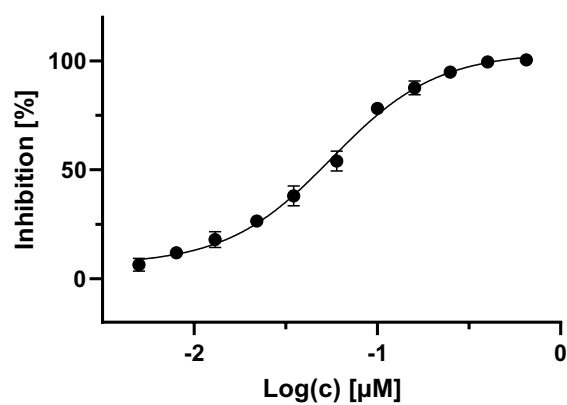


Fig. S12. Structure and inhibitory activity of selenoether analogue of 1 (Sec-1) against SARS-CoV-2 M^{PRO}.

Table S3. Data collection and refinement statistics. For the low resolution SARS-CoV-2 M^{pro}:1 complex we provide data collection statistics to demonstrate the SARS-CoV-2 M^{pro}:Se-1 crystal has similar space group/unit cell dimensions. The quality of the electron density in the SARS-CoV-2 M^{pro}:1 complex was not sufficient to build a high-quality model or resolve the binding of the ligand.

	SARS-CoV-2 M ^{pro} -Se-1	SARS-CoV-2 M ^{pro} -1
PDB ID	7RNW	N/A
Data collection		
Space group	P 1 2 ₁ 1	P1 2 ₁ 1
Cell dimensions		
<i>a, b, c</i> (Å)	48.4 201.7 60.5	47.6, 190.1, 59.15
α, β, γ (°)	90.0 113.5 90.0	90, 113.64, 90
Resolution (Å)	33.31-2.35 (2.43-2.35)*	39.66-3.45 (3.78-3.45)*
R _{merge}	0.254 (1.542)	0.658 (2.249)
R _{pim}	0.103 (0.629)	0.370 (1.297)
I/σI	6.4 (1.4)	4.4 (1.4)
CC _{1/2}	0.999 (0.512)	0.933 (0.315)
Completeness (%)	99.9 (99.6)	99.5 (99.3)
Redundancy	7.0 (6.9)	7.2 (7.0)
Refinement		
Resolution (Å)	33.31-2.35 (2.41-2.35)	
No. reflections	44079 (4410)	
R _{work} /R _{free}	0.171/0.231 (0.243/0.340)	
No. atoms	9819	
Protein	9732	
Ligand/ion	40	
Water	47	
B-factors (overall)	37.90	
Protein	37.92	
Ligand/ion	47.30	
Water	25.19	
R.m.s. deviations		
Bond lengths (Å)	0.009	
Bond angles (Å)	1.727	

*Statistics for the highest resolution shell are shown in parentheses

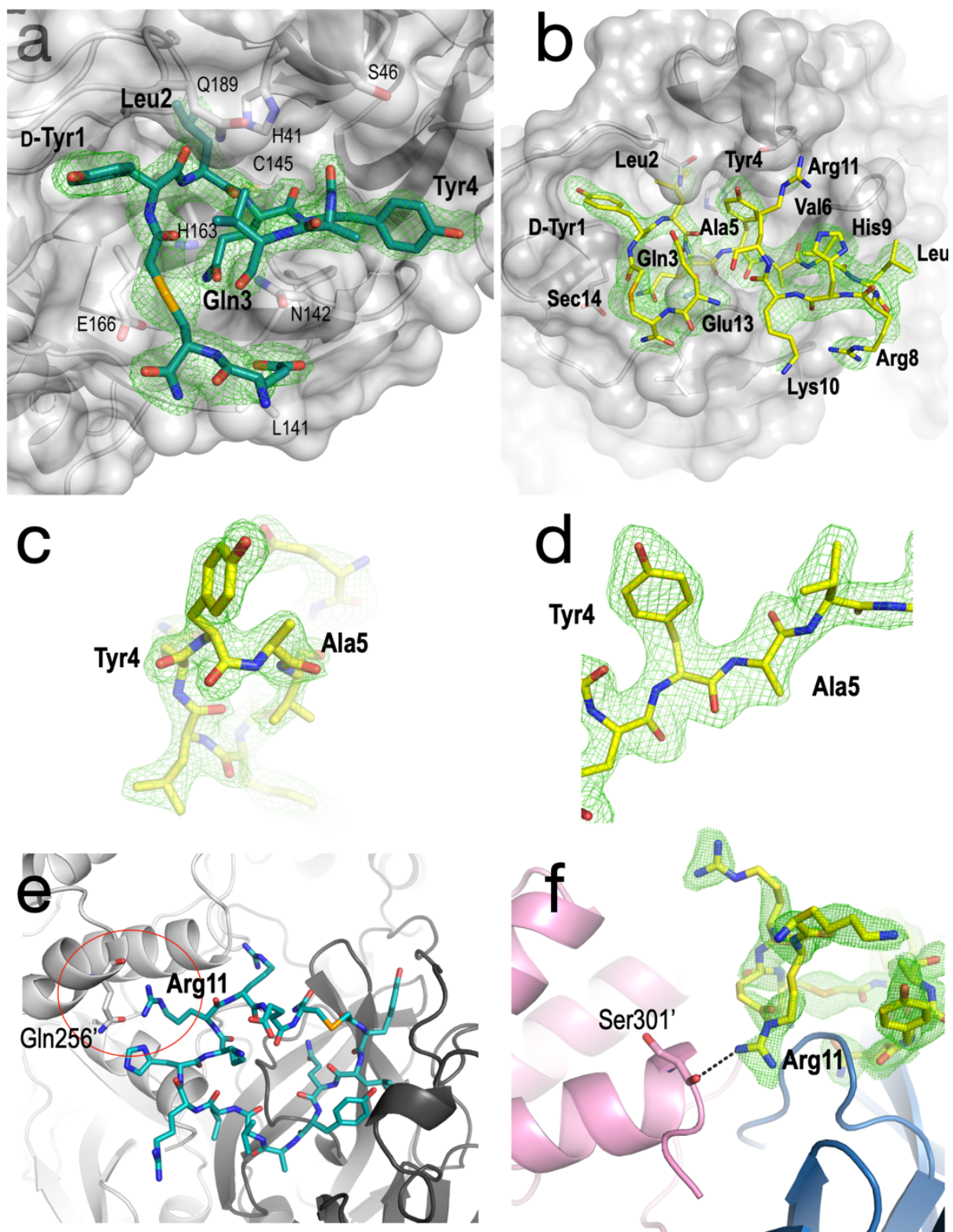


Fig. S13. Structural analysis of the complex between selenoether analogue of 1 (Se-1) and SARS-CoV-2 M^{Pro}. **a** Comparison between the binding mode of the peptide in chains A, C, D and **b** chain B shown as sticks with 3.0 σ omit electron density map. While the Tyr4-Ala5 *cis*-peptide bond causes a tight turn in the peptide in chains A, C, D, the Tyr4-Ala5 *trans*-peptide bond in chains B results in the main chain running through the site otherwise occupied by Tyr4 in the other chains. **c** and **d** show

3.0 σ omit electron density maps of the Tyr4-Ala5 *cis*-peptide bond in chain C and the Tyr4-Ala5 *trans*-peptide bond in chain B. **e** Molecular dynamics simulations reveal the peptide can transiently interact with the neighbouring chain in the dimer *via* Arg11. **f** Arg11 can be modelled into weak electron density consistent with a transient interaction with the carbonyl carbon of Ser301 in the neighbouring monomer.

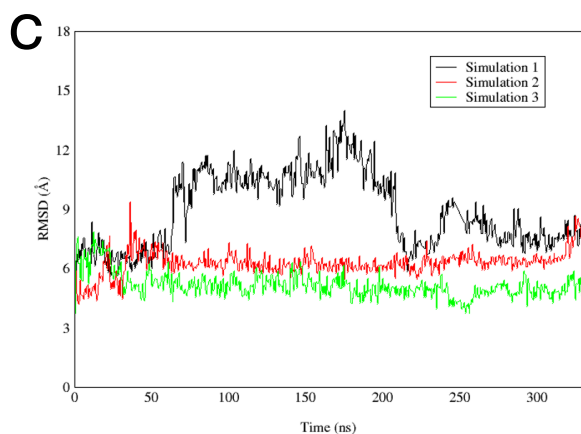
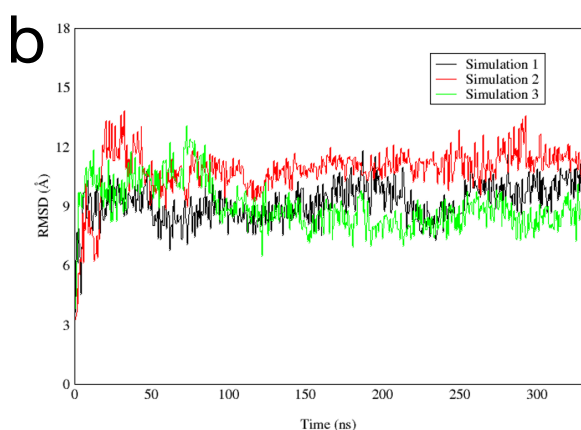
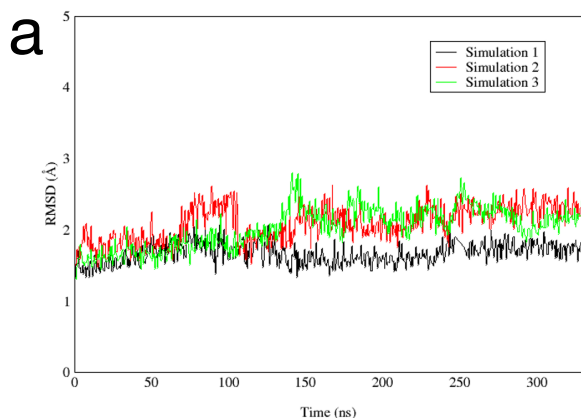
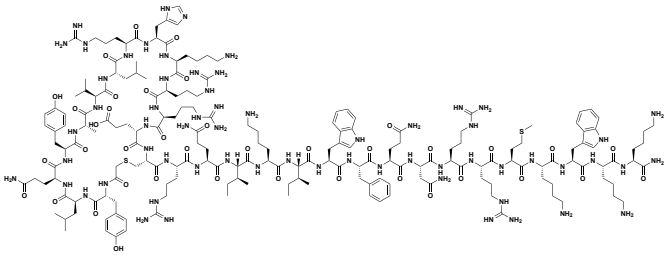
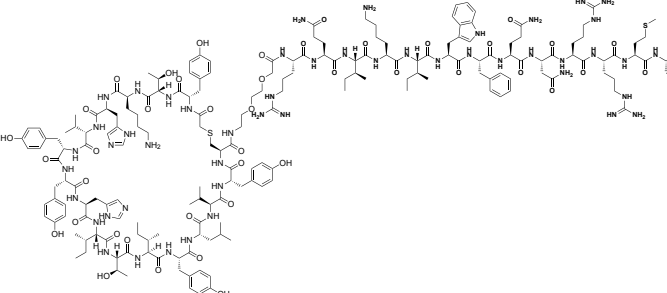
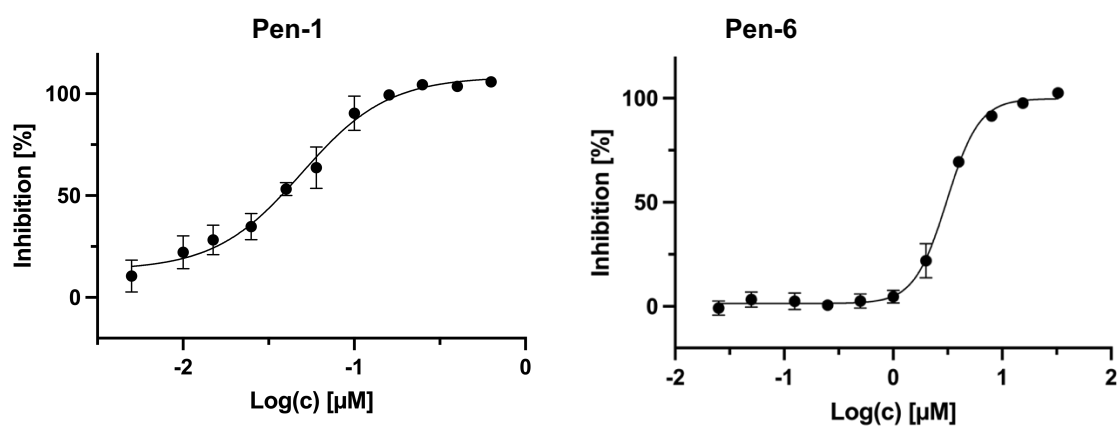


Fig. S14. RMSD plots of MD simulations. For chain A, the peptide Gln3 and Leu2 (P1 and P2 respectively) groups were oriented towards the S1 and S2 subcavities, respectively. As a negative control, for chain B, the peptide was modelled in the opposite orientation where the S2 subcavity was occupied by Tyr4 group. RMSD plots were obtained from the three independent 330 ns simulations. **a** Protein backbone RMSD; **b** RMSD of ligand (bound to chain A) fit to the protein; **c** RMSD of ligand (bound to chain B) fit to protein. The canonical model (Gln3-Leu2 = P1 & P2) was more stable than the alternative reverse model.

A

Peptide	Structure	IC ₅₀ (μM)
pen-1		0.049 ± 0.009
pen-6		3.1 ± 0.2



B

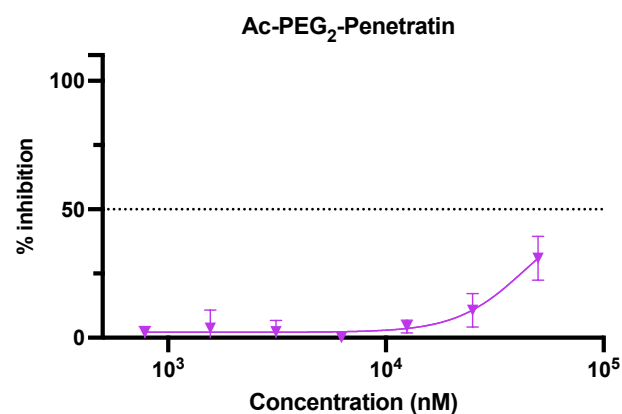


Fig. S15. A. Structures and inhibitory activities of penetratin conjugates of 1 and 6 (pen-1 and pen-6) against SARS-CoV-2 M^{PRO}. B. Antiviral activity of Ac-PEG₂-Penetratin negative control

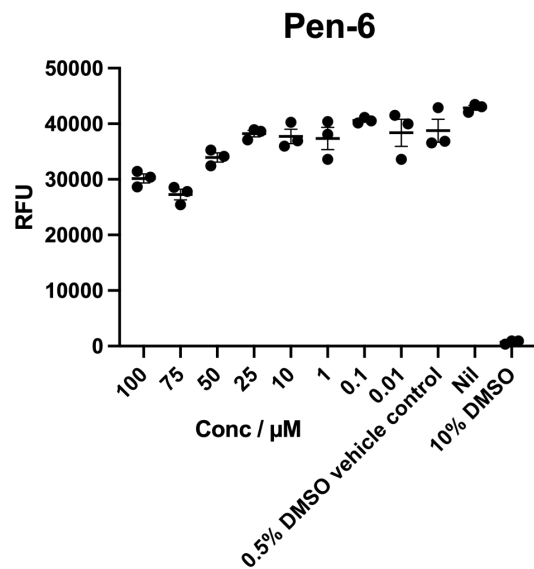
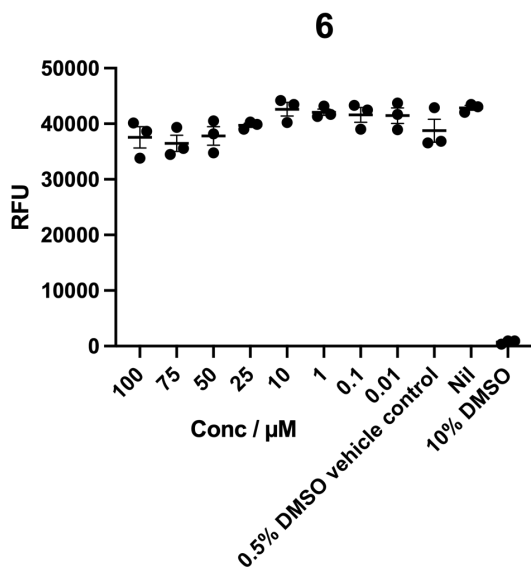
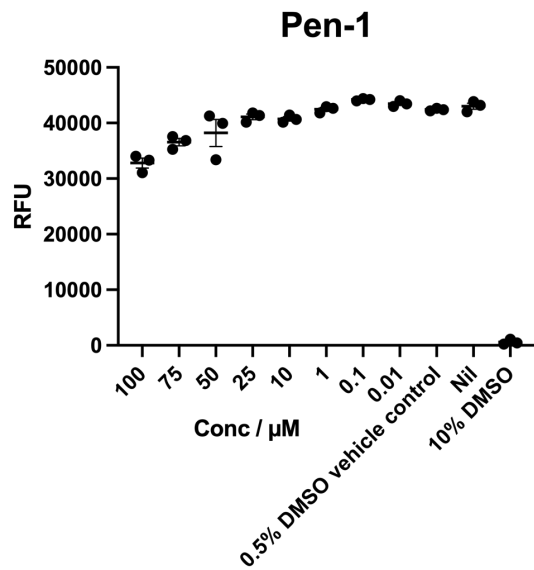
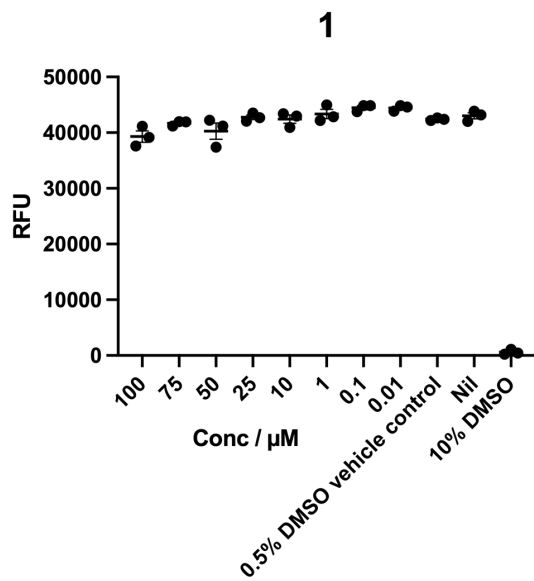
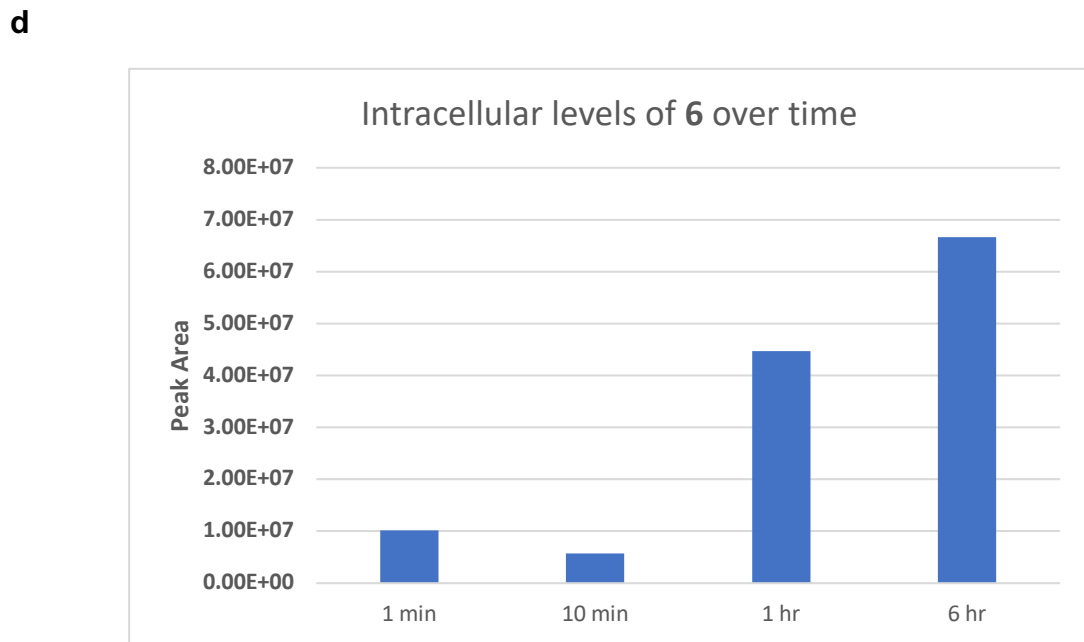
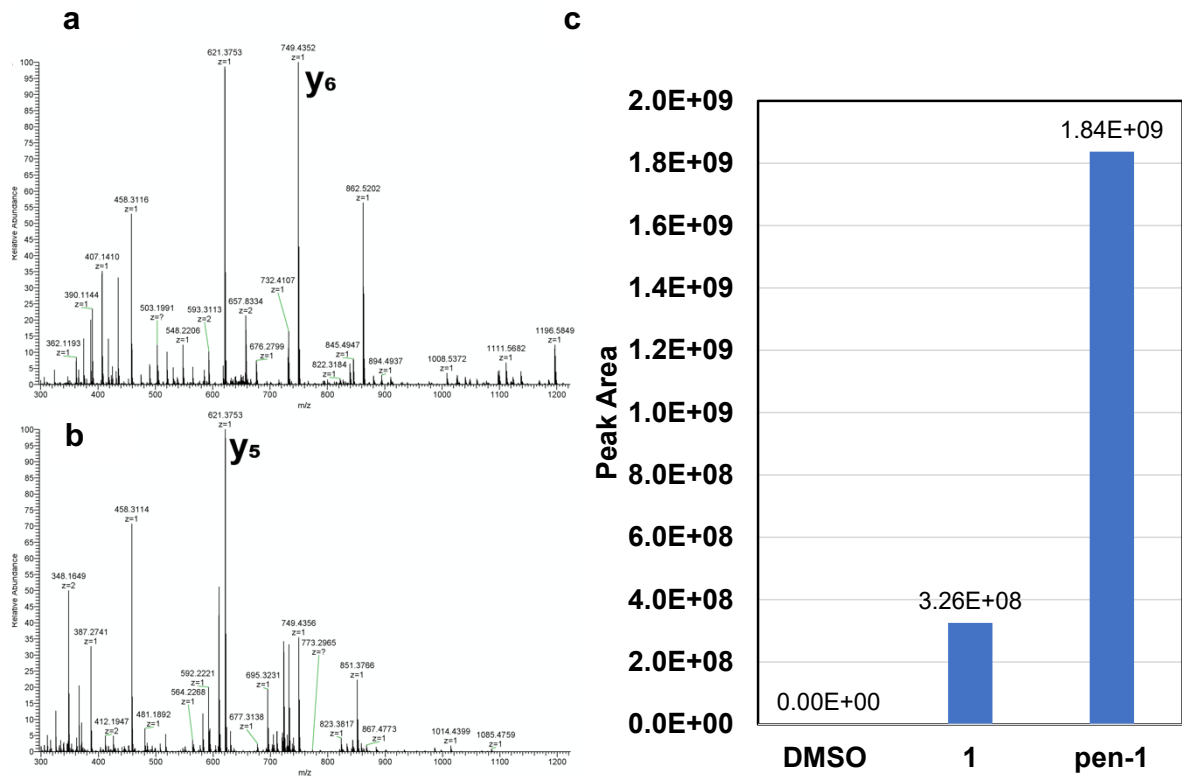


Fig. S16. Cytotoxicity of 1, pen-1, 6 and pen-6 against HEK293-ACE-2-TMPRSS2 cells. No cytotoxicity was observed for 1 and 6 whilst pen-1 and pen-6 resulted in minimal cytotoxicity over 50 μM .



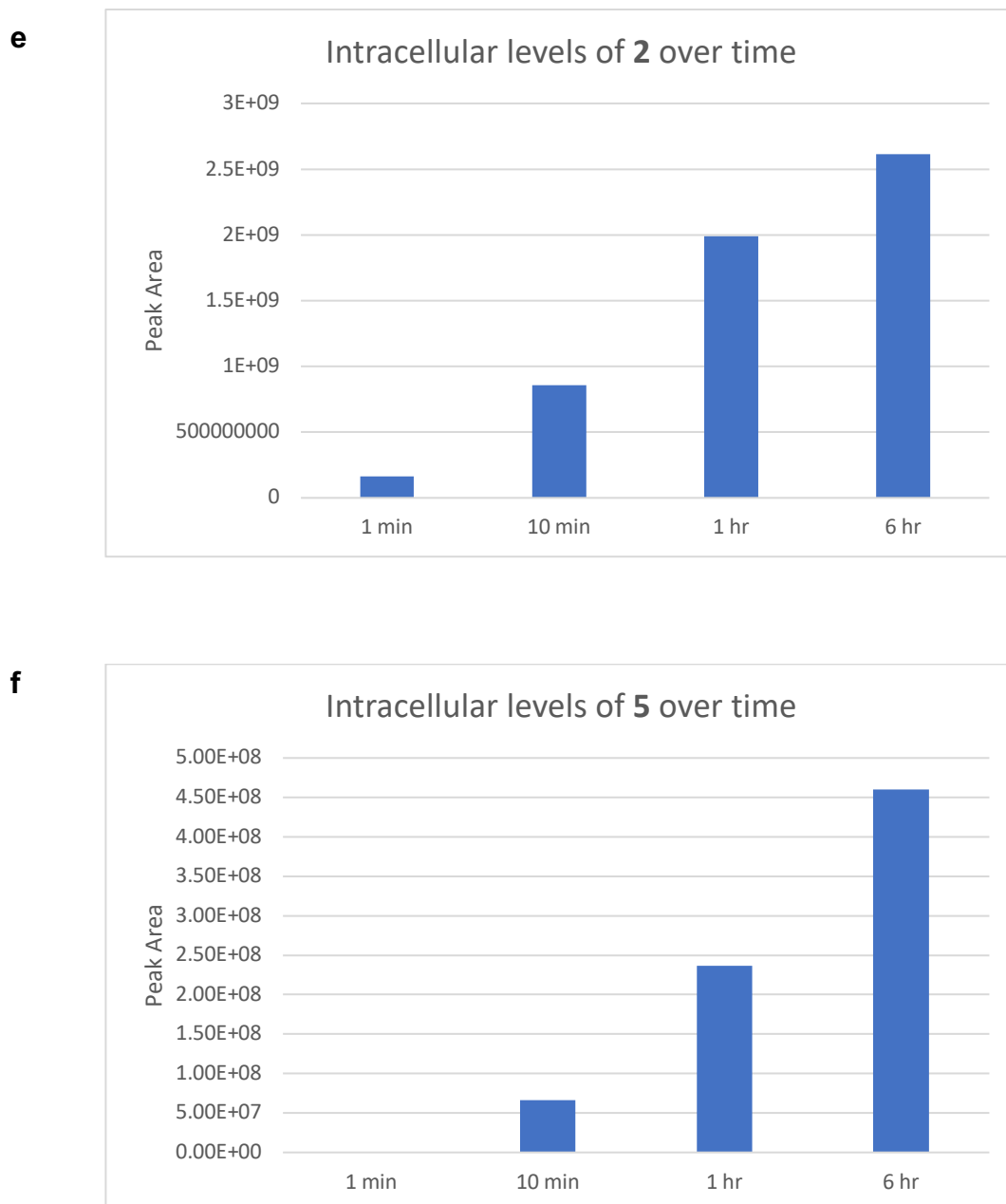


Fig. S17. Cyclic peptide M^{pro} inhibitor **1**, its penetratin conjugate (**pen-1**) and **6** were incubated with HEK293-ACE2-TMPRSS2 cells. After 10 mins (as well as 1 and 6 hours in the case of **6**) aliquots of cells were washed before lysis. Analysis of trypsin digested cell-lysates by data-independent acquisition (DIA) LC-MS/MS enabled the quantification by peak area of both **1** and **pen-1**. **a** Quantification of **1** used the y₆ ion (749.4304, +1) in the 648.500 DIA window from precursor m/z 657.8292 (+2). **b** Quantification of **pen-1** used the y₅ ion (621.3719, +1) in the 490.500 DIA window from precursor m/z 491.2503 (+3). **c** **pen-1** was observed to have >5.5-fold larger peak area compared to **1** under the same conditions. This shows that while both **pen-1** and **1** can enter cells to inhibit SARS-CoV-2 M^{pro}, **pen-1** does so more efficiently. **d** Intracellular levels of **6** in HEK293-ACE2-TMPRSS2 cells over a time course of 6 hours. **e** Intracellular levels of **2** in HEK293-ACE2-TMPRSS2 cells over a time course of 6 hours. **f** Intracellular levels of **5** in HEK293-ACE2-TMPRSS2 cells over a time course of 6 hours.

Characterization of recombinant SARS-CoV-2 M^{pro}

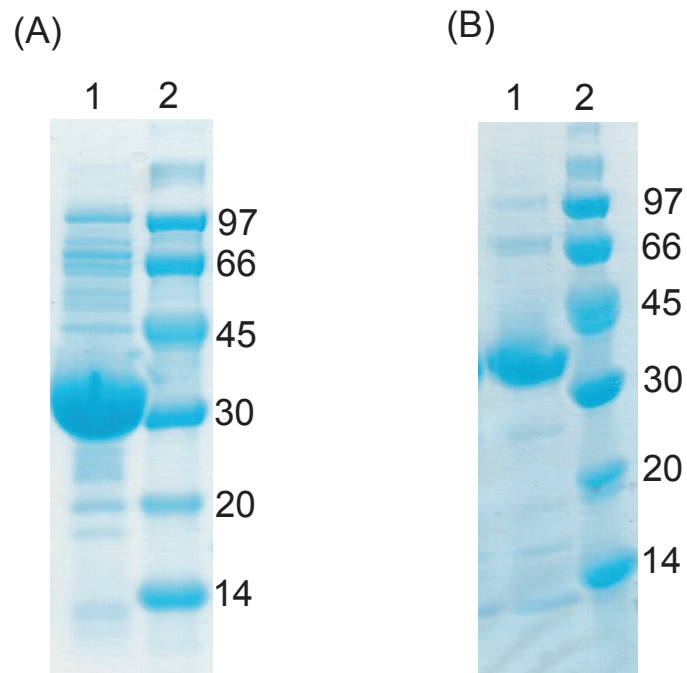


Fig. S18. 12 % SDS-PAGE of purified proteins. Lane 1 shows the purified protein and lane 2 the protein markers. (A) Wild-type M^{pro}. (B) R298A mutant.

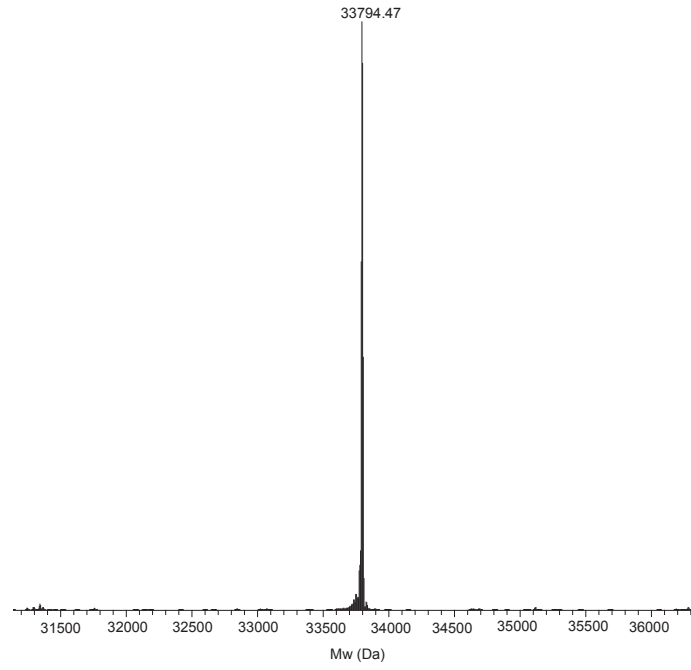


Fig. S19. Intact protein mass spectrometric analysis of wild-type M^{pro} (calculated mass 33796.72 Da).

Characterization of peptides

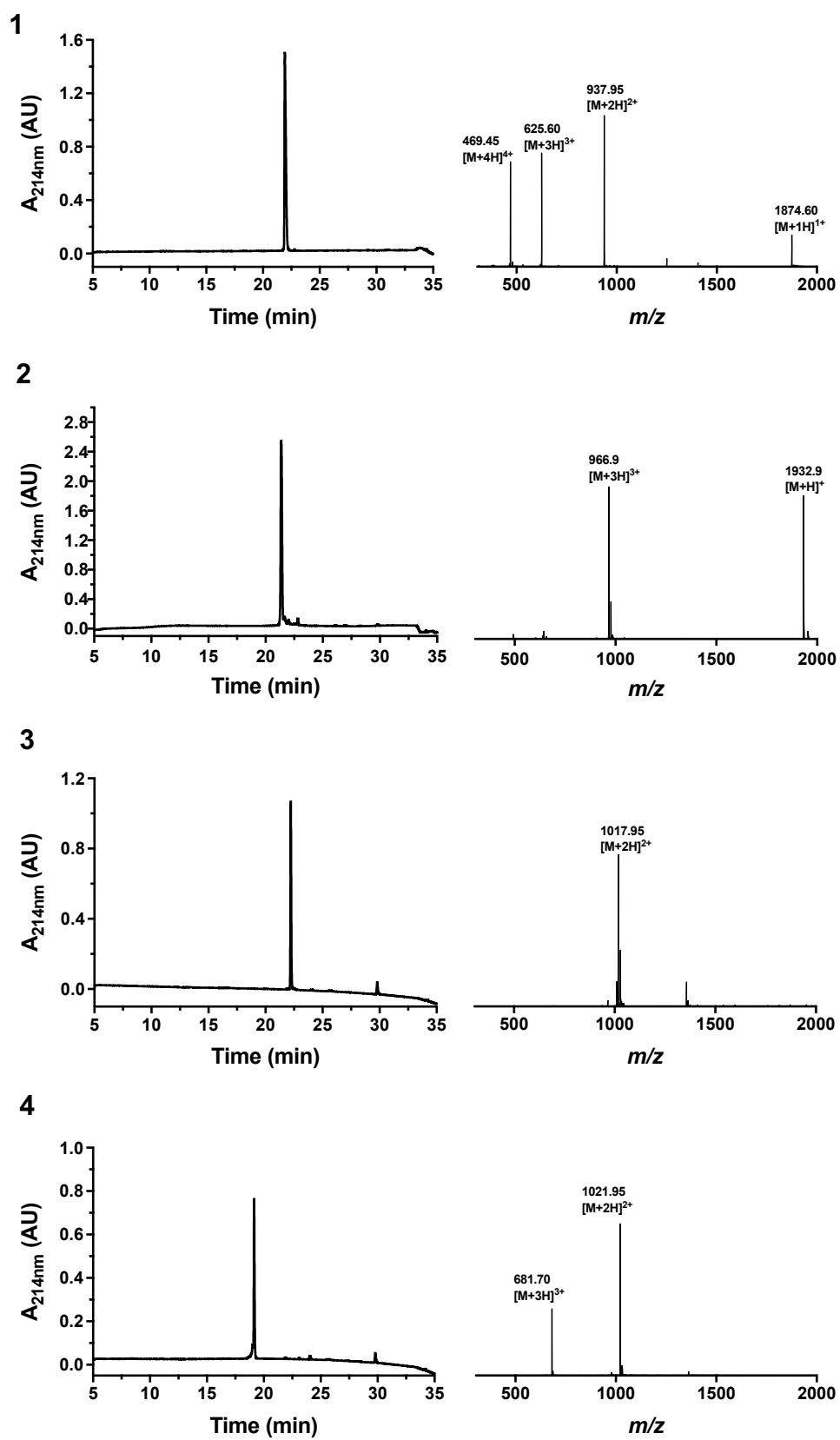


Fig. S20. Analytical HPLC traces and ESI+ mass spectra of peptides 1-4.

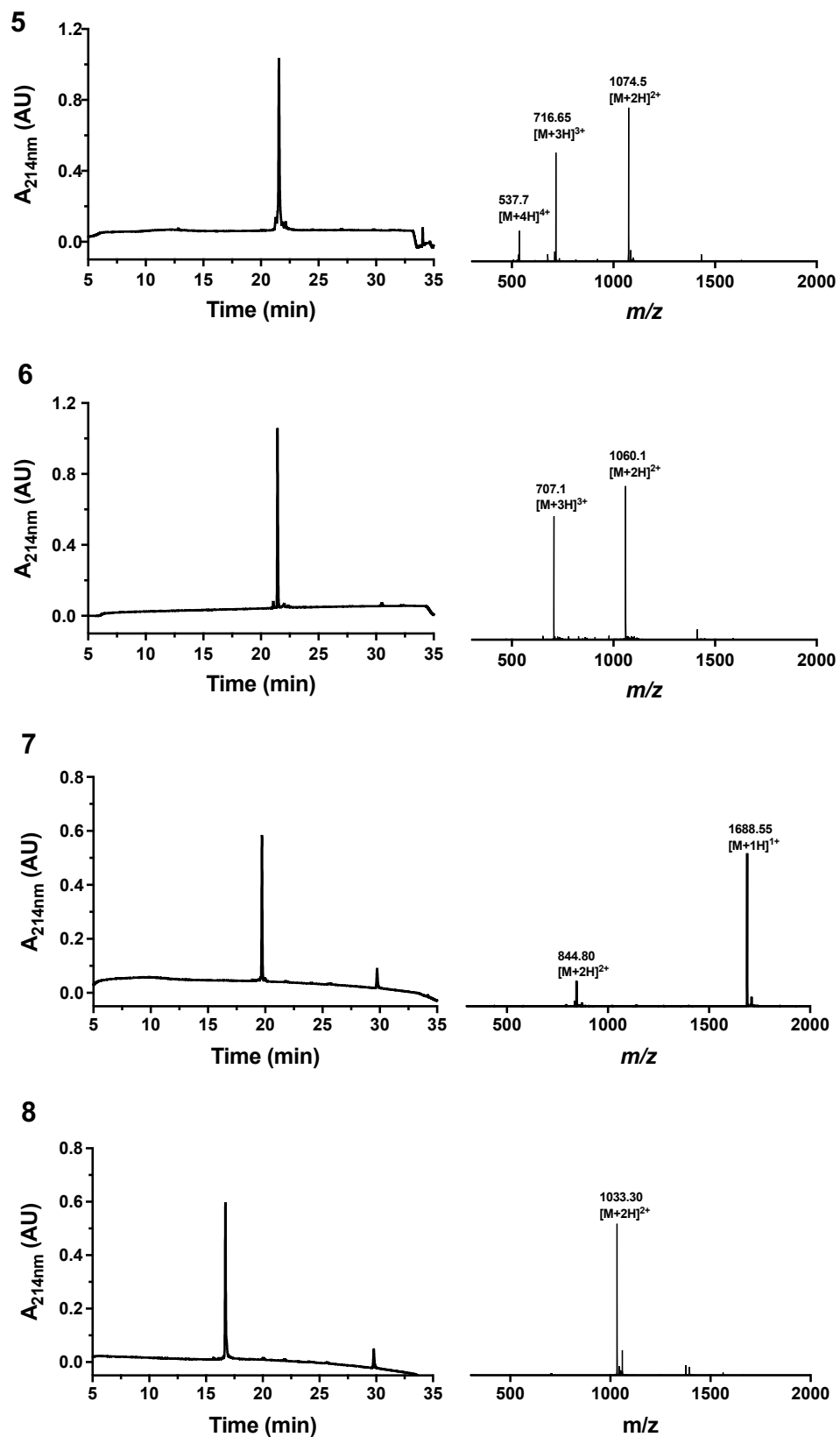


Fig. S21. Analytical HPLC traces and ESI+ mass spectra of peptides 5-8.

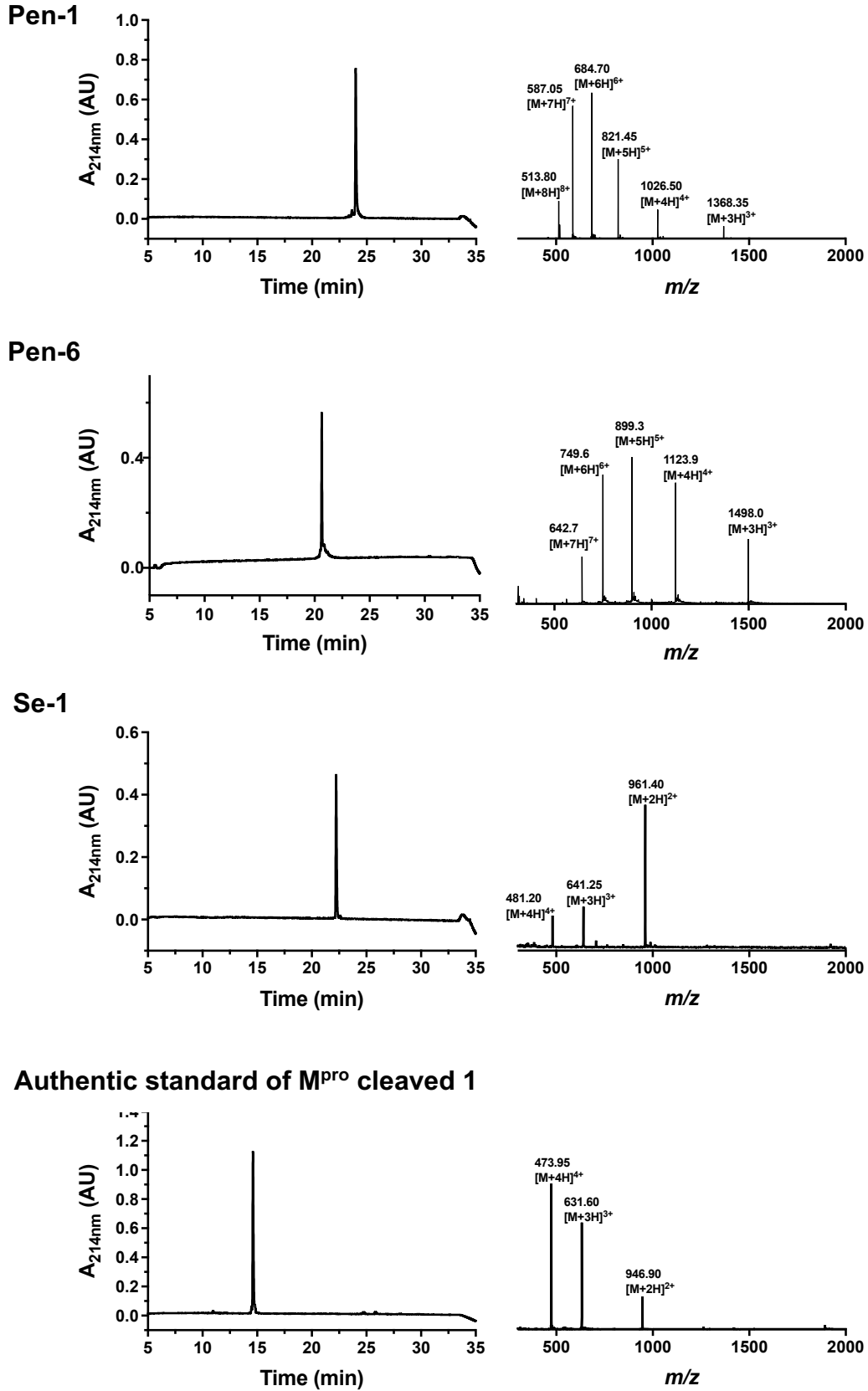


Fig. S22. Analytical HPLC traces and ESI+ mass spectra of Pen-1, Pen-6, Se-1 and authentic standard of M^{pro} cleaved 1.

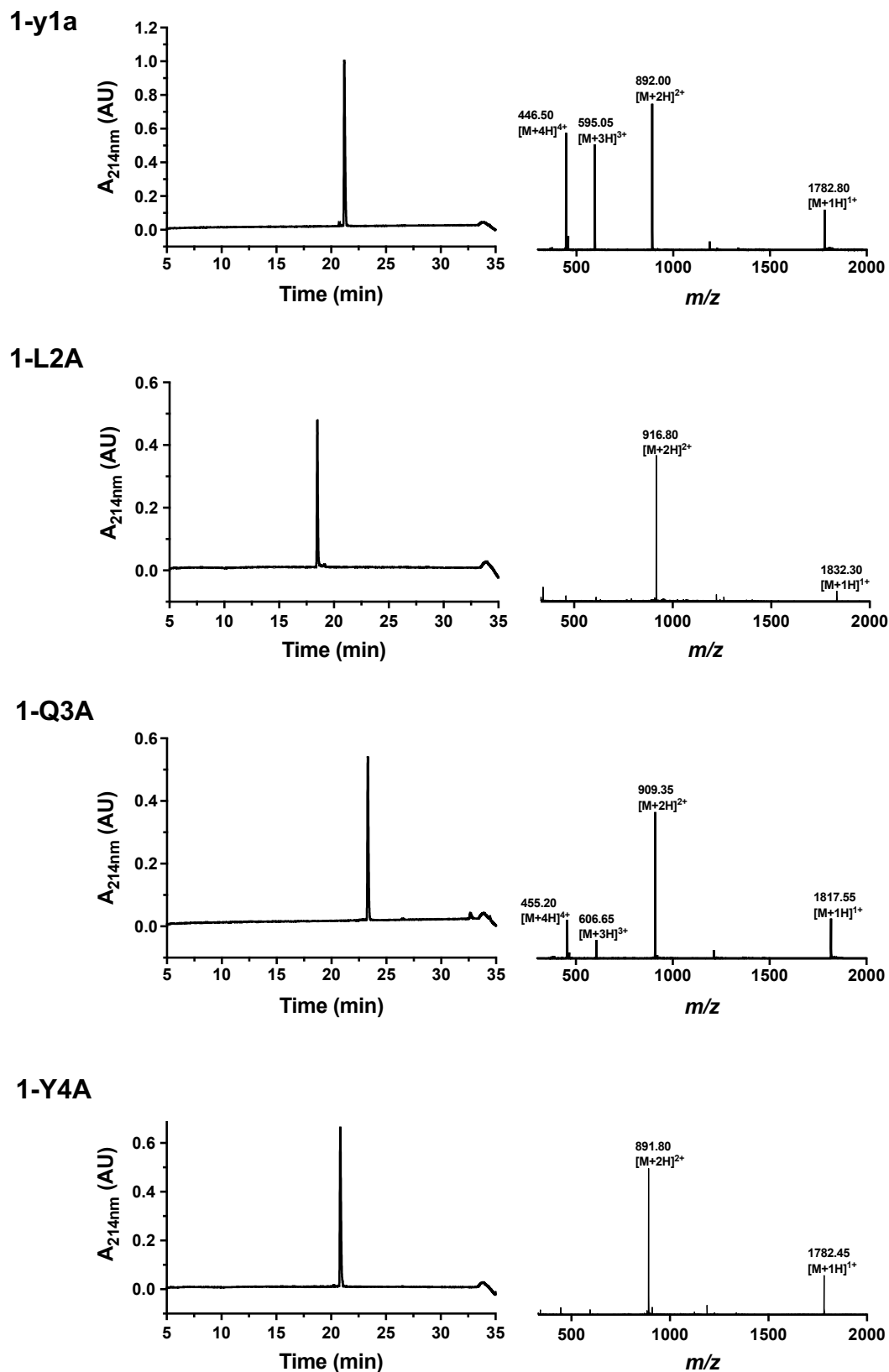


Fig. S23. Analytical HPLC traces and ESI+ mass spectra of 1-y1a, 1-L2A, 1-Q3A and 1-Y4A.

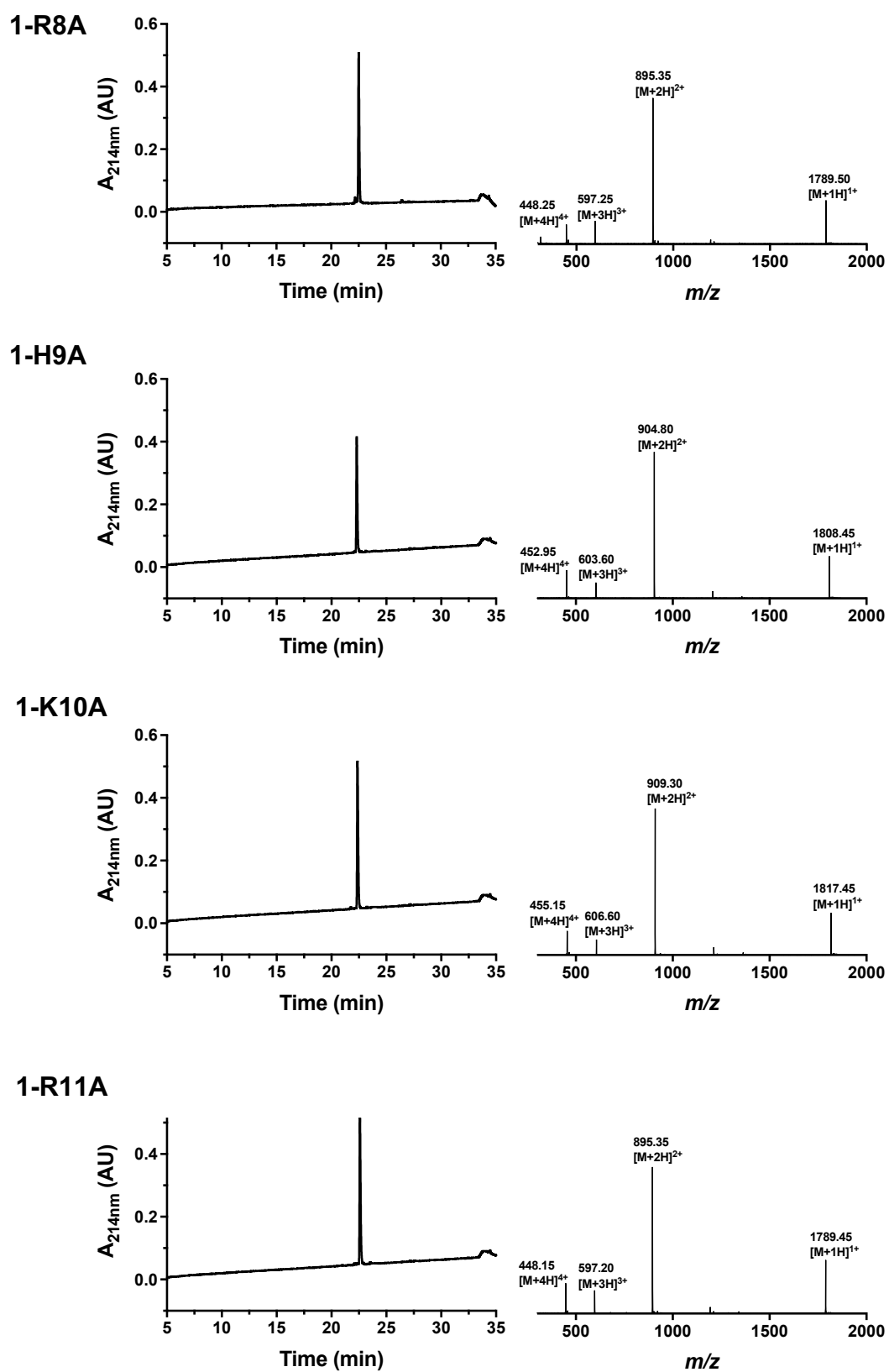
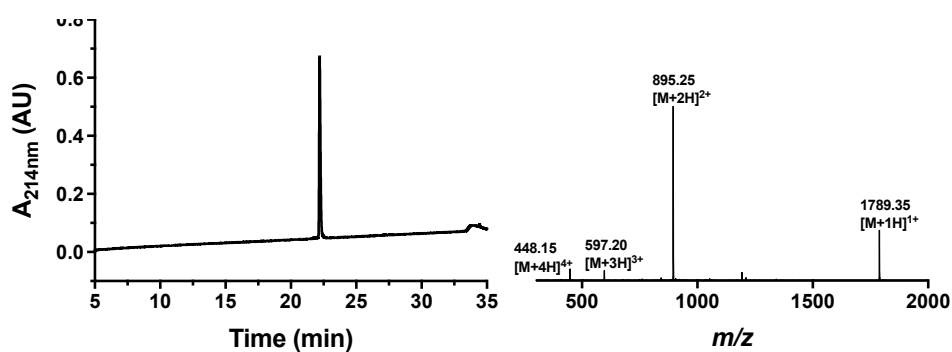
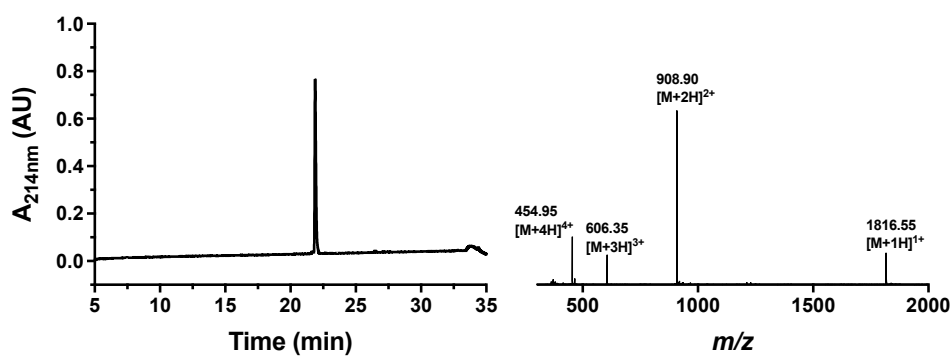


Fig. S24. Analytical HPLC traces and ESI+ mass spectra of 1-R8A, 1-H9A, 1-K10A and 1-R11A.

1-R12A



1-E13A



Ac-PEG₂-Penetratin

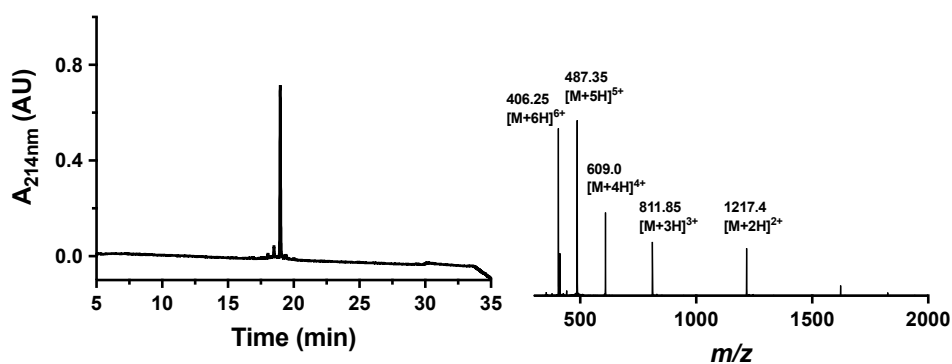


Fig. S25. Analytical HPLC traces and ESI+ mass spectra of 1-R12A, 1-E13A and Ac-PEG₂-Penetratin.

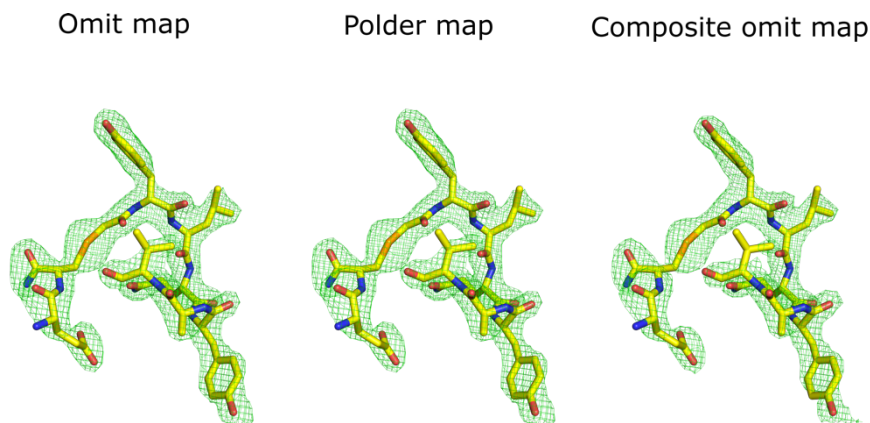


Fig. S26. The peptide bound in Chain C is shown in 3.0σ omit electron density maps generated by phenix (using twin refinement), a Polder omit map and a composite omit map (10% atoms) with refinement. The omit maps are essentially identical and all indicate the placement and modelling of the peptide is correct.

SI References

1. K. Ozawa, M. J. Headlam, P. M. Schaeffer, B. R. Henderson, N. E. Dixon and G. Otting, *Eur. J. Biochem.*, 2004, **271**, 4084-4093.
2. M. A. Apponyi, K. Ozawa, N. E. Dixon and G. Otting, in *Structural Proteomics*, Springer, 2008, pp. 257-268.
3. P. S. Wu, K. Ozawa, S. P. Lim, S. G. Vasudevan, N. E. Dixon and G. Otting, *Angew. Chem. Int. Ed.*, 2007, **46**, 3356-3358.
4. D. P. Teufel, G. Bennett, H. Harrison, K. van Rietschoten, S. Pavan, C. Stace, F. Le Floch, T. Van Bergen, E. Vermassen, P. Barbeaux, T. T. Hu, J. H. M. Feyen and M. Vanhove, *J. Med. Chem.*, 2018, **61**, 2823-2836.
5. Z. Jin, X. Du, Y. Xu, Y. Deng, M. Liu, Y. Zhao, B. Zhang, X. Li, L. Zhang and C. Peng, *Nature*, 2020, **582**, 289-293.
6. A. J. Robertson, J. Ying and A. Bax, *Magn. Reson.*, 2021, **2**, 129-138.
7. F.-X. Cantrelle, E. Boll, L. Brier, D. Moschidi, S. Belouzard, V. Landry, F. Leroux, F. Dewitte, I. Landrieu, J. Dubuisson, B. Deprez, J. Charton and X. Hanouille, *Angew. Chem. Int. Ed.*, 2021, **60**, 25428-25435.
8. S. C. Cheng, G. G. Chang and C. Y. Chou, *Biophys. J.*, 2010, **98**, 1327-1336.
9. Schrödiner Release 2019-1: Protein Preparation Wizard, Schrödinger, LLC, New York, NY (2019).
10. Schrödiner Release 2019-1: Desmond Molecular Graphics System, D. E. Shaw Research, New York, NY (2019).
11. The PyMOL Molecular Graphics System, Version 2.0, Schrödinger, LLC.
12. L. Zhang, D. Lin, X. Sun, U. Curth, C. Drost, L. Sauerhering, S. Becker, K. Rox and R. Hilgenfeld, *Science*, 2020, **368**, 409-412.
13. S. Wang, S. R. Foster, J. Sanchez, L. Corcilius, M. Larance, M. Canals, M. J. Stone and R. J. Payne, *ACS Chem. Biol.*, 2021, **16**, 973-981.
14. Y. Goto, T. Katoh and H. Suga, *Nat. Protoc.*, 2011, **6**, 779-790.
15. Y. Hayashi, J. Morimoto and H. Suga, *ACS Chem. Biol.*, 2012, **7**, 607-613.
16. A. Norman, C. Franck, M. Christie, P. M. E. Hawkins, K. Patel, A. S. Ashurst, A. Aggarwal, J. K. K. Low, R. Siddiquee, C. L. Ashley, M. Steain, J. A. Triccas, S. Turville, J. P. Mackay, T. Passioura and R. J. Payne, *ACS Cent. Sci.*, 2021, **7**, 1001-1008.
17. Y. Yamagishi, I. Shoji, S. Miyagawa, T. Kawakami, T. Katoh, Y. Goto and H. Suga, *Chem. Biol.*, 2011, **18**, 1562-1570.

18. L. Zhu, S. George, M. F. Schmidt, S. I. Al-Gharabli, J. Rademann and R. Hilgenfeld, *Antiviral Res.*, 2011, **92**, 204-212.
19. C. Ma, M. D. Sacco, B. Hurst, J. A. Townsend, Y. Hu, T. Szeto, X. Zhang, B. Tarbet, M. T. Marty, Y. Chen and J. Wang, *Cell Res.*, 2020, **30**, 678-692.
20. D. Aragão, J. Aishima, H. Cherukuvada, R. Clarken, M. Clift, N. P. Cowieson, D. J. Ericsson, C. L. Gee, S. Macedo, N. Mudie, S. Panjikar, J. R. Price, A. Riboldi-Tunncliffe, R. Rostan, R. Williamson and T. T. Caradoc-Davies, *J. Synchrotron Radiat.*, 2018, **25**, 885-891.
21. W. Kabsch, *Acta Crystallogr., Sect. D: Biol. Crystallogr.*, 2010, **66**, 125-132.
22. P. R. Evans and G. N. Murshudov, *Acta Crystallogr., Sect. D: Biol. Crystallogr.*, 2013, **69**, 1204-1214.
23. A. J. McCoy, R. W. Grosse-Kunstleve, P. D. Adams, M. D. Winn, L. C. Storoni and R. J. Read, *J. Appl. Crystallogr.*, 2007, **40**, 658-674.
24. P. Emsley, B. Lohkamp, W. G. Scott and K. Cowtan, *Acta Crystallogr., Sect. D: Biol. Crystallogr.*, 2010, **66**, 486-501.
25. G. N. Murshudov, P. Skubák, A. A. Lebedev, N. S. Pannu, R. A. Steiner, R. A. Nicholls, M. D. Winn, F. Long and A. A. Vagin, *Acta Crystallogr., Sect. D: Biol. Crystallogr.*, 2011, **67**, 355-367.
26. G. N. Murshudov, A. A. Vagin and E. J. Dodson, *Acta Crystallogr., Sect. D: Biol. Crystallogr.*, 1997, **53**, 240-255.
27. P. D. Adams, P. V. Afonine, G. Bunkóczi, V. B. Chen, I. W. Davis, N. Echols, J. J. Headd, L. W. Hung, G. J. Kapral, R. W. Grosse-Kunstleve, A. J. McCoy, N. W. Moriarty, R. Oeffner, R. J. Read, D. C. Richardson, J. S. Richardson, T. C. Terwilliger and P. H. Zwart, *Acta Crystallogr., Sect. D: Biol. Crystallogr.*, 2010, **66**, 213-221.
28. D. Liebschner, P. V. Afonine, N. W. Moriarty, B. K. Poon, O. V. Sobolev, T. C. Terwilliger and P. D. Adams, *Acta Crystallogr., Sect. D: Biol. Crystallogr.*, 2017, **73**, 148-157.
29. T. C. Terwilliger, R. W. Grosse-Kunstleve, P. V. Afonine, N. W. Moriarty, P. D. Adams, R. J. Read, P. H. Zwart and L.-W. Hung, *Acta Crystallogr., Sect. D: Biol. Crystallogr.*, 2008, **64**, 515-524.
30. F. Tea, A. Ospina Stella, A. Aggarwal, D. Ross Darley, D. Pilli, D. Vitale, V. Merheb, F. X. Z. Lee, P. Cunningham, G. J. Walker, C. Fichter, D. A. Brown, W. D. Rawlinson, S. R. Isaacs, V. Mathivanan, M. Hoffmann, S. Pöhlman, O. Mazigi, D. Christ, R. J. Rockett, V. Sintchenko, V. C. Hoad, D. O. Irving, G. J. Dore, I. B. Gosbell, A. D. Kelleher, G. V. Matthews, F. Brilot and S. G. Turville, *PLoS Med.*, 2021, **18**, e1003656.
31. G. J. Walker, V. Clifford, N. Bansal, A. O. Stella, S. Turville, S. Stelzer-Braid, L. D. Klein and W. Rawlinson, *J. Paediatr. Child Health*, 2020, **56**, 1872-1874.
32. D. J. Harney, M. Cielesh, R. Chu, K. C. Cooke, D. E. James, J. Stöckli and M. Larance, *Cell Rep.*, 2021, **34**, 108804.
33. S. F. Martinez-Huenchullan, I. Shipsey, L. Hatchwell, D. Min, S. M. Twigg and M. Larance, *Mol. Cell. Proteomics*, 2020, **20**, 100027.
34. E. F. Pettersen, T. D. Goddard, C. C. Huang, G. S. Couch, D. M. Greenblatt, E. C. Meng and T. E. Ferrin, *J. Comput. Chem.*, 2004, **25**, 1605-1612.